Journal of Translational Medicine

REVIEW

Open Access

Fluorescent probes in autoimmune disease research: current status and future prospects

Junli Chen[1,2], Mingkai Chen[1,2] and Xiaolong Yu[1,3*]

Abstract

Autoimmune diseases (AD) present substantial challenges for early diagnosis and precise treatment due to their intricate pathogenesis and varied clinical manifestations. While existing diagnostic methods and treatment strategies have advanced, their sensitivity, specificity, and real-time applicability in clinical settings continue to exhibit significant limitations. In recent years, fluorescent probes have emerged as highly sensitive and specific biological imaging tools, demonstrating substantial potential in AD research.

This review examines the response mechanisms and historical evolution of various types of fluorescent probes, systematically summarizing the latest research advancements in their application to autoimmune diseases. It highlights key applications in biomarker detection, dynamic monitoring of immune cell functions, and assessment of drug treatment efficacy. Furthermore, this article analyzes the technical challenges currently encountered in probe development and proposes potential directions for future research. With ongoing advancements in materials science, nanotechnology, and bioengineering, fluorescent probes are anticipated to achieve higher sensitivity and enhanced functional integration, thereby facilitating early detection, dynamic monitoring, and innovative treatment strategies for autoimmune diseases. Overall, fluorescent probes possess substantial scientific significance and application value in both research and clinical settings related to autoimmune diseases, signaling a new era of personalized and precision medicine.

Keywords Fluorescent probe, Autoimmune disease, Early diagnosis, Precision medicine, Nanotechnology, Multimodal imaging

Introduction

Autoimmune diseases (AD) [1] comprise a group of complex and challenging chronic conditions characterized by the immune system's aberrant attack on its own tissues, resulting in widespread inflammation and tissue damage. To date, over 80 distinct types of autoimmune diseases have been identified, capable of affecting any organ system [2]. AD can be categorized based on the extent of the lesions they cause, including systemic and organ-specific disorders. Systemic diseases encompass conditions such as systemic lupus erythematosus, rheumatoid arthritis, and systemic sclerosis, whereas organ-specific diseases comprise type 1 diabetes, multiple sclerosis, and myasthenia gravis [1]. In recent years, the global incidence of autoimmune diseases (AD) has shown a significant upward trend, affecting approximately 3–5% of the population [3] and occurring in individuals of all ages. The annual incidence and prevalence rates have risen by 19.1% and 12.5% [4], respectively, positioning AD as one of the most pressing public health concerns. According to the National Health and Nutrition Examination Survey (NHANES) [4], 18% of U.S. adults test positive for

*Correspondence:
Xiaolong Yu
yuxiaolong@wjrmyy.cn
[1] Wujin Hospital Affiliated With Jiangsu University, Changzhou, Jiangsu, China
[2] School of Medicine, Jiangsu University, Zhenjiang, Jiangsu, China
[3] The Wujin Clinical College of Xuzhou Medical University, Changzhou, Jiangsu, China

thyroid autoantibodies, and 32% of adults aged 60 and older possess at least one of four specific autoantibodies: rheumatoid factors, anti-thyroglobulin, anti-thyroid peroxidase autoantibodies, or anti-tissue transglutaminase autoantibodies. An epidemiological study [5] involving eight autoimmune diseases among Chinese adults estimated that 2.7–3.0% of this population (over 31 million individuals) suffer from one or more autoimmune diseases, with the majority of the burden stemming from autoimmune thyroid diseases and rheumatoid arthritis. These statistics suggest that AD are likely to emerge as a significant healthcare challenge in the future, underscoring the need for heightened attention and research efforts to mitigate the disease's progression.

Autoimmune diseases are notoriously challenging to treat. Beyond the substantial physical and psychological harm they cause to patients, the potential for complications warrants significant attention [6]. AD can substantially elevate the risk of developing cardiovascular diseases, malignancies, and various other health conditions [7]. A survey of the American population indicates that several autoimmune diseases are linked to an elevated risk of hepatobiliary cancers [8]. The presence of any autoimmune condition is associated with a higher risk of anal squamous cell carcinoma (OR = 1.11, 95%CI = 1.02 to 1.21; population attributable fraction = 1.8%). Furthermore, systemic lupus erythematosus, sarcoidosis, and psoriasis demonstrate moderate associations with increased squamous cell carcinoma risk [9]. Large-scale cohort studies conducted in China have revealed that patients with five types of autoimmune diseases—SLE, RA, Sjögren's syndromes (SS), systemic sclerosis (SSc), and idiopathic inflammatory myopathies (IIM)—exhibit a heightened cancer risk [10]. Some studies imply a close relationship between SLE and myasthenia gravis (MG) [11]. Research by L. Sumelahti indicates that patients with multiple sclerosis (pwMS) experience a median life expectancy reduction of 8–9 years compared to healthy controls [12]. Additionally, a study involving 20,266 patients with Sjögren's syndrome found that this population has a higher prevalence of hearing loss, dizziness, tinnitus, and sudden deafness [13].

Imaging diagnosis is integral to the evaluation of AD. Common imaging methods [14] include conventional radiography (CR), ultrasound, computed tomography (CT), and magnetic resonance imaging (MRI). CR [15] is a simple and rapid technique often employed to assess joint damage, such as bone erosion, joint space narrowing, and misalignment in patients with AD. However, CR exhibits poor sensitivity in detecting early structural changes at the joint and soft tissue levels. Ultrasound [16] offers advantages such as being non-invasive, cost-effective, and devoid of radiation hazards, making it an ideal diagnostic tool. It is frequently utilized to evaluate synovial inflammation and provide diagnostic support, particularly in detecting bone erosion that CR fails to identify. Nevertheless, the accuracy of ultrasound results is contingent upon the operator's skill, and its application in the management of AD has yet to be systematized. CT is effective for identifying pulmonary lesions [17], assessing bone destruction, and precisely evaluating bone pathology; however, it is limited in differentiating between various soft tissue structures, which restricts its use in certain clinical scenarios. MRI [18], characterized by high resolution and multi-planar imaging capabilities, provides clear visualization of soft tissue structures, including muscles, ligaments, and nerve pathology. Consequently, MRI is pivotal in diagnosing and monitoring autoimmune diseases such as RA and MS. However, its high cost and longer examination times present significant barriers to widespread clinical application. Each imaging modality possesses specific advantages and limitations; therefore, clinicians typically select the most appropriate diagnostic approach based on the patient's individual condition and needs. Ultimately, imaging diagnosis alone cannot yield conclusive evidence and must be integrated with clinical presentation and laboratory test results to enhance diagnostic accuracy.

Autoantibody testing serves as a crucial biomarker for diagnosing autoimmune diseases, as autoantibodies that target the body's own tissue components are present in nearly all patients with autoimmune diseases. For instance, patients with SLE typically test positive for antinuclear antibodies (ANA) and anti-double-stranded DNA (dsDNA) antibodies [19], while those with RA may show elevated levels of rheumatoid factor (RF) and anti-citrullinated protein antibodies (ACPA) [20]. Research into various autoantibodies and their characteristics offers valuable insights into the underlying pathophysiological mechanisms of these diseases. However, the specificity of these antibodies is limited [21, 22], and a positive antibody test alone cannot definitively confirm the diagnosis of AD; such results must be interpreted in conjunction with clinical presentation and other diagnostic findings. Patients with autoimmune diseases often display abnormal immunoglobulin levels [23] and complement system activation [24]. Testing for immunoglobulins and complement components, such as C3 and C4, can aid in evaluating disease activity. Nevertheless, these markers also lack specificity and cannot be used in isolation for diagnosing autoimmune diseases. Similarly, elevated levels of cytokines (e.g., IL-1, IL-6, TNF-α) are frequently observed in patients with AD [25, 26]. While these cytokines are helpful for assessing disease activity and monitoring treatment responses, their lack of specificity precludes them from serving as definitive

diagnostic criteria. Pathological examination through tissue biopsy can provide direct evidence for diagnosing and distinguishing AD by revealing the infiltration of inflammatory cells and the destruction of tissue architecture. However, since pathological examination is invasive, and some pathological features of autoimmune diseases lack high specificity, this may compromise the reliability of the diagnosis [27].

In the early stages of AD, patients often exhibit subtle symptoms that lack specificity [28]. Consequently, by the time a definitive clinical diagnosis is established, patients are typically in the mid-to-late stages of the disease, often experiencing multi-organ damage and severe complications. This diagnostic delay results in the loss of opportunities for early intervention, significantly impacting the long-term prognosis for patients. Thus, early diagnosis and timely intervention are crucial for enhancing disease outcomes in AD. Currently, no single diagnostic method provides adequate sensitivity and specificity for AD; therefore, diagnosis typically relies on a combination of multiple methods. While this approach improves diagnostic accuracy, it also introduces challenges such as increased diagnostic and treatment costs, reduced efficiency in the utilization of medical resources, and the potential to exacerbate doctor-patient conflicts, which may adversely affect patient compliance. Consequently, the development of a diagnostic method that is low-cost, highly specific, and accurate is not only of great importance for the early diagnosis of AD but will also significantly enhance treatment outcomes and long-term prognosis while facilitating the optimization of healthcare resource allocation.

With the ongoing advancements in diagnostic and imaging fields, fluorescence imaging technology has emerged as an indispensable method for monitoring changes in biochemical indicators and detecting biomarkers within living systems. Optical imaging techniques based on fluorescence have gained significant attention due to advancements in therapeutic diagnostics. Fluorescent probes, as a core component of this technology, offer several notable advantages over traditional imaging modalities (such as conventional radiography, ultrasound, CT, and MRI), including high sensitivity, real-time imaging capabilities, and the potential for multiplexing [29]. These characteristics allow fluorescent probes to be utilized non-invasively and with high precision for diagnosing various diseases and measuring the concentrations of biological substances within the body. Furthermore, fluorescent probes can intricately depict dynamic intracellular processes and visualize biological activities in response to specific parameters [30, 31]. They excel in detecting inorganic ions, biological thiols, reactive oxygen species (ROS), antigen–antibody interactions, and large macromolecules [32] while targeting subcellular structures [33] such as the nucleus, mitochondria, endoplasmic reticulum, and lysosomes. Consequently, they find widespread application in research domains such as biology, pathology, pharmacology, biochemistry, and medical science.

As the incidence of autoimmune diseases continues to rise, coupled with an enhanced understanding of their pathogenesis, there is an urgent need for the development of more precise diagnostic and therapeutic methods. Fluorescent probe technology, an innovative biological imaging technique, offers remarkable sensitivity and specificity. This review examines the response mechanisms and historical evolution of various types of fluorescent probes, systematically summarizing the latest research advancements in their application to autoimmune diseases. It highlights key applications in biomarker detection, dynamic monitoring of immune cell functions, and assessment of drug treatment efficacy. Unlike previous reviews, this work provides a comprehensive overview of fluorescent probes across a wide spectrum of autoimmune diseases, offering a unique perspective on their potential in this field. To further distinguish this review, we introduce a comparative table (Table 4) summarizing the key characteristics of different probe types and propose a novel classification framework based on their clinical applications: diagnostic, theranostic, and multimodal probes.

Fundamentals and development history of fluorescent probes

The development history of fluorescent probes

The concept of fluorescence was first proposed in 1852 by Stokes [34], who, while observing the fluorescence of chlorophyll and quinine in solution, discovered that the wavelength of emitted light was longer than that of the excitation light. This phenomenon, defined as Stokes Shift [35], spurred in-depth research into fluorescence phenomena and their mechanisms of generation. In 1905, Noelting and Dziewonsky [36] synthesized the organic dye rhodamine, which possesses an oxanthrene structure and remains one of the most widely used fluorescent groups to this day. In 1955, Albert H. Coons and colleagues successfully employed fluorescein to label antibodies [37]. Three years later, in 1958, tetramethylrhodamine was reported as a fluorescent marker in the study of chronic thyroiditis [38], marking the onset of widespread applications of organic dyes in the life sciences. In 1964, Mortimer Litt discovered that fluorescent dyes could visualize immune complexes in individual cells [39], revealing the potential applications of fluorescent probes in autoimmune diseases.

In 1962, Shimomura discovered green fluorescent protein in the Victoria multi-tentacled jellyfish [40]. In 1994, Martin Chalfie demonstrated that gene-encoded green fluorescent protein (GFP) could express its biological functions in the neurons of Escherichia coli and Caenorhabditis elegans [41], thereby establishing the wide application of fluorescent proteins in biological research. In 1988, Mark A. Reed discovered quantum dots [42], and subsequently, Bruchez and colleagues synthesized CdSe/CdS structured quantum dots, employing them as fluorescent probes to label tissue cells in mice [43]. In 1999, red fluorescent protein was discovered in non-biological luminescent corals [44], followed by the identification of monomeric red fluorescent protein in 2002 [45]. In 2004, Shaner and collaborators expanded the range of fluorescent protein colors through various modifications [46].

In laboratory settings, extensive studies on cellular and animal models are necessary to evaluate the safety of these probes. Beyond laboratory research, fluorescent probes are increasingly employed in clinical settings for applications such as guiding surgical procedures [47], assessing treatment efficacy, and predicting prognosis. Concurrently, researchers are continually improving techniques and developing new applications, such as utilizing near-infrared (NIR-II) fluorescence imaging-guided photothermal therapy to achieve integrated diagnosis and treatment through dual-targeted nanotherapy [48].

Reflecting on the evolution of fluorescent probes (Fig. 1), it is evident that, despite significant advancements over the past few decades, the development of these probes for disease diagnosis and treatment remains in its early stages, constrained by numerous limitations and challenges. Certain probes, such as heavy metal quantum dots and nanoparticles, are hindered by biotoxicity, which restricts their in vivo applications, and their prolonged retention in the body poses potential risks of eliciting immune responses and organ toxicity. Probes that utilize visible light exhibit limited tissue penetration capabilities, whereas most near-infrared probes are still in the nascent phases of development, facing unresolved issues concerning low stability and quantum yield [49]. Future advancements in fluorescent probes for the diagnosis and treatment of various diseases are anticipated to be at the forefront of fluorescent imaging research. Ongoing improvements will likely facilitate the rapid detection of key biomarkers in deeper biological sites, at lower concentrations, and during the early stages of disease progression, thus enabling more accurate clinical diagnosis and treatment monitoring while enhancing our understanding of the physiological roles of bioactive molecules in targeted diseases.

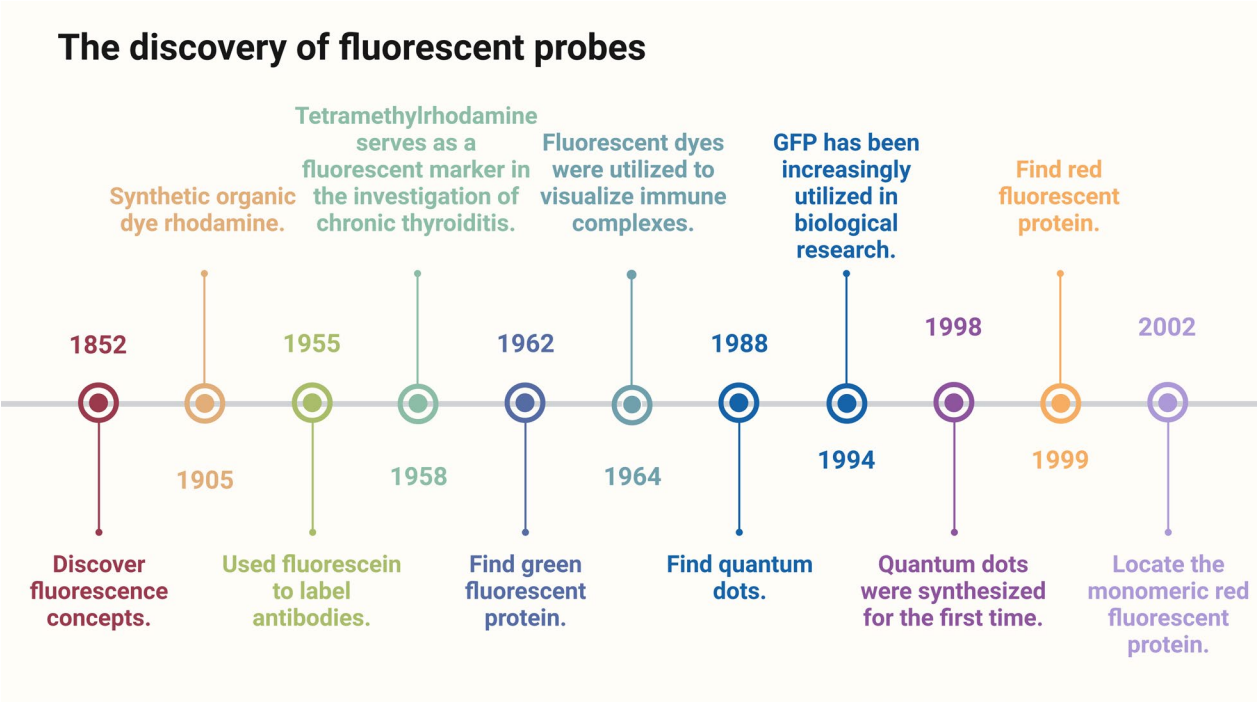

Fig. 1 Development history of fluorescent probes (Created in https://BioRender.com)

Principle of fluorescence probes

Fluorescent probes are typically composed of a fluorophore, a linking group, and a recognition group, with their fundamental principle based on the phenomenon of fluorescence [50]. When fluorescent probe molecules absorb light energy at a specific wavelength (usually ultraviolet or visible light), the excited electrons transition from the ground state to the excited state. Due to the instability of this high-energy excited state, electrons rapidly undergo non-radiative relaxation, converting to the lowest energy singlet excited state, a process known as internal conversion [51]. When electrons return from the excited state to the ground state, energy is released in the form of light, emitting at a longer wavelength than the excitation light, which results in fluorescence (Fig. 2a). The ratio of the number of emitted photons to the number of absorbed photons by a fluorescent probe is termed fluorescence quantum yield (FQY) [52], reflecting the efficiency with which the probe converts absorbed light energy into fluorescence. This parameter can be used to screen suitable fluorescent materials. Fluorescence lifetime, the average time a molecule spends in the excited state before returning to the ground state, is sensitive to the probe's

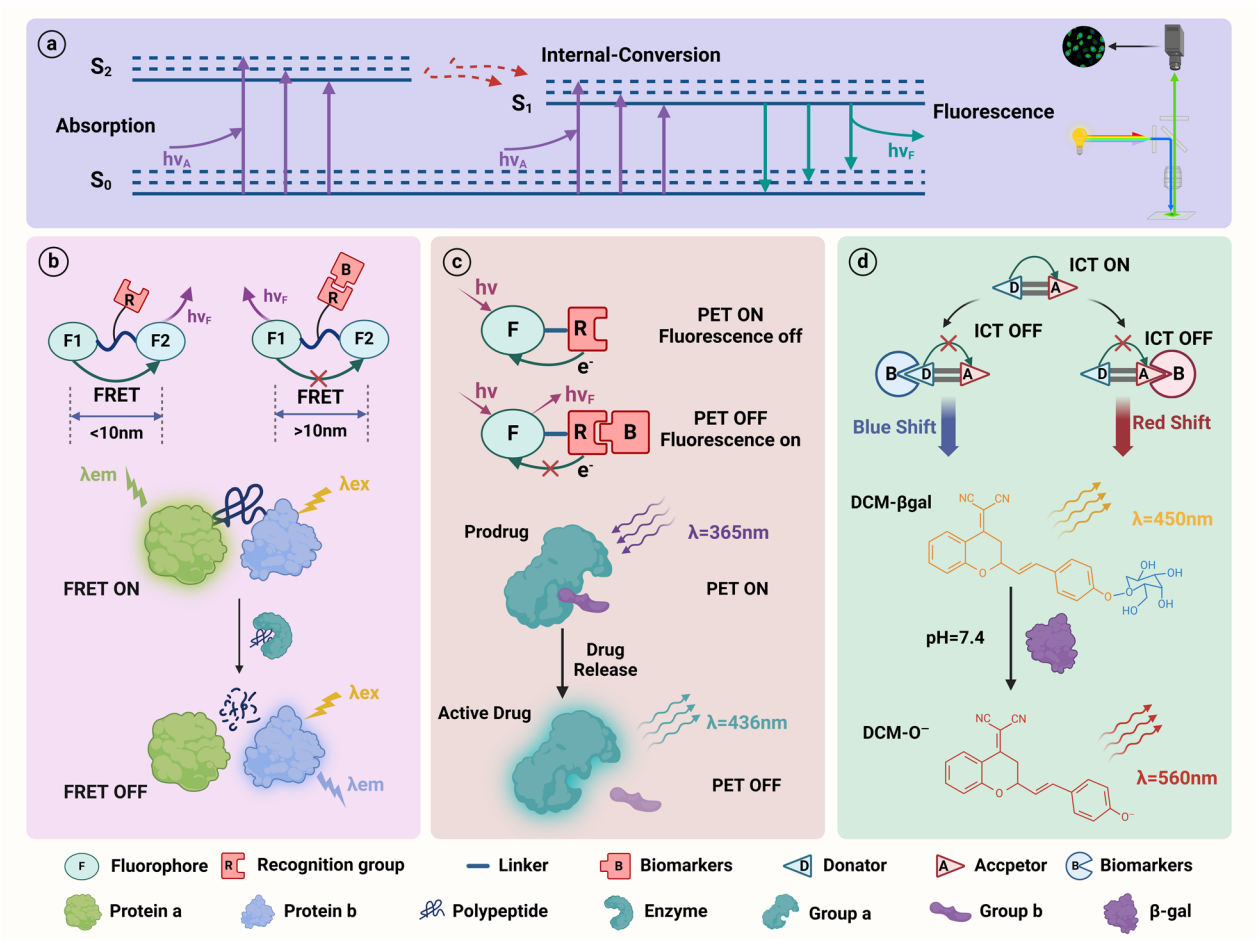

Fig. 2 Basic principle of fluorescence probe (Created in https://BioRender.com). **a** pattern of fluorescence excitation: When fluorescent molecules absorb light energy of a specific wavelength, excited electrons transition from the ground state S0 to the excited state S2. After internal conversion to S1, electrons can return to S0 and produce fluorescence. **b** FRET mechanism: One fluorescent molecule absorbs light energy and non-radiatively transfers this energy to another fluorescent molecule, resulting in a decrease in the fluorescence intensity of the donor and an increase in the fluorescence intensity of the acceptor [54]. The FRET mechanism can clearly detect interactions between proteins. **c** PET mechanism: Upon binding of the target molecule to the receptor, the PET process is inhibited, leading to the recovery of the probe's fluorescence [55]. The PET mechanism has significant importance in drug screening and efficacy monitoring [56]. **d** ICT mechanism: When the donor component interacts with a cation, the electron-donating properties of the probe diminish, causing a blue shift in the absorption spectrum. Conversely, when the acceptor component interacts with a cation, the absorption spectrum exhibits a significant red shift [57]. The ICT mechanism aids in monitoring biochemical processes such as enzyme-catalyzed reactions in vivo [58]

microenvironment and provides valuable information [53].

Fluorescent probes utilize various sensing mechanisms, including Förster Resonance Energy Transfer (FRET) [54], Photoinduced Electron Transfer (PET) [55, 56], and Intramolecular Charge Transfer (ICT) [57, 58]. FRET involves non-radiative energy transfer between two fluorescent molecules (Fig. 2b), while PET relies on electron transfer between the receptor and fluorophore (Fig. 2c). ICT refers to electron transfer within a molecule, leading to spectral shifts upon interaction with cations (Fig. 2d). These mechanisms enable probes to detect various targets and processes.

Types of fluorescence probes

Fluorescent probes are widely utilized across various fields, including biology, physiology, medicine, pharmacology, and environmental science. Depending on the excitation light source, they can be categorized as single-photon, two-photon, and multiphoton fluorescent probes. Based on the type of substances to be measured, they can be classified into metal ion fluorescent probes and biomolecule fluorescent probes. Furthermore, according to their structural characteristics, fluorescent probes can be divided into organic molecular dye probes, quantum dot probes, fluorescent protein probes, and other categories. In this article, we briefly introduce the main types of probes based on their structural features (Table 1).

Fluorescent organic dye

Fluorescent organic dyes are among the earliest and most widely used chemical assays and labeling agents for cells and tissues [59]. Commonly employed fluorophores include rhodamine, fluorescein, anthocyanins, and their derivatives, such as fluorescein isothiocyanate (FITC) and tetramethylrhodamine isothiocyanate (TRITC). These fluorescent dyes serve as common labels for various detection formats, characterized by their clear structures, low cytotoxicity, good biocompatibility, and high selectivity and sensitivity. Small organic fluorescent probes are favored for their strong emission, tunable wavelengths, and versatility in probe construction [60]. However, their application in the biomedical field has been somewhat restricted due to limitations such as rapid self-quenching, photostability issues, and poor water solubility [61, 62].

FITC, with good water solubility and biocompatibility [63], is widely used for protein localization [64], antibody labeling [65], and immunological research. In preclinical studies of rheumatoid arthritis, FITC has been used in the CAR system to eliminate autoreactive B cells [66]. However, FITC exhibits fluorescence quenching characteristics when its concentration varies [67]; thus, factors such as pH must be considered in probe design.

Rhodamine is a catechol-derived fluorophore comprising rhodamine B, rhodamine 6G, and rhodamine 123, with rhodamine B being the most commonly utilized. Rhodamine presents several advantages, including excellent photostability, a wide wavelength range, and a high fluorescence quantum yield [68]. However, some studies have indicated that rhodamine B can induce apoptosis in the hypothalamic cells of rats, disrupt hormonal balance, and may possess carcinogenic and teratogenic effects [69]. In 2022, Chen and colleagues developed a fluorescent probe named Probe 9, which incorporates both rhodamine and BODIPY fluorophores [70]. This probe exhibits low cytotoxicity and good biocompatibility, along with high selectivity and sensitivity for nitric oxide (NO) and glutathione (GSH), making it suitable for guiding the treatment of heart failure with preserved ejection fraction (HFpEF).

Quantum dots

In 1988, Mark A. Reed invented quantum dots [42], which are colloidal semiconductor nanocrystals that have become widely utilized nanomaterials due to their unique quantum effects. Compared to traditional organic dyes, quantum dots possess characteristics such as high brightness and strong photostability, providing high signal-to-noise ratio fluorescence for extended periods. They are extensively used in cell labeling, molecular tracking, and in vivo imaging, showcasing immense potential in biomedical diagnostics and therapies [71]. Quantum dots have a broad absorption spectrum, allowing for simultaneous or multiplex emission under a single light source, with emission wavelengths covering ultraviolet, visible light, and infrared. Their nanoscale size enables conjugation with multiple copies of dye molecules, resulting in high optical sensitivity and chemical stability. However, the preparation of quantum dots requires various reagents and involves complex steps, leading to variability in the composition of their final structures [72]. When applied to living cells or animals, quantum dots containing heavy metals exhibit cytotoxicity, potentially causing DNA damage, endoplasmic reticulum stress, mitochondrial dysfunction, and lysosomal rupture [73]. Additionally, oxidative stress and inflammatory responses can elicit toxic reactions from quantum dots, and these potential threats to human health limit their widespread application in the life sciences [73].

Coating ZnS shells onto the surface of ZnSe/CdS quantum dots can enhance their quantum yield and optical stability while reducing biological toxicity [74]. ZnSe/CdS/ZnS quantum dots exhibit high sensitivity in the quantitative determination of C-reactive protein, making

Table 1 Common types of fluorescent probes

Type	Fluorophore	Structure (From: https://pubchem.ncbi.nlm.nih.gov/)	Application	Feature	Deficiency	References
Organic dye probe	FITC	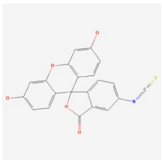	It is capable of binding to a diverse array of antibody proteins	Excellent water solubility and biocompatibility	The characteristics of fluorescence quenching are influenced by concentration	[67, 87]
	Rhodamine B	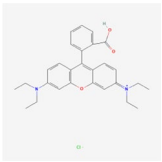	Monitoring acidic organelles such as lysosomes with a pH range of 4.5–5.5	Water-soluble and high fluorescence under acidic conditions	Carcinogenic and teratogenesis	[82]
	Rhodamine 6G	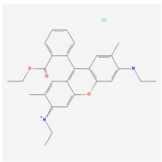	PH-sensitive probe. It can measure the intracellular glutathione content	High stability and water-soluble	Carcinogenic and teratogenesis	[88–90]
	Rhodamine 123	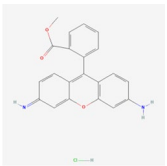	Monitoring intracellular H_2O_2 and mitochondrial membrane potential	Good cell permeability	The staining effects are influenced by cell type and status	[91, 92]
	Fluorescein	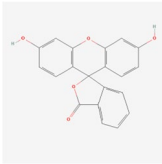	Detection of metal cations, various anions, small molecules such as amino acids, and biological macromolecules such as enzymes	Good biocompatibility and high sensitivity	Photobleaching; Influenced by experimental conditions	[83]
	Coumarin	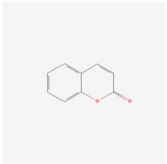	Detection of metal ions, pH, biological small molecules, and cellular microenvironments	Good solubility, large stokes shift and widely applicable	Fluorescence quenching occurs under acidic conditions	[93]

Table 1 (continued)

Type	Fluorophore	Structure (From: https://pubchem.ncbi.nlm.nih.gov/)	Application	Feature	Deficiency	References
Quantum dots	Carbon quantum dots		Drug delivery, cancer therapy, bioimaging, photothermal therapy, photodynamic therapy, and biosensors, etc	Photostability, low toxicity, high water solubility, and conductivity	Complex preparation	[85]
	CdTe quantum dots	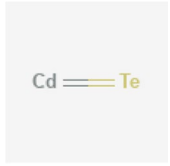	Bioimaging, drug delivery, and cellular labeling	Relatively strong fluorescence intensity; small volume; Photostability	Influenced by pH value	[94]
	InP quantum dots		Cellular imaging	Low cost; Low toxicity, good biocompatibility, and excellent photochemical stability	Surface oxidation defects	[84]
Fluorescent protein	GFP		Protein fusion, subcellular localization, cellular visualization, protein–protein interactions, and gene-encoded sensors	Low phototoxicity and convenient for intracellular expression	Larger molecular weight and can induce DNA damage	[86]
	Red fluorescent probe		Protein fusion expression and intracellular redox imaging	Lower autofluorescence, low phototoxicity, and high quantum yield	Photobleaching and oligomerization	[95, 96]

them suitable for the early detection of infections and autoimmune diseases. In recent years, carbon-based quantum dots have garnered considerable research attention due to their excellent biocompatibility and low toxicity [75]. Studies have shown that carbon quantum dots can alleviate dysregulated immune processes in a non-obese diabetic mouse model of Sjögren's syndrome, potentially mitigating the apoptosis of submandibular gland epithelial cells in patients during the early stages of the disease [76].

Fluorescent proteins

Fluorescent proteins were originally derived from marine organisms such as jellyfish, corals, and sea anemones. In 1962, Shimomura and colleagues first discovered green fluorescent protein in Aequorea Victoria [77]. Fluorescent proteins can be categorized into green fluorescent proteins and their derivatives, red fluorescent proteins and their derivatives, and near-infrared fluorescent proteins [78]. These proteins possess the capability for imaging in live cells and are extensively employed to monitor dynamic changes in proteins within tissues and organisms, as well as to observe cell behavior. Their spectral characteristics cover a wide range, providing advantages for multicolor imaging. However, green fluorescent proteins, when excited, can generate singlet oxygen, which induces significant DNA damage in cells expressing the fusion proteins, leading to shrinkage, aggregation, and apoptotic cell death [79]. Additionally, fluorescent proteins exhibit issues such as photobleaching and low light stability, which limit their reliability as tools for biological applications [80]. Therefore, in practical applications, researchers must consider these potential drawbacks to optimize the use of fluorescent proteins.

A radar chart (Fig. 3e) illustrates the performance of four types of probes: organic dyes, quantum dots, fluorescent proteins, and nanoparticle carriers, clearly delineating the advantages and disadvantages of each type. Organic dyes demonstrate high sensitivity and specificity, exemplified by the dynamic quenching constant Ksv = 9.8L/mol for FTIC, indicating low sensitivity to quenching agents. However, they are susceptible to photobleaching, and the emission wavelength of FITC shifts red to 491 nm, which may influence penetration depth [67]. Quantum dots exhibit the highest quantum yield (nearly 90%) and outstanding sensitivity, and their photostability is remarkable, with minimal photobleaching. Nevertheless, their biocompatibility is relatively low; this issue has been mitigated by employing a ZnS outer shell to reduce toxic cadmium exposure [74]. Quantum dots provide good tissue penetration depth but are costly and involve complex synthesis processes. Fluorescent proteins display exceptional biocompatibility due to their natural, non-toxic composition, allowing for direct expression in cells without exogenous labeling. They also possess high sensitivity, and gene-editing capabilities confer considerable specificity, although their cost warrants consideration. The sensitivity of nanoparticle carriers varies by material, and their specificity is akin to that of quantum dots. They demonstrate favorable biocompatibility; for example, the cell survival rate of psi-tGC-NPs exceeds 80%, while the hemolysis rate remains below 5% [81]. It is important to note that the diversity of nanoparticle materials may lead to a broader range of performance variations.

Fluorescent probes are essential tools in biomedical research, and their diverse classification reflects the specific needs of various application scenarios. Based on differences in excitation light sources, target substances, and structural characteristics, fluorescent probes can be subdivided into multiple types (Fig. 3), each with its own advantages and limitations. Among organic dyes, despite their high biocompatibility and selectivity, issues such as photobleaching and poor water solubility still limit their application in long-term imaging. Quantum dots, on the other hand, demonstrate broad potential for cell labeling and molecular tracking due to their excellent photostability and multiplex emission capabilities; however, their potential heavy metal toxicity and complex synthesis processes present challenges for clinical applications. The emergence of fluorescent proteins offers new possibilities for live cell imaging; however, the risks of photobleaching and DNA damage necessitate careful consideration of their use. In the study of autoimmune diseases, selecting appropriate fluorescent probes is crucial. Researchers should comprehensively evaluate the optical characteristics, biocompatibility, and potential cytotoxicity of the probes to optimize experimental design and enhance imaging effectiveness.

Application of fluorescent probes in the study of different autoimmune diseases

Systemic autoimmune diseases

Systemic autoimmune diseases represent a class of disorders marked by the aberrant activation of the immune system, which results in the extensive assault of self-antibodies and inflammatory mediators on multiple organs and tissues. Key characteristics of these diseases include the production of autoantibodies, such as ANA, and involvement of various organ systems. Common manifestations include RA, SLE, and MS. The incidence of RA may be as high as 0.5% [97], while the global incidence of SLE ranges from approximately 20–150 cases per 100,000 individuals [98]. Clinical presentations are complex and diverse, often commencing with nonspecific systemic symptoms (e.g., fever and fatigue) in the initial stages,

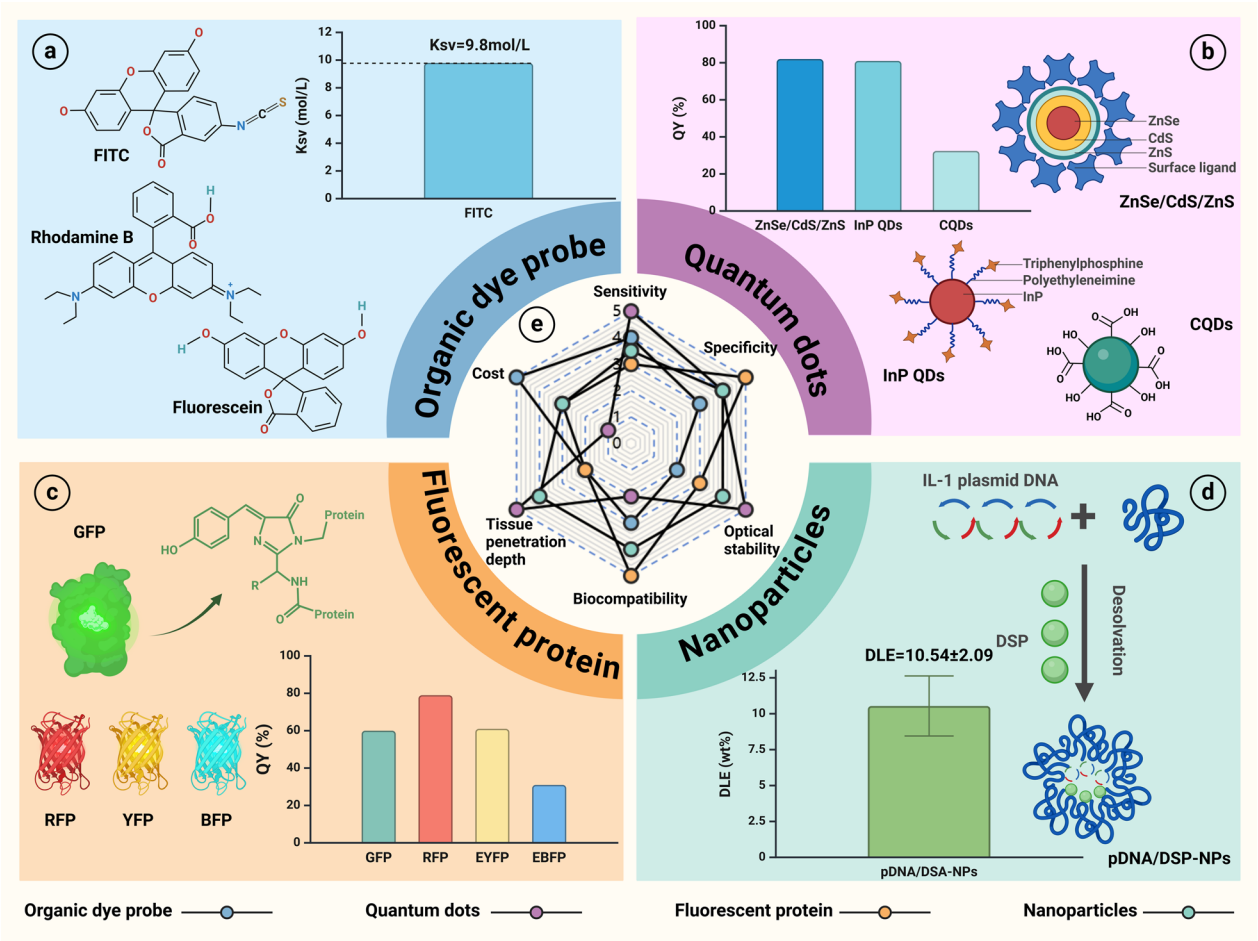

Fig. 3 Comparison of different types of fluorescent probes (Created in https://BioRender.com) **a** Organic dye probe: Chemical structures of FITC [67], rhodamine B [82] and fluorescein [83]. The bar graph indicates that FITC has a low sensitivity to the quencher (Ksv = 9.8L/mol), suggesting its high stability in complex environments [67]. **b** Quantum dots: Schematic representation of ZnSe/CdS/ZnS, InP QDs and CQDs structures. The bar graph compares the quantum yield (QY) of different quantum dots (ZnSe/CdS/ZnS QY = 82% [74], InP QDs QY = 81% [84], CQDs QY = 32.4% [85]), demonstrating their excellent optical stability. **c** Fluorescent protein: Schematic representation of GFP chemical structure and RFP, YFP, and BFP structures [86]. The bar graph compares the quantum yield (QY) of various fluorescent proteins (GFP QY = 60%, RFP QY = 79%, EYFP QY = 61%, EBFP QY = 31% [86]), proving their good optical stability. **d** Nanopariticles: Schematic diagram of pDNA/DSP-NPs preparation. It exhibits a very high drug loading capacity, with a drug loading efficiency (DlE) of up to 10.54 ± 2.09 wt% [81]. **e** Based on the design characteristics of probes in the literature and practical application scenarios, a radar chart compares the performance of organic dyes, quantum dots, fluorescent proteins, and nanoparticles across six key performance indicators (such as sensitivity, specificity, optical stability, biocompatibility, tissue penetration depth, and cost)

which subsequently progress to multi-organ damage. For example, RA is characterized by symmetrical joint swelling and deformities [99] and SLE manifests with butterfly-shaped rashes, lupus nephritis, and hematological abnormalities [100], thereby significantly increasing patient mortality risk.

Rheumatoid arthritis (RA)

Abnormal activation of T cells and B cells plays a central role in the pathogenesis of RA, and their accumulation in the synovium can trigger a persistent inflammatory response. Consequently, fluorescent probes that specifically detect T cells or B cells hold significant potential for the non-invasive diagnosis of RA. Figure 4 provides a detailed visualization of fluorescent probes targeting different immune cells and inflammatory in RA, highlighting their potential for early diagnosis and disease monitoring. The CD molecules on the surfaces of T cells and B cells serve as specific targets for labeling. For instance, methods such as labeling with FITC against CD4 and using r-phycoerythrin (PE) to label CD39 can be employed to observe the frequency and phenotypic changes of regulatory T (Treg) cells in RA patients [101]. By staining with monoclonal CD3-FITC and CD26-PE,

the percentage of activated T cells in peripheral blood can be analyzed to assess disease activity [102]. Furthermore, targeting molecules that induce T cell activation is also an important strategy. For example, fluorescently labeling CD1c + myeloid dendritic cells (mDCs) in synovial fluid (SF) can indicate their ability to induce the proliferation of CD4 + T cells [103]. Using MR1-5-OP-RU tetramers to detect changes in mucosal-associated invariant T (MAIT) cells can aid in diagnosing early untreated RA patients [104]. The IRDye-680RD-OX40 monoclonal antibody (mAb) probe exhibits high sensitivity and specificity for OX40, achieving an area under the curve (AUC) of 1.0 in the receiver operating characteristic (ROC) curve constructed using the ratio of RP to LP fluorescence intensity. This finding indicates that the probe can effectively differentiate between the RA model and the healthy control group, and it can be utilized to detect T cell activation in early RA tissues, demonstrating notable predictive potential (Fig. 4b) [105]. Additionally, IRDye-680RD-4-1BB mAb fluorescent probes can track 4-1BB + activated T cells in vivo for the non-invasive diagnosis of RA [106]. Fluorescent labeling of B cells provides a valuable method for diagnosing RA. Following intra-articular injection of anti-CD20 antibodies conjugated with Cy5 fluorescent dye, the signal intensity (representing B cell density) within the lesions was observed to be 3.2 times higher than that in normal tissue ($p < 0.001$), highlighting the distribution of B cells in plasma and lymphatic fluid (Fig. 4c) [107]. Fluorescein-labeled antigens targeting CD80, CD24, and CD21 can visualize the autoreactivity of B cells [108]. Labeling with FITC against CD38, PE against CD27, and APC against CD19 can categorize B cell subsets, with their percentages serving as early diagnostic indicators for RA [109].

The primary feature of RA is the immune regulatory imbalance within the joint synovium, where disruption of cytokine and chemokine pathways promotes persistent inflammation in the joints. Numerous cytokines play critical roles in the pathological processes of RA (Table 2), and understanding their functions and mechanisms provides essential insights for the diagnosis and treatment of this condition. By labeling cytokines with fluorescent probes, new pathways for monitoring and diagnosing RA can be established, significantly enhancing diagnostic efficiency and therapeutic outcomes. In addition to the labeling and detection of individual cytokines, novel fluorescent probes have also been developed for the simultaneous detection of multiple cytokines. For example, multiplex antibody chips and the Quantibody Human Inflammatory Array 1 can detect a variety of cytokines, including IFN-γ, IL-1α, IL-1β, IL-4, IL-6, IL-8, IL-10, IL-13, MCP-1, and TNF-α [110]. Li et al. designed a multi-molecular fluorescent probe composed of three fluorescent molecules and one dangling single-chain domain, which significantly enhances the fluorescent signal and enables accurate quantification of cytokines under complex conditions [111]. Its high sensitivity allows for the clinical diagnosis of low-concentration biomarkers, providing a powerful tool for the early clinical diagnosis of RA.

Visualizing pathological changes in RA joint tissue is crucial for the early diagnosis of the condition. The near-infrared ratio fluorescent probe, Ratio-A, is composed of an enhanced rhodamine scaffold, which exhibits a linear relationship between the logarithm of its fluorescence intensity($lg(F_{564}nm/F_{700}nm)$) and $ONOO^-$ concentration(0-10 μM) ($y = 0.2221x - 0.4495$, $R^2 = 0.9931$). This relationship facilitates real-time monitoring of the intracellular fluctuations of $ONOO^-$ in mouse ankle joint tissues (Fig. 4d) [123]. These probes demonstrate high selectivity and low detection limits, underscoring their potential in RA diagnosis. Nanobody 119 (Nb119), labeled with Alexa Fluor 647, exhibits significant signal intensity in macrophages of inflamed joint synovium,

(See figure on next page.)

Fig. 4 Comparison of probes for different targets of RA (Created in https://BioRender.com) **a** Pathogenesis of RA: The pathogenesis of RA involves the presentation of autoimmune antigens by APC, which activate T cells and initiate an immune response. Additionally, activated B cells, macrophages, synovial fibroblasts, and various inflammatory mediators play significant roles in this process [97]. **b** T cell targets: A schematic diagram of the detection of activated T cells in early RA tissues using IRDye-680RD-OX40 mAb. The ROC curve constructed using the RP/LP fluorescence intensity ratio achieved an AUC of 1.0, indicating that the probe can completely discriminate between the collagen-induced arthritis model (CIA) and the healthy control group, demonstrating high sensitivity and high specificity (redrawn based on data from the literature [105]). **c** B cell targets:A schematic diagram of the distribution of B cells using Cy5-labeled anti-CD20 antibodies. Immunofluorescence images: Left: healthy control group (few blue fluorescent spots); Right: RA model group (a large number of green fluorescent spots, clustered in the synovial area of the joint). It indicates that the density of B cells in the lesion area is 3.2 times higher than that in the healthy group ($p < 0.001$). (Redrawn based on data from the literature [107].) **d** Small molecule targets: A schematic diagram for the quantitative monitoring of $ONOO^-$ using Ratio-A. The curve graph demonstrates a linear relationship between the logarithm of fluorescence intensity and $ONOO^-$ concentration (0-10 μM) ($y = 0.2221x - 0.4495$, $R^2 = 0.9931$), intuitively showing the high sensitivity and linear response of Ratio-A to $ONOO^-$ (redrawn based on data from the literature [123]). **e** Cytokine targets: A schematic diagram of TNF-α gene silencing using psi-tGC-NPs. The bar graph shows that both the MTX group ($P < 0.01$) and the psi-tGC-NPs group ($P < 0.05$) significantly inhibit the expression of TNF-α mRNA. This intuitively reflects the potential of the nanoparticle delivery system in gene silencing, comparable to the efficacy of MTX (redrawn based on data from the literature [133])

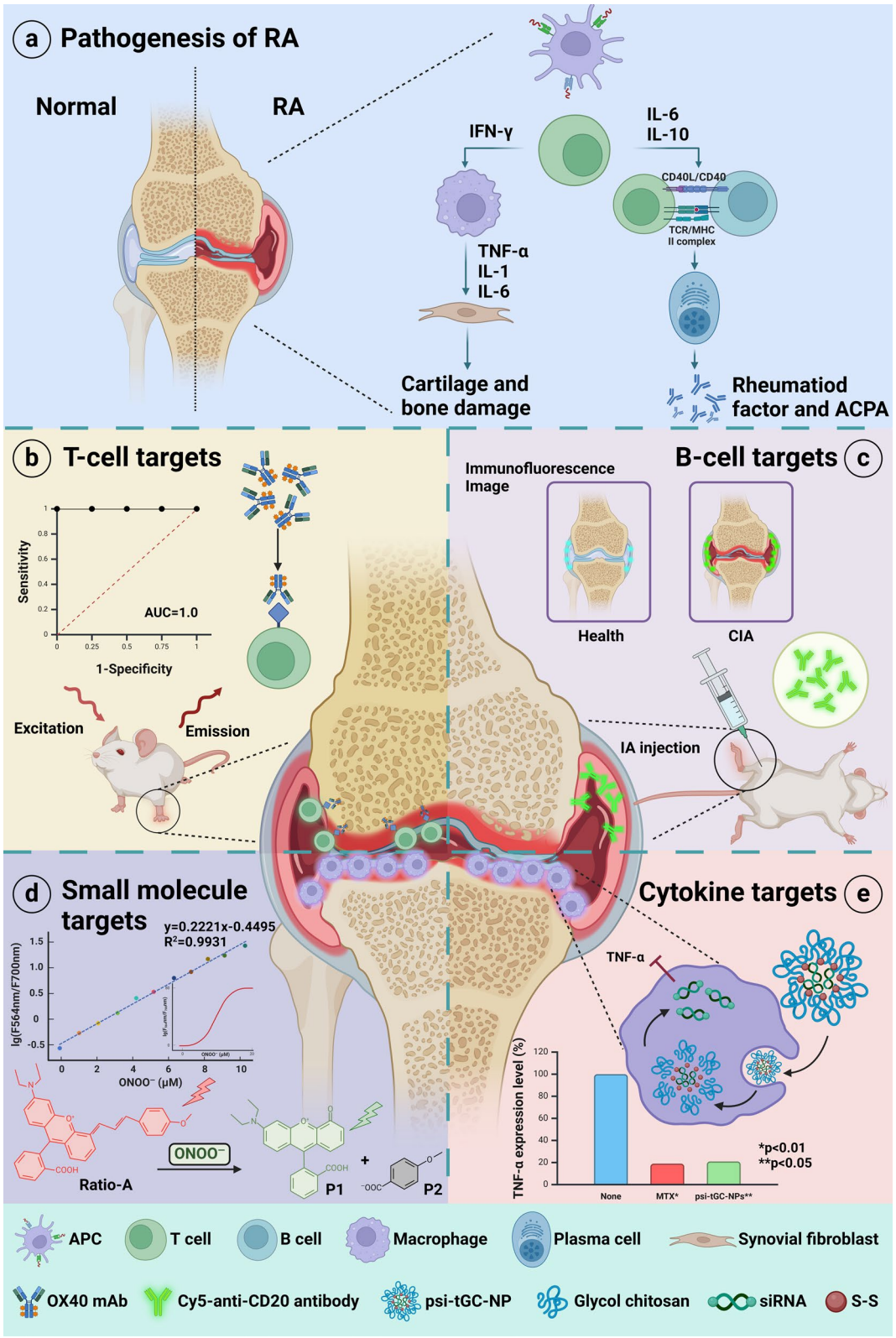

Fig. 4 (See legend on previous page.)

Table 2 Cytokines involved in the pathogenesis of RA that can be detected by fluorescence

Cytokines	Source	Function	Detection method	Main distribution position	References
IL-1	Macrophages, monocytes, and dendritic cells	Stimulates the production of RANKL, which is involved in osteoclastogenesis, and matrix metalloproteinases (MMPs) that are involved in cartilage degradation	DAB reagent conjugated with IL-1R antibody	In bone, cartilage, and joint synovial fluid	[112]
IL-6	Produced by almost all stromal cells and immune cells	Mediates the differentiation of fibroblasts into rheumatoid arthritis-fibroblast-like synoviocytes (RA-FLSs), and excessive production can promote disease progression and chronicity	After labeling with IL-6 antibody, staining with Alexa Fluor 488 conjugate or fluorescein-labeled vector	In synovial fluid	[113, 114]
IL-10	T cells, B cells, and macrophages	Inhibits cytokine production and affects cytokine balance	Hybridizing IL-10 gene nucleotide 1082 through gene-specific fluorescent-labeled probes	In the serum of patients	[115]
IL-17	Th17 and other T cells	Works synergistically with other cytokines to activate synoviocytes and induce cytokine production, leading to chronic inflammation	Staining with anti-IL-17-PE or anti-IL-17-PerCP-Cy5.5 labeled antibodies	Synovial membrane	[116]
IL-18	Macrophages, dendritic cells, and epithelial cells	The upregulation of endothelial cell adhesion molecules, the release of chemokines from synovial fibroblasts, and the direct action as a chemotactic agent for monocytes, lymphocytes, and neutrophils collectively induce leukocyte extravasation	Anti-IL-18 labeling and fluorescein staining	Aberrantly high expression in synovial tissue and synovial fluid	[117]
IL-20	Activated monocytes and dendritic cells	Promotes neutrophil chemotaxis, induces synovial fibroblasts to produce IL-6 and IL-8, and activates the migration of synovial fibroblasts, as well as the proliferation of endothelial cells and the expansion of osteoclasts	Following anti-IL-20 labeling, staining is performed using Alexa 488	Relatively abundant in the intima and sublayer of the synovial membrane	[118]
IL-40	Neutrophils and activated B cells	Elevated levels are associated with disease activity, autoantibodies, and the externalization of neutrophil extracellular traps (NETosis)	Following anti-IL-40 labeling, staining is performed using STAR 580	In the serum of early RA patients	[117]
TNF-α	Monocytes, macrophages, and certain T cells	Induces synovial cells from patients to produce IL-6, coordinates tissue recruitment and the survival of inflammatory immune cells, and promotes tissue destruction	Anti-Infliximab and certolizumab antibody-modified elongated gold nanorods	Within the synovial membrane	[119]

Table 2 (continued)

Cytokines	Source	Function	Detection method	Main distribution position	References
Vascular endothelial growth factor A (VEGFA)	Vascular endothelial cells, macrophages, and smooth muscle cells	Inducing angiogenesis is positively correlated with the levels of inflammatory markers, including C-reactive protein (CRP), erythrocyte sedimentation rate(ESR), MMP-3, and TNF-α, as well as disease activity	Luminex-based fluorescent bead assay system, or the addition of Cy5-labeled 5′-amino ssDNA probes to the surface of Mn-ZIF-NPs	Peripheral blood and synovium	[120, 121]
Granulocyte-monocyte colony-stimulating factor (GM-CSF)	Synovial stromal cells and subglial macrophages	This process involves down-regulating the elevated expression of CD90 + FAP + synovial fibroblasts, CD90 + activated endothelial cells, and CD163 + macrophages across various types of arthritis	Conjugation of anti-GM-CSF antibody with a fluorescent dye	In synovial fluid and blood	[122]

allowing for the production of a targeted nanobody, Cy7-Nb119, which binds to the V-set and Ig domain 4 (Vsig4) present on synovial macrophages [124]. This labeling technique enables high-contrast rapid imaging within three hours, indicating its promise for arthritis monitoring. Fluorescently labeled Cy3-tilmanocept generates notable fluorescence in mouse knee and elbow joints, demonstrating its effectiveness in the early detection of in vivo inflammation associated with RA [125]. Beyond fluorescent probes targeting synovial macrophages, the visualization of RA's pathological structures can also be accomplished by targeting joint bone and cartilage tissues. The LS301 fluorescent probe selectively accumulates within the cartilage cells of arthritic joints, with fluorescent signal intensity positively correlated to disease severity, signifying its potential application in RA monitoring [126]. Fluorescent probes that bind to the integrin αvβ3 receptor effectively target inflamed joints with high sensitivity and accuracy [127]. Probes such as C700-OMe and P800SO3 enable clear differentiation between cartilage and bone tissues within the same individual, facilitating real-time dual-channel fluorescent imaging [128]. This approach provides visual evidence for assessing the severity of inflammation and disease progression. Through the use of tissue-specific fluorescent probes, it is feasible to visualize pathological changes in inflammatory tissues with high sensitivity and resolution, utilizing a safe, non-invasive method that offers a novel perspective for RA detection.

Timely and effective treatment of diseases is crucial for improving the prognosis of RA. Methotrexate (MTX) is currently one of the first-line treatment drugs for RA; however, its systemic side effects limit its long-term use. Consequently, achieving targeted drug delivery and real-time monitoring of therapeutic effects has emerged as a significant research focus. Experiments have demonstrated that MTX can enhance the activity of Treg cells by increasing adenosine production, and a fluorescently labeled anti-CD39 ATP probe has been shown to predict the therapeutic effects of MTX [129]. The fluorescent probe Probe-2, developed by Feng et al., can rapidly respond to and monitor dynamic changes in HOCl in vivo and in vitro, providing a novel tool for early evaluation of MTX efficacy [130]. In addition to real-time monitoring of drug efficacy to mitigate adverse reactions, employing targeted drug delivery systems to specific cells or tissues has significantly reduced the toxicity of MTX. Single-walled carbon nanotubes (SWCNTs) synthesized from high-pressure carbon monoxide (HiPco) and carboxyl-functionalized SWCNTs (carboxyl-SWCNTs) can function as effective drug carriers. SWCNTs loaded with siRNA/MTX selectively accumulate in arthritic joints and interact with monocytes and neutrophils in a dose-dependent manner, thereby reducing drug toxicity, prolonging the drug's half-life, diminishing immunogenicity, and enhancing bioavailability [131]. By encapsulating MTX with indocyanine green (ICG) fluorescent probes in iRGD peptide-modified echogenic liposomes (iELPs), efficient targeted accumulation can be achieved, enabling controlled release through near-infrared fluorescence imaging and ultrasound triggering [132]. In addition to MTX, therapies targeting specific cytokines also exhibit therapeutic potential. The siRNA nanocomplex (poly-siRNA), composed of thiolated polyethylene glycol-chitosan (tGC) targeting TNF-α and labeled with the dye Flamma FPR-675, can accumulate at the site of the joint. Treatment with psi-tGC-NPs (100 nmol/L) resulted in a 78% inhibition of TNF-α expression, demonstrating efficacy comparable to that of MTX (Fig. 4e) [133]. The combination of IL-10 pDNA with the chemotherapy drug dexamethasone sodium phosphate (DSP), incorporated into human serum albumin (HSA), results in pDNA/DSP nanoparticles that target macrophages in synovial tissue [81]. This combination can be labeled with a red cell membrane fluorescent probe, showcasing advantages such as high drug loading capacity, real-time imaging, and no liver toxicity, thereby underscoring the application potential of fluorescent probes in the treatment of RA.

Systematic lupus erythematosus (SLE)

The formation of autoantibodies and immune complexes (ICs) plays a significant role in the pathogenesis of SLE [134]. ANA serve as key biomarkers for the diagnosis of SLE and are an essential component of its classification criteria [135]. Immunofluorescence testing using human epithelial cell tumor (HEp-2) cells is considered the gold standard for ANA detection [136]. The International Consensus on ANA Patterns (ICAP) categorizes 30 distinct HEp-2 indirect immunofluorescence assay (IFA) patterns into four major groups: negative, nuclear fluorescence patterns, cytoplasmic fluorescence patterns, and mitotic fluorescence patterns [137]. SLE is associated with patterns AC-1, AC-4, AC-5, AC-13, AC-19, AC-24, and AC-26, and the clinical relevance of these patterns has become a focus of research in recent years [138]. Studies have found a positive correlation between ANA levels in saliva and serum ANA titers, suggesting the potential for a non-invasive alternative to blood tests [139]. This provides a new strategy for developing targeted fluorescent probes for autoantibodies. In addition to ANA, other fluorescence labeling techniques targeting autoantibodies are also extensively explored. Fluorescently labeled caspase-1 inhibitor probes can illuminate the relationship between autoantibodies and disease activity [140]. Other techniques, such as using

fluorescently labeled TaqMan probes, enhance the diagnostic performance of autoantibodies in identifying SLE [141]. By introducing fluorescently labeled cells into nanopores, B cells producing anti-SSA/Ro and anti-SSB/La antibodies—and their secretion levels—can be simultaneously detected to assess disease activity [142]. The quantification of immune complex deposition in SLE mice using Alexa Fluor 594-conjugated IgG provides a basis for the diagnosis of SLE [143]. Additionally, using FITC staining for autoantibodies enables visualization of immune complex deposition in glomerular basement membranes, facilitating the diagnosis of lupus nephritis [144]. These fluorescent labeling methods provide a vital technical foundation for developing targeted fluorescent probes for ICs and point towards new directions for early diagnosis and disease monitoring in SLE.

LN represents a subtype of glomerulonephritis and significantly influences the morbidity and mortality rates associated with SLE [145]. Approximately 50% of patients with SLE are likely to develop LN, rendering it one of the most severe organ manifestations of the disease [146]. Early and accurate diagnosis of LN is thus crucial for enhancing the prognosis of SLE patients. Percutaneous kidney biopsy remains a commonly utilized method in the assessment of renal diseases, providing precise diagnostic information. However, this procedure may lead to complications, such as bleeding [147], and has limitations in terms of treatment guidance and prognosis prediction in patients with LN [148]. As a result, the development of non-invasive diagnostic fluorescent probes for LN presents considerable clinical significance. Takuji et al. designed an activatable fluorescent probe, gGlu-HMRG, which facilitates the clear identification of the renal cortex in kidney biopsy specimens by quantifying fluorescence intensity [149]. This demonstrates the potential applications of fluorescent probes in clinical nephrology. Furthermore, Tang et al. employed small molecule amino acids to create a lysosome-targeted two-photon fluorescent probe, Cys-j, which effectively visualizes cysteine levels in renal diseases [150]. This probe demonstrates adequate depth of penetration, making it a promising tool for the imaging diagnosis of kidney disorders. A characteristic feature of LN is the accumulation of polyclonal immunoglobulin G (IgG) in various regions of the glomeruli. Edwin et al. observed IgG deposition in the glomerular mesangium, subendothelial, and subepithelial regions using immunofluorescence probes [151]. Additionally, they measured the thickness of the kidney basement membrane, thereby facilitating rapid imaging for detecting the ultrastructure of glomeruli. This enhances the classification of lesion stages and contributes to a deeper understanding of the mechanisms of renal tissue damage, as well as the early diagnosis of the disease.

Skin manifestations are often the initial indicators of SLE [152], including butterfly-shaped erythema on the cheeks [153] and scarring alopecia [154]. Cutaneous lupus erythematosus (CLE) is an autoimmune skin disease characterized by diverse clinical presentations, which may either reflect one of the many clinical manifestations of SLE or occur as an independent skin condition, exhibiting an incidence rate double that of SLE [155]. As the disease progresses, CLE may evolve into SLE, with the average duration from the diagnosis of skin disease to the development of systemic disease being approximately eight years [156]. Early and accurate identification of CLE is crucial for effective treatment and improved prognosis. The lupus band test (LBT) [157] performed on lesional skin can reveal the deposition of IgM, IgG, and C3 at the dermal–epidermal junction [158], which aids in distinguishing between various CLE subtypes and is of significant importance for CLE diagnosis. Additionally, the LBT, in conjunction with monitoring anti-chromatin responses and complement levels, can predict the transition from CLE to SLE [159]. The use of ex vivo confocal laser scanning microscopy facilitates simultaneous histopathological and immunofluorescent examinations of CLE, significantly enhancing diagnostic efficiency [160]. Ultraviolet (UV) exposure serves as a critical trigger for CLE, leading to keratinocyte apoptosis and the activation of immune responses [161, 162]. Utilizing fluorophore derivatives to stain keratinocytes enables real-time monitoring of their dynamic changes and tracking of disease progression [163]. Katsuyama et al. developed a fluorescent probe, Fluo-4AM, for detecting intracellular calcium levels in keratinocytes to assess the impact of UV exposure on cellular function, thus providing new insights into the diagnosis of CLE [164]. While fluorescent probes can enhance detection sensitivity, they may also influence keratinocyte functions and induce cytotoxicity [165]. Therefore, the development of efficient and biocompatible fluorescent probes remains a significant challenge in the field of CLE diagnosis.

In the pathogenesis of SLE, the destruction of central and peripheral immune tolerance mechanisms leads to abnormal apoptosis of B cells, resulting in the production of autoreactive B cells and pathological autoantibodies that induce autoimmune responses [166]. Abnormal expression of the Fas/FasL signaling pathway may impede the apoptosis process [167], while a decreased clearance function of apoptotic cells further fosters the occurrence of autoimmune responses [168]. These mechanisms indicate that the development of probes targeting

cell apoptosis provides novel approaches for the diagnosis and monitoring of SLE. MicroRNA-21 (miRNA-21) and caspase-3 are key signaling molecules within the apoptosis pathway. Fluorescent probes targeting apoptosis, such as dsDNA-AuNP-pep [169], allow for real-time monitoring of this process in SLE. Other probes, like TBCI [170] and PPCN [171], can distinguish cellular states during apoptosis. Additionally, fluorescent probes targeting metal ions, such as Zn^{2+}, including SPI [172] and DCSH [173], can visualize changes in ion concentrations during apoptosis, providing significant non-invasive examination tools for visualizing the progression of SLE. The application of these probes not only enhances the sensitivity of detecting apoptosis but also establishes a technical foundation for precise diagnosis and dynamic monitoring of SLE.

Other systemic autoimmune diseases

Sjogren's syndrome (SS) is primarily characterized by the autoimmune destruction of salivary and lacrimal glands, resulting in dry mouth and dry eyes [174]. A polarity-sensitive fluorescent probe, DIM, exhibits increased fluorescence intensity with heightened polarity, which can be employed to monitor changes in the polarity of the submandibular gland, aiding in the diagnosis of salivary gland abnormalities [175]. The novel near-infrared organic fluorescent probe CyA-B2 facilitates highly effective in vivo imaging of the vascular endothelial layer [176]. This probe integrates a three-dimensional vascular model with a Diversity-Oriented Fluorescent Library (DOFL) screening strategy, overcoming the limitations of conventional targeted probe development and offering a robust tool for the dynamic investigation of autoimmune vasculitis.

Organ-specific autoimmune disease

Organ-specific autoimmune diseases constitute a category of disorders characterized by the aberrant targeting of specific organs or tissues by the immune system, primarily mediated by self-antibodies or T cells that cause localized damage. Common examples include multiple sclerosis, type 1 diabetes, inflammatory bowel disease, pemphigus, myasthenia gravis, autoimmune hepatitis, idiopathic pulmonary fibrosis, psoriasis, autoimmune myocarditis, Sjögren's syndrome, and autoimmune thyroiditis. The etiology of these diseases is frequently unknown, presenting a subtle onset and a chronic course characterized by recurrent and persistent symptoms. Clinical manifestations predominantly involve functional impairments in the target organs, such as visual disturbances and motor ataxia in multiple sclerosis [177], the classic "three polys and one less" symptoms in type 1 diabetes [178], erythematous plaques in psoriasis, and myasthenic crisis in myasthenia gravis. Diagnosis relies on specific antibody assays, imaging modalities, and histopathological examination; however, current methods possess substantial limitations, including fluctuating disease symptoms, elevated risks associated with invasive procedures, inadequate sensitivity of antibody tests, and disease heterogeneity, underscoring an urgent need to develop novel diagnostic strategies to improve diagnostic accuracy.

Multiple sclerosis (MS)

MS is a T cell-mediated autoimmune disease characterized by the immune system mistakenly attacking its own tissues, resulting in inflammation and demyelination [179]. A comprehensive understanding of T cell behavior and function in the central nervous system can enhance the diagnosis of the disease and inform the development of treatment strategies. By utilizing GFP-labeled myelin basic protein (MBP)-specific T cells, in vivo imaging facilitates the monitoring of brain autoantigen-specific T cell behavior before the onset of disease symptoms, thereby allowing for the formulation of more targeted treatment plans [180]. Employing two-photon microscopy to observe GFP and TdTomato-labeled Treg cells in conjunction with Th17 cells enables a systematic comparison of cell behavior and activation status, elucidating the cellular mechanisms by which T cells inhibit spinal cord neuroinflammation [181]. By visualizing the relationship between immune cell distribution and disease progression, this research contributes to the development of more precise therapeutic intervention strategies.

Oligodendrocytes are responsible for forming myelin around neuronal axons [182]. In MS, peripheral immune cells cross the blood–brain barrier and release various cytokines that attack oligodendrocytes, leading to their death and subsequent demyelination [183]. The utilization of the chromis-1 probe to visualize changes in intracellular Zn^{2+} levels in oligodendrocytes allows for the identification of their developmental stages, providing new insights for the diagnosis of MS [184]. Phospholipid fragments that accumulate in demyelinated areas must be cleared by microglia, making the study of microglial activity essential for monitoring the clinical progression of MS. By employing the fluorescent dye acridine orange, researchers can monitor the status and function of microglia, as real-time imaging of microglia phagocytosing cell debris during neurological demyelination offers deeper insights into the pathogenesis of MS and enables dynamic monitoring of the disease [185]. Kim et al. developed a high-performance fluorescent probe, CDr20, which can visualize microglia both in vivo and in vitro, serving as a potential imaging tool for identifying MS [186]. Boronic acid-based fluorophores can penetrate

the central nervous system and co-localize with microglia, enabling the identification of active phagocytic cells in demyelinating regions and providing insights into the demyelination process, with potential applications for monitoring disease progression and diagnostic staging [187]. The targeted fluorescent probe Rhp-pip-C1 can be delivered across the blood–brain barrier via ultrasound and microbubbles, selectively accumulating in activated microglia, thereby facilitating the imaging of inflammatory sites and supporting research on the inflammatory mechanisms associated with MS and the development of therapeutic drugs [188]. Furthermore, administering fluorescently labeled dendritic PAMAM dendrimers through the subarachnoid space allows for the localization of activated microglia, enabling targeted delivery of therapeutic drugs for MS [189].

The primary feature of MS is the demyelination of neuronal axons [190]. Visualizing myelin fibers can significantly facilitate the rapid diagnosis of the disease. The non-toxic dye FluoroMyelin™ Red selectively stains myelin, enabling real-time imaging of myelin without significant adverse effects on the myelin or axons [191]. Case Imaging Compounds (CIC) are targeted fluorescent imaging agents that selectively bind to myelin lipids, accurately reflecting differences in the content of healthy and pathological myelin, which can be utilized for assessing MS [192]. The near-infrared aggregation-induced emission fluorescent probe PM-ML provides high penetration depth, allowing for three-dimensional visualization of myelin [193]. The FA-CND, made from carbon nanodots, can display the spatial distribution of myelin images from multiple directions, dynamically monitoring the process of neuronal demyelination [194]. The probe 1-MeNHNR is capable of crossing the blood–brain barrier and can specifically bind to myelin fibers, aiding in the diagnosis and efficacy evaluation of MS [195]. Another fluorescent probe, Cy5-MBP81-99-QXL680, can distinguish newly occurring lesions from long-term active lesions through targeted recognition of myelin basic protein, thereby supporting disease classification [196]. The DBT-NIRF probe serves as a cost-effective imaging tool for myelin lipids, with fluorescent intensity quantifying levels of demyelination and myelin regeneration, complementing existing imaging methods [197]. Furthermore, the use of the fluorescent neuronal tracer Dil allows for tracking of the corticospinal tract to monitor axon damage, providing a quantitative method for assessing MS progression and evaluating treatment efficacy [198]. Table 3 summarizes the fluorescent probes utilized for myelin imaging.

Damage to neuronal axons in MS is driven by inflammation, and monitoring inflammatory activity in MS is crucial for diagnosis and treatment. Using the 5-HT_{1A} ligand UCM-2550, Gloria and colleagues developed a fluorescent probe capable of detecting the specific expression of the 5-HT_{1A} receptor in $CD4^+$ T cells [199]. This probe dynamically displays pro-inflammatory or anti-inflammatory responses induced by the pathological environment or drug treatment, serving as a key indicator for assessing the severity of MS. Additionally, oxidative stress levels are closely related to the severity of neuroinflammation. The far-red fluorescent probe DCI-H rapidly responds with fluorescence changes, allowing for real-time monitoring of hypochlorous acid (HOCl) activity in vivo and in vitro with high sensitivity and selectivity, showcasing its potential value in diagnosing neuroinflammation [200]. Currently, INF-β is one of the first-line treatments for MS. The use of fluorescent probe-labeled nanoparticles carrying INF-β (INF-β-NPs) enables the delivery of INF-β to the central nervous system via intranasal administration, significantly reducing drug dosage requirements and providing an effective, non-invasive, and cost-efficient treatment option for MS [201]. Furthermore, elevated levels of peptidylarginine deiminase (PAD) 2 lead to the citrullination of MBP, which represents a significant mechanism in the pathogenesis of MS [202]. The probe 4MeBz-FluME effectively monitors the activity of PAD isoforms, providing a reliable method for high-throughput screening of PAD inhibitors and facilitating the development of new drugs targeting this pathological pathway [203].

Type 1 diabetes (T1D)

The onset of T1D is primarily attributed to the infiltration of $CD4^+$ and $CD8^+$ T cells into the pancreatic islets, leading to the destruction of islet β-cells and insufficient insulin secretion [204, 205]. Consequently, the autoimmune responses occurring within the β-cells provide new avenues for the diagnosis and monitoring of T1D. Research indicates that employing the improved fluorescent dye 5,6-carboxyfluorescein diacetate can assess T cell proliferation, enabling the determination of disease heterogeneity and tracking disease progression. Imaging and accurately measuring the quality of islet β-cells are pivotal for monitoring T1D progression and developing personalized treatment plans [206]. Bertrand et al. designed a small molecule fluorescent probe targeting free fatty acid receptor 1 (FFAR1/GPR40) that can specifically image β-cells and stimulate the FFAR1 receptor to promote insulin secretion, offering the potential for accurately assessing the quantity and viability of residual β-cells in patients' pancreases [207]. The fluorescent probe E4×12-VT750 can rapidly bind to β-cells, facilitating in vivo imaging and precise measurement of β-cell viability, thereby serving as a crucial tool for monitoring diabetes progression [208]. Additionally, the fluorescent

dyes NG-DCF/PI [209] and the ligand 12 [210] are novel Zn^{2+}-specific fluorescent dyes capable of locating pancreatic β-cells for continuous fluorescent bioimaging, allowing for the dynamic assessment of β-cell function. The activation of the pro-inflammatory NF-κB signaling pathway in pancreatic tissue is a significant factor contributing to β-cell destruction. Measuring the fluorescence intensity of the NIR-ODND probe can visualize NF-κB levels in pancreatic tissue and cells, which is critical for early disease assessment and enables the detection of changes in pro-inflammatory signals prior to disease onset, facilitating early intervention [211].

Advancements in technology have led to the emergence of smartphone-based microfluidic fluorescence imaging systems, providing novel tools for the physiological research of pancreatic islets [212]. This system enables real-time analysis of β-cell metabolic activity and ionic signaling through high-resolution dynamic imaging, offering a convenient solution for monitoring islet function. Significant progress has been made in the development of fluorescent probes for monitoring T1D, which offer advantages such as ease of synthesis, low cost, and specific labeling, thereby facilitating their application in clinical diagnosis. The decline in pancreatic β-cell quality accompanies the progression of T1D; therefore, the development of related fluorescent probes further promotes the advancement of personalized medicine.

Inflammatory bowel disease (IBD)

Monitoring biomarkers serves as an important supplementary method for assessing disease activity in IBD. After intravenous injection of the fluorescent probe Cy-DM, the probe is taken up by inflammatory cells in the intestine, visualizing endogenous HClO and providing a means for early diagnosis of IBD [213]. The fluorescent probe LS-NO can sensitively monitor levels of NO in the intestine and shows promise as a diagnostic reagent for real-time monitoring of IBD [214]. The fluorescent probe BPan-CL, prepared using a dual-lock strategy, circumvents the issue of false positives by co-activating multiple biomarkers, enabling it to differentiate between various states of disease activity in IBD after injection [215].

The core issue in IBD is primarily the disruption of intestinal barrier function. Utilizing fluorescent probes for in vivo imaging of inflammatory regions in the intestine provides new insights into the diagnosis and localization of inflammatory lesions. Xu et al. developed the PTZB-FR probe, which enables in vivo imaging through oral administration and assesses intestinal barrier function, making it applicable for research, diagnosis, and treatment monitoring of IBD [216]. The near-infrared fluorescent probe WS-1-NO_2 has been successfully used for in vivo imaging, facilitating differentiation between ulcerative colitis and healthy colon tissue, thereby serving as an early diagnostic tool for IBD in clinical practice

Table 3 Fluorescent probes for neuromyelin imaging

Fluorescent probe	Excitation wavelength (λex/nm)	Emission wavelength (λem/nm)	Feature	Application	References
FluoroMyelin^{TM}Red	490	655	Large Stokes shift, good photostability, and non-toxic	Selectively stains myelin and enables real-time imaging of myelin	[191]
CIC	448–467	466–517	The preparation process is simple and sensitive to differences in the levels of healthy and pathological myelin	Targeted binding to myelin lipids can be used to assess the disease course of MS and develop treatment strategies	[192]
FA CND	355	446	Low cost, photobleaching resistance, high spatial resolution, and good biocompatibility	Visualization of the three-dimensional distribution of myelin lipids	[194]
PM-ML	495	708	High contrast, good photostability, and greater penetration depth	High-resolution 3D imaging for the visualization of myelin	[193]
1-MeNHNR	667	691	High specificity and high affinity	Can be used to diagnose MS and assess treatment efficacy	[195]
Cy5-mbp81-99-QXL680	643	663	The synthesis process is simple, with high sensitivity and high specificity	Can be used for early diagnosis of MS and to predict disease progression	[196]
DBT-NIRF	782	797	High specificity and high sensitivity	Monitoring the demyelination process and the level of myelin regeneration	[197]
DiI	–	–	High fluorescence intensity, photobleaching resistance, and non-cytotoxicity	Monitoring axonal injury and assessing the efficacy of MS treatment regimens	[198]

[217]. The Cy-Azo probe exhibits high sensitivity and specificity, allowing precise targeting of inflammatory sites, which is significant for the diagnosis and treatment of IBD [218]. DCM-KPV is a fluorescent probe that targets oligopeptide transporters, enabling real-time tracking and visualization of inflammatory cells while non-invasively observing inflammatory responses in the colonic mucosa, thus assisting in the differentiation of acute and chronic IBD [219]. Coupling the Pyr1 fragment to infliximab forms a probe with high affinity for TNF-α, which can be utilized for monitoring treatment and evaluating therapeutic efficacy [220]. After intravenous injection of BPN-BBTD nanoparticles, the probe specifically localizes to inflammatory sites, and the fluorescence intensity in the affected colon reflects the severity of IBD and the response to therapeutic interventions, providing a powerful tool for developing new treatment strategies [221].

Pemphigus

Pemphigus encompasses a group of rare acantholytic mucocutaneous autoimmune skin diseases, including various subtypes such as pemphigus vulgaris, pemphigus foliaceus, and IgA pemphigus [222]. These conditions are mediated by autoantibodies that target desmoglein (Dsg) 1 and Dsg3, disrupting their adhesive function in keratinocytes, which leads to acantholysis and the formation of subepithelial blisters [223]. The significant differences in prognosis and treatment between pemphigus and other pemphigoid diseases underscore the critical importance of accurate diagnosis. Utilizing FITC staining of immunoglobulins and C3 can reveal intercellular deposition of IgG and IgA, thus assisting in the diagnosis and classification of pemphigus [224, 225]. Even in cases of partial epidermal loss, the honeycomb-like fluorescence of skin appendages such as sweat glands, sweat ducts, and hair follicles can contribute to an accurate diagnosis. Currently, a multiplex immunofluorescence technique known as BioCHIP has been validated for diagnosing and screening various disease subtypes, thereby providing a simpler and more efficient diagnostic method for pemphigus [226]. With advances in technology, additional fluorescent probe methods are anticipated to play significant roles in the research of pemphigus and other autoimmune skin diseases.

Autoimmune hepatitis (AIH)

The dual-modal probe hCy-Tf-CA can visualize intracellular oxidative stress, accurately detecting cellular oxidative damage; it exhibits excellent photostability and has potential for dynamic monitoring, making it an effective tool for the early diagnosis of AIH [227]. The Q-SNAP nanoprobe allows for deep tissue imaging, enabling differentiation between autoimmune hepatitis and healthy liver tissue as early as four hours post-injection, thus facilitating real-time in situ monitoring of the T cell-mediated processes in AIH and assessing the efficacy of prophylactic immunosuppressive treatment [228]. Additionally, the bimodal fluorescent probe ETYZE-GGT shows dose-dependent fluorescence signal changes when detecting pathological states of liver tissue, providing corresponding quantitative analysis results and indicating its potential as an early diagnostic tool for AIH [229].

Idiopathic pulmonary fibrosis (IPF)

Fluorescent probes not only serve as essential research tools for elucidating the pathogenesis of IPF but also present a promising approach for aiding in the clinical diagnosis of the disease. Immune-mediated damage to alveolar epithelial cells constitutes a critical step in the progression of IPF; thus, the detection of circulating antibodies targeting these cells may facilitate early diagnosis. Imaging with fluorescently labeled anti-IgG antibodies reveals a linear deposition of IgG along the alveolar epithelial cells of lung tissue in IPF patients [230], providing a detailed representation of the severity of alveolar epithelial cell dysfunction and contributing to the early confirmation of the disease.

The progression of IPF is closely associated with elevated levels of oxidative stress, where excessive stimulation by reactive oxygen species promotes the apoptosis of alveolar epithelial cells, leading to the activation of fibroblasts and the deposition of extracellular matrix (ECM), ultimately resulting in persistent inflammation and fibrosis. Consequently, oxidative stress has garnered significant attention as a novel strategy for the specific diagnosis of IPF. The fluorescent probe Cy-GGT can effectively demonstrate changes in oxidative stress during the lung fibrosis process, displaying remarkable potential for real-time monitoring and serving as an effective tool for detecting the progression of pulmonary fibrosis [231]. Additionally, the probe DCM-NO can respond to in vivo NO levels in IPF patients at a low detection limit and reacts within 60 s, allowing for the rapid visualization of fluctuations in NO levels [232]. This capability renders it a valuable tool for real-time monitoring of lung fibrosis damage. The two-photon imaging probe FS-MnCl penetrates deeper into tissues, yielding improved imaging results and enhancing the capacity to assess the extent of lung fibrosis damage, potentially playing a significant role in the early detection and later treatment of IPF [233]. Another two-photon probe, rTPONOO-1, can visualize the transition of lung tissue from healthy to inflamed and fibrotic states via ONOO-, thereby predicting the early progression of IPF [234].

In the monitoring of treatment for IPF, fluorescent probes play a crucial role. The mitochondria-targeted near-infrared responsive emitting probe NIR-PTZ-HClO rapidly responds within 2 s to monitor fluctuations of HClO during nintedanib treatment, providing real-time evaluation of the drug's therapeutic effects [235]. The fluorescent probe Bcy-HS, designed and synthesized by Hou et al., not only monitors changes in sulfur elements in IPF in real time but also alleviates oxidative damage to alveolar epithelial cells and inhibits the activation of fibroblasts [236]. Its therapeutic effect on lung fibrosis is significantly enhanced when used in combination with pirfenidone. The fluorescence signal of the probe Cy-GST increases with the severity of lung fibrosis, and the combined administration of the glutathione S-transferase (GST) inhibitor TLK117 alongside pirfenidone yields better therapeutic outcomes than either treatment alone, indicating that the probe Cy-GST has potential for the diagnosis and treatment of IPF [237]. Wei et al. developed the fluorescent probe Cy-HDAC, which targets histone deacetylase (HDAC) and can reflect the severity of lung fibrosis by monitoring fluctuations in HDAC levels in IPF [238]. The efficacy of HDAC inhibitors combined with pirfenidone for treating IPF is superior to that of using either treatment alone, offering a novel auxiliary diagnostic tool and treatment approach for IPF.

Psoriasis

Abnormal activation of T cells is considered a key factor in the pathogenesis of psoriasis. Schwenck et al. utilized substrate-like protease-activating probes, known as ProSense, to achieve non-invasive in vivo imaging, facilitating the assessment of T cell activation during delayed-type hypersensitivity and the expression levels of tissue cathepsin B [239]. This strategy not only aids in understanding the mechanisms underlying delayed-type hypersensitivity reactions in the skin but also provides new insights for the early diagnosis and treatment of psoriasis. By using PE and BV421 staining to label HLA-C*06:02 tetramers containing self-peptides, researchers can directly identify CD8 + T cells in patients, revealing the potential role of cross-reactive T cells between environmental antigens and self-peptides in psoriasis [240]. This method can be used to evaluate the impact of different environmental antigens on the risk of developing psoriasis, thereby contributing to the formation of personalized multimodal management plans for psoriasis patients through dietary adjustments and lifestyle improvements.

ROS play a significant role in the pathogenesis of psoriasis by promoting the release of inflammatory factors, which, in turn, stimulate the proliferation of keratinocytes. Therefore, fluorescent probes that target ROS are advantageous for the early diagnosis and treatment monitoring of psoriasis. The specific fluorescent probes G1 and G2 undergo highly selective reactions with HOCl, enabling the in situ identification and imaging of HOCl and providing a novel method for diagnosing psoriasis [241]. Based on the finding that the concentration of HOCl in the skin is positively correlated with the degree of inflammation in psoriasis, Zhao et al. designed the lipid droplet imaging probe CN2-CF3-5, which has been successfully employed to track endogenous HOCl in psoriasis cells and skin [242]. This probe can simultaneously visualize lipid droplets while monitoring HOCl in real time, offering an innovative and promising imaging tool for the diagnosis of psoriasis.

In psoriasis treatment research, the application of nanotechnology has paved the way for the development of novel therapeutic strategies. Lin et al. Designed PLGA nanoparticles that enhance targeting capabilities toward skin dendritic cells by controlling particle size, while also reducing systemic side effects [243]. These nanoparticles can be utilized not only for the treatment of psoriasis but can also be expanded for other immune-related skin diseases, offering new insights for customizing personalized nanoparticle treatment plans.

Myasthenia gravis (MG)

The concentration of anti-muscle-specific kinase (MuSK)-specific IgG4 is significantly correlated with the severity of MG. Han et al. developed a method based on a MuSK antibody cell-based assay (CBA) utilizing fluorescent dye-labeled specific antibodies, allowing for the determination of anti-MuSK-specific IgG4 antibody concentrations through the intensity of fluorescent signals, which reflect the severity of the disease [244]. This method features a low detection limit and high sensitivity, enabling early detection of MG. For patients who are negative for anti-acetylcholine receptor (AchR) antibodies and MuSK antibodies, Pevzner et al. found that antibodies against low-density lipoprotein receptor-related protein 4 (LRP4) can serve as an important biomarker for MG [245]. By employing an enhanced green fluorescent protein (EGFP)-labeled detection method, anti-LRP4 autoantibodies can be efficiently and clearly detected, providing a new diagnostic pathway for patients for whom traditional methods fail to yield a definitive diagnosis. This finding has opened new avenues for the early diagnosis of MG. Recently, Álvarez-Velasco et al. established a connection between reduced Treg cells expression and the prevalence of MG through dual immunofluorescence staining (CD4-FOXP3), suggesting that functional deficits in Treg cells may play a significant role in the pathogenesis of MG [246]. This discovery aids in the deeper understanding of the immunological basis of MG and offers new perspectives for the

early detection, diagnosis, and treatment of the disease. In summary, fluorescent probes have played a crucial role in the diagnosis of MG, particularly in detecting relevant autoantibodies, thereby enhancing the sensitivity and specificity of MG diagnostics.

Autoimmune myocarditis

Research conducted by Martinez et al. demonstrated that the fluorescently labeled targeting peptide MyH-PhD-05 can co-localize with CD4 + T cells and monocytes, enabling the early identification of severe myocarditis even in the absence of changes in cardiac function, thus providing a novel approach for early diagnosis [247]. In another study, a nanoprobe that assesses granzyme B activity can localize with CD8 + T cells, facilitating visualization of myocardium-related autoimmune responses induced by myosin and evaluating the efficacy of dexamethasone treatment for myocarditis, thereby promoting the development of non-invasive imaging technologies for autoimmune myocarditis [248]. Sun et al. constructed a high-performance near-infrared emitting nanofluorescent probe, TNP, which specifically targets CXCL9 + macrophages, aiding in the early diagnosis of acute myocarditis [249]. By monitoring changes in NIR-II fluorescence intensity at the lesion site, researchers can accurately assess the pathological progression of the disease and simultaneously evaluate the therapeutic effects of drugs on myocarditis, providing a powerful tool for screening anti-myocarditis drugs. The dye-doped polymer probe SDPP, constructed using fluorescent dyes as a scaffold, can accurately image •OH radicals in vivo, evaluate the severity of myocardial inflammation, and significantly reduce the incidence of false-positive signals, thus providing a new direction for the diagnosis of autoimmune myocarditis [250].

With an enhanced understanding of disease pathogenesis, various nanodrug delivery systems are increasingly being utilized in the study of autoimmune myocarditis. Keiji Okuda et al. developed PEG-modified liposomes capable of encapsulating the immunosuppressant FK506 [251]. Following intravenous administration, fluorescence nanoprobes loaded with FK506 can reach the affected myocardial sites on the same day as administration, significantly inhibiting the expression of cytokines such as IFN-γ, TNF-α, IL-17, and IL-1β. The results in a reduction of myocardial inflammatory responses and fibrosis area, markedly improving cardiac dysfunction by day seven post-administration. This finding demonstrates the broad potential of this treatment approach for acute autoimmune myocarditis. Xiong et al. developed a novel fluorescence probe that employs T lymphocyte-macrophage hybrid membranes to coat zeolitic imidazolate framework-8 (ZIF-8) nanoparticles loaded with targeted small interfering RNA against interferon regulatory factor 1 (siIRF1) (siIRF1@ZIF@HM NPs) [252]. This probe utilizes the selective uptake of pro-inflammatory macrophages (M1 macrophages) to specifically target these cells, achieving high targeting accuracy, effectively silencing IRF1, and inhibiting IFN-γ-mediated macrophage pyroptosis. As a result, it significantly relieves myocardial inflammation and curtails disease progression. This strategy not only has significant clinical application value but also offers a novel targeted therapeutic approach for autoimmune myocarditis.

Other organ-specific autoimmune diseases

In addition to the aforementioned diseases, the application of fluorescent probes in other organ-specific autoimmune disorders has also advanced significantly. The probe Ox-PGP1 can accurately differentiate between normal, inflammatory, and cancerous thyroid cells, demonstrating the potential for rapid and sensitive distinction between autoimmune thyroiditis and undifferentiated thyroid cancer, thereby facilitating early intervention in thyroid illnesses [253]. Dong and colleagues devised a fluorescent protein-conjugated probe, PM Q-probe, which selectively binds to anti-thyroid IgG and detects T4 concentration in serum, offering a tool for early detection and diagnosis of Graves' disease and thereby enhancing the diagnosis and treatment for patients afflicted with this condition [254].

The application of fluorescent probes in autoimmune diseases primarily involves real-time monitoring of abnormal immune response processes, which is essential for the early diagnosis of these conditions and facilitates timely intervention. These probes can visualize the activation status of immune cells, providing a foundation for adjusting immunotherapy regimens and enhancing treatment efficacy. Furthermore, fluorescent probes enable precise imaging of target tissues and organs, mitigating the risks associated with traditional invasive procedures, reducing the likelihood of misdiagnosis and missed diagnoses, and making image interpretation more objective and reliable. In summary, fluorescent probes play a crucial role in the diagnosis, differential diagnosis, and treatment monitoring of autoimmune diseases, particularly demonstrating significant potential for non-invasive real-time visualization.

The scope of this review goes beyond traditional applications of fluorescent probes, incorporating cutting-edge research in biomarker detection, dynamic monitoring of immune cell functions, and evaluating the efficacy of drug treatments. While previous reviews have focused on specific applications or limited subsets of autoimmune diseases, our work provides a more comprehensive perspective, covering a broad range of autoimmune

conditions and their unique challenges. By systematically summarizing the latest advancements in the field, this review highlights the growing potential of fluorescent probes as versatile and powerful tools for both diagnostics and therapeutic interventions. To differentiate this work from earlier reviews, we introduce a novel comparative framework (Table 4) for classifying fluorescent probes based on their clinical applications. Specifically, we categorize probes into four main types: diagnostic probes, theranostic probes, multimodal probes and prognostic probes. This classification not only offers a clearer understanding of the probes' applications in the clinical setting but also enables a more nuanced exploration of their respective advantages and limitations. This table serves as an invaluable resource for clinicians and researchers alike, enabling them to select the most appropriate probes for specific diagnostic and therapeutic needs in autoimmune diseases.

Technical challenges

Biocompatibility and toxicity issues

The design of fluorescent probes must prioritize safety, particularly given their potential applications in biomedicine. A prevalent concern is the toxicity associated with these probes, especially those represented by quantum dots, which can induce harmful reactions such as oxidative stress, alterations in gene expression, autophagy, apoptosis, and the release of metal ions [257]. These factors significantly impede the use of probes in clinical diagnosis and treatment. Consequently, reducing the cytotoxicity of probes and enhancing their biocompatibility are critical advancements necessary to promote their clinical application.

Fluid dynamics, particle surface charge, core composition, and surface coatings are four common factors influencing the toxicity of fluorescent probes [258]. At equivalent concentrations, smaller-sized fluorescent probes can penetrate the nucleus and cause DNA damage, leading to apoptosis [259]. In contrast, spherical probes diffuse more rapidly than rod-shaped probes, exhibiting stronger toxicity. Therefore, under identical functional conditions, optimizing the size and shape of probes to facilitate their entry and exit from cells within the constraints of natural pore size structures can significantly reduce their cytotoxicity [260, 261]. Coating probe surfaces with protective layers, such as Si polymer bilayer encapsulation [262] or GSH-Ag_2S conjugated quantum dots [263], offers robust protection against degradation while enhancing both the biocompatibility and optical performance of the probes. Additionally, modifying probes with ionic liquids can improve the biocompatibility of carbon quantum dot probes and induce varying fluorescence emission characteristics [264]. In recent years, probes synthesized without heavy metals (e.g., Fe [265], carbon [266], or Mn/ZnS [267]) have gained attention due to their low cost, minimized toxicity, and ease of use, significantly advancing probe applications. However, probe distribution at the same dosage varies among different cell lines due to differences in cell viability. Consequently, there remains a need for a comprehensive standardized guideline to assess probe toxicity, allowing for accurate evaluation of their toxicity and facilitating the selection of suitable probes for clinical applications.

Recent advancements in toxicology have led to significant progress in reducing the toxicity of fluorescent probes and enhancing their biocompatibility. Nevertheless, research into the potential toxicity mechanisms of nanoprobes, particularly quantum dots, remains in its early stages. The metabolic and excretion pathways of these probes in vivo are still not fully understood, and most quantum dots are composed of non-degradable materials, such as heavy metals, which raises concerns regarding their biocompatibility and chronic toxicity. While modifications in variables such as fluid dynamics and the physicochemical properties of the probes can help mitigate their biological toxicity, the assessment of their biosafety must also account for various factors influencing the organism, underscoring the need for more systematic toxicological analyses. This entails extensive studies and a standardized protocol for evaluating the cytotoxicity and biocompatibility of probe materials, which will facilitate comparisons across different laboratories. Furthermore, translating the effects of probe toxicity from animal models to human applications necessitates further breakthroughs in future research.

Insufficient sensitivity and specificity

Prolonged excitation-emission cycles of fluorescent groups can result in permanent chemical damage due to oxidative free radicals, leading to gradual decay or complete disappearance of the fluorescence signal [268]. The phenomenon of photobleaching in fluorescent probes poses a significant challenge in the development of fluorescence imaging techniques, adversely affecting imaging quality and constraining the feasibility of long-term dynamic observations, thereby significantly limiting their widespread application. Researchers have currently gained a deeper understanding of the photobleaching mechanism at the molecular level, which has spurred the development of various innovative solutions. Inducing structural changes in fluorescent proteins is an effective strategy to enhance the photostability of these probes, as it mitigates photobleaching damage without requiring dynamic adjustments to light intensity or sampling time [269]. However, this method may lead to reduced quantum yield. Simultaneous Photo-Activated Imaging

Table 4 Characteristics of the different probe types

Probe type	AD	Probe name	Target spot	Applications	Advantages	Limitations	References
Diagnostic probes	RA	IRDye-680RD-OX40	T cell	Detection of T cell activation in early RA	Non-radioactive; convenient; easy to prepare; low cost; high specificity; high sensitivity	Poor penetration of deep tissues; discrepancies exist between animal models and the chronic disease progression of RA	[105]
		Ratio-A	ONOO-	Visualizing ONOO- fluctuations for the diagnosis of RA	High selectivity; low detection limit; low cytotoxicity	Discrepancies exist between animal models and the chronic disease progression of RA	[123]
		Cy7-Nb119	Macrophage	Monitoring arthritis	High sensitivity; no radioactivity; easy to produce; and rapid response	Suitable for short-term use only; fluorescent dye not quantified	[124]
	SLE	Single-cell antibody nanopores	Autoantibody	Detection of B cells that produce anti-SSA/Ro and anti-SSB/La antibodies and their secretion levels	High sensitivity; high specificity; quantitative detection; large-scale simultaneous detection	Clinical translation has not yet been achieved	[142]
		Cys-j	Cys	Visualizing the Cys levels in kidney disease	Fast response; simple synthesis; good stability; deep penetration ability	Clinical translation has not yet been achieved	[150]
		dsDNA-AuNP-pep	Signaling pathway molecules	Detection of the expression levels of miRNA-21 and caspase-3 to monitor the progression of apoptosis	Simple preparation; high specificity; high stability; in situ real-time monitoring	Clinical translation has not yet been achieved	[169]
	MS	Rho-pip-C1	Inflammatory cell	Localization of the activated microglia	Low cytotoxicity	It cannot penetrate the blood–brain barrier on its own and requires the assistance of ultrasound and microbubbles	[188]
		PM-ML	Cellular structure	Achieving three-dimensional visualization of myelin	High contrast; good stability; deeper penetration capability	Unable to distinguish myelin fibers in different brain regions	[193]
		DCI-H	HOCl	Dynamic monitoring of HOCl levels in the brain	High sensitivity; high selectivity; fast response; good stability; low detection limit	Clinical translation has not yet been achieved	[200]
	T1D	NIR-ODND	Signaling pathway molecules	Quantitative measurement of NF-κB levels in the pancreas	High sensitivity; deeper penetration capability	Clinical translation has not yet been achieved	[211]
	IBD	Cy-DM	HClO	Imaging of HClO within lysosomes	High sensitivity; high selectivity; rapid response; high signal-to-noise ratio	Clinical translation has not yet been achieved	[213]

Table 4 (continued)

Probe type	AD	Probe name	Target spot	Applications	Advantages	Limitations	References
		DCM-KPV	oligopeptides	Localization and visualization of the tripeptide KPV (Lys-Pro-Val, C-terminal sequence of α-MSH) to differentiate colonic inflammation	Low photobleaching; good biocompatibility; rapid response; noninvasive imaging	Complex preparation	[219]
	AIH	Q-SNAP	T cell	Dynamic monitoring of T cell dysfunction and evaluation of preventive immunosuppressive therapy	High signal-to-noise ratio; high sensitivity; rapid response; deep penetration capability	Complex preparation	[228]
	IPF	FS-MnCl	NO	Detection of NO levels in cells and IPF mouse models	Low detection limit; resistance to photobleaching	Clinical translation has not yet been achieved	[233]
	Psoriasis	ProSense	T cell	Assessment of T cell activation status and expression levels of tissue cathepsin B	Non-invasive imaging	Insufficient specificity	[239]
	Autoimmune myocarditis	MyH-PhD-05	Cell	Co-localization with CD4 + T cells and monocytes (CD11b)	Non-invasive imaging	Low resolution; the long-term application value remains to be studied	[247]
	SS	DIM	Lysosome and ratio polarity	Monitoring of the polarity changes in the submandibular glands	High selectivity; real-time dynamic imaging	The quantitative relationship between fluorescence intensity and disease severity still needs to be studied	[175]

Table 4 (continued)

Probe type	AD	Probe name	Target spot	Applications	Advantages	Limitations	References
Therapeutic probes	RA	Probe-2	HOCl	Real-time monitoring of HOCl to assess the early therapeutic effects of MTX treatment	Fast fluorescence response; high sensitivity; high specificity; and good biocompatibility	Lower penetration in deep tissues	[130]
		psi-tGC-NPs	TNF-α	Blocking TNF-α to inhibit progressive joint destruction	High stability; sequence specificity; and efficacy comparable to MTX	Further exploration of potential immune responses is needed	[133]
		pDNA/DSP-np	Macrophage	Promoting macrophage polarization to alleviate arthritis inflammation and bone erosion	High specificity; high drug loading capacity; no hepatotoxicity; prolonged drug half-life	Complex design	[81]
	MS	FITC-G4-OH	Inflammatory cell	Targeted delivery of therapeutic drugs to localized microglia and astrocytes	High specificity; prolonging drug half-life; low cytotoxicity	Complex preparation. Clinical translation has not yet been achieved	[189]
		IFN-β-NPs	IFN-β	Nasal administration to modulate cell activation and control neuroinflammation	Good biocompatibility; low cost; drug dose reduction	Clinical translation has not yet been achieved	[201]
	IBD	BPN-BBTD NPs	Inflammatory cell	Monitoring the level of inflammation and the response to pharmacological intervention	High signal to noise ratio; clear spatial resolution	Background fluorescence interference	[221]
	IPF	Bcy-HS	S	Real-time monitoring of changes in S to alleviate oxidative damage to alveolar epithelial cells and inhibit fibroblast activation	High sensitivity; high yield; low background interference; good biocompatibility	Clinical translation has not yet been achieved	[236]
	Psoriasis	PLGA NPs	Dendritic cell	Dendritic cell uptake for the treatment of psoriasis	Prolonging drug half-life; reducing systemic side effects	Particle size must be accurately controlled	[243]
	Autoimmune myocarditis	ZIF-8 NPs	Macrophage	Inhibition of macrophage pyroptosis to alleviate myocardial inflammation and slow down disease progression	High specificity; high nucleic acid effective load	Limited in vivo toxicity data	[252]

Table 4 (continued)

Probe type	AD	Probe name	Target spot	Applications	Advantages	Limitations	References
Multimodal probes	AIH	hCy-Tf-CA	O_2^-	In vivo imaging of O_2^- and early diagnosis of liver inflammation	High sensitivity; optical stability; deep penetration ability	Low quantum yield; complex design	[227]
	—	Synthesis of Magnetic-Plasmonic NPs	Cell	Imaging of in vitro cells and ex vivo tissues	Low cytotoxicity; multimodal synchronous imaging; high sensitivity; fast deep penetration imaging	Clinical translation has not yet been achieved	[255]
	T1D	PiF	Pancreatic β cell	Fluorescence imaging and PET imaging of pancreatic β-cells	High specificity; fast response	Clinical translation has not yet been achieved	[256]
Prognostic probes	RA	Cy5-αCD20	B cell	Assessment of B cell distribution, absorption, and plasma pharmacokinetics in RA joints	Enhancing efficacy while reducing off-target side effects	Clinical translation has not yet been achieved	[107]
	MS	Fluorescent 5-HT_{1A} probe	5-HT_{1A}	Detection of the expression of 5-HT_{1A} in T cells to assess the inflammatory response after treatment	Photostability; high fluorescence quantum yield; high molar extinction coefficient; and high specificity	Clinical translation has not yet been achieved	[199]
	T1D	E4 × 12-VT750	Pancreatic β cell	In vivo imaging and measurement of pancreatic β-cell vitality	Easy to synthesize; high specificity; high synthetic yield; good optical features	Clinical translation has not yet been achieved	[208]
	IPF	NIR-PTZ-HClO	HOCl	Monitoring the fluctuations of HOCl in mice with pulmonary fibrosis treated with the IFP drug Nintedanib	High sensitivity; high selectivity; fast response	Complex preparation	[235]
	Autoimmune thyroiditis	Ox-PGP1	Pyroglutamate aminopeptidase 1 (PGP-1)	Detection and quantitative analysis of PGP-1 to evaluate the therapeutic effects of medication	High sensitivity; high specificity; rapid response; photostability	Complex preparation	[253]

(SPI) fluorescent groups facilitate photactivation and excitation with a single light source, thereby eliminating the need for repeated switching between excitation and emission light, which addresses the problem of signal depletion during prolonged imaging [270]. A competitive relationship exists between FRET and photobleaching kinetics; incorporating small molecules that act as FRET receptors into probes can suppress rapid photobleaching, though this approach may reduce imaging brightness [271]. While photobleaching is a common characteristic of probes, it has evolved from a mere technical obstacle into an important research tool. Probes designed using photobleaching can also serve as valuable detection tools, offering more robust observation methods for biomedical imaging research [272].

In the practical application of fluorescent probes, background fluorescence represents a significant concern. High background signals not only diminish detection sensitivity but may also result in false-positive results [273]. Non-specific binding of fluorescent probes to substrates can lead to considerably elevated background signals, thus constituting a key challenge in enhancing the selectivity of these probes. Hydrophobicity is a primary determinant of the binding affinity between fluorescent dyes and substrates, and the main focus in probe design is to select hydrophilic dyes with favorable photophysical properties [274]. Encapsulating quantum dots probes with bovine serum albumin (BSA) can increase the water solubility of quantum dots, effectively reducing non-specific cellular binding [275]. Furthermore, introducing neutral auxiliary groups to control the hydrophilicity of the probes can decrease their non-specific accumulation on hydrophobic cellular components [276]. However, these methods may suffer from challenges such as leakage and operational complexity. Novel protein cavity-encapsulated fluorescent probes can effectively address these issues by encapsulating the probes within protein cavities and utilizing SNAP-tag as a protein barrier to block non-specific interactions [277, 278]. Additionally, single-target fluorescent probes, which rely solely on a single biomarker, often face specificity issues. Equipping a single probe with two recognition sites allows it to detect two specific biomarkers or microenvironmental conditions simultaneously, thereby reducing non-specific activation of a single probe and improving diagnostic accuracy [279]. Moreover, the mechanism of twisted intramolecular charge transfer (TICT) can enhance probe specificity [280]; when the probe undergoes conformational twisting and enters the TICT state, the emitted light is significantly weakened or may not emit at all. Designing TICT-emitting fluorescent probes with protein ligands that emit fluorescence exclusively upon binding to the target can substantially enhance labeling selectivity [281].

Tu et al. introduced steric hindrance and competitive binding designs in fluorescent probes to suppress background signals, successfully enhancing sensitivity and minimizing interference from elevated background noise during detection [282]. By incorporating fluorescence quenching groups into the probe design, they further inhibited the fluorescence of the fluorophore [283]. The synergistic effect of multiple quenching groups allowed for the complete elimination of background signals, resulting in a zero-background signal CuFS fluorescent probe. This strategy facilitates the clear identification of subtle fluorescence changes; however, the preparation process is relatively complex, necessitating further research to evaluate its applicability to other probe types. Recently, Mela et al. improved the signal-to-noise ratio of fluorescent imaging by more than twofold using a dense light flow point tracking mechanism, pulsed fluorescence excitation, and interleaved collection techniques [284]. Nevertheless, this method relies on high-quality equipment and requires minimizing signal delays or desynchronization, which presents challenges for practical implementation. Consequently, designing a simple and efficient fluorescent probe structure that effectively reduces background signals remains a critical issue that warrants further investigation.

Barriers to clinical translation

Translating developed fluorescent probes from preclinical stages to clinical applications is a vital step in their implementation, yet it faces challenges such as funding, mass production, and regulatory approvals. The high demands for costly synthesis equipment and associated expenses significantly restrict the large-scale production and application of fluorescent probes, making the exploration of simple and low-cost synthesis processes an essential task in their development. Natural diatoms yield over 10 million tons annually, providing a continuous supply of affordable raw materials for producing high-quality SiNP probes [285]. Wang et al. identified a novel fluorescent dye that can be produced at low cost and scaled up through a user-friendly and environmentally sustainable reaction pathway, presenting significant potential for the clinical application of fluorescent probes [286]. Yan et al. introduced an effective method for the large-scale preparation of probes by integrating hydrothermal treatment, sintering, and ultrasonic processing [287]. Wang et al. demonstrated that high-quality fluorescent probes can be produced in large quantities using a molecular fusion approach [288]. Mass production of fluorescent probes often entails multiple steps and technologies; effectively addressing these challenges could

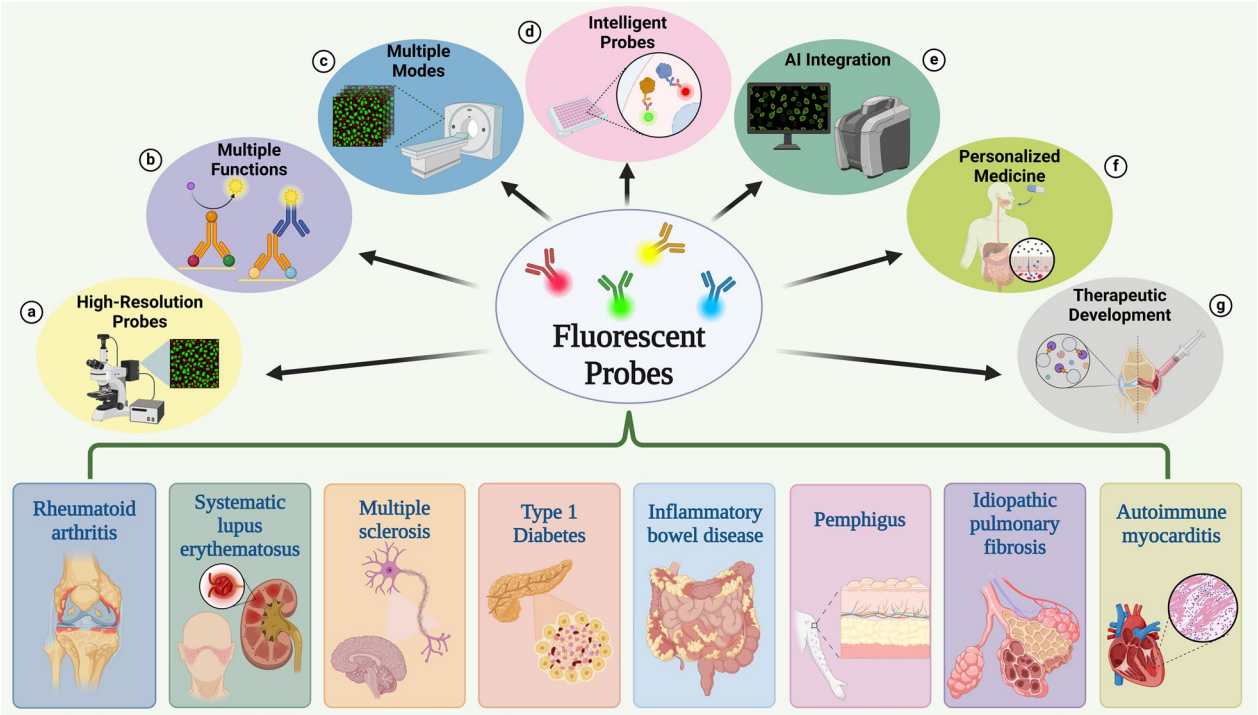

Fig. 5 The prospect of fluorescent probes (Created in https://BioRender.com) **a** High-Resolution Probes: The utilization of high-resolution fluorescent probes significantly enhances spatiotemporal resolution and deep tissue penetration, facilitating high-precision imaging. **b** Multiple Functions: Multifunctional fluorescent probes enable the simultaneous detection of multiple biomarkers, thereby improving detection efficiency. **c** Multiple Modes: Multimodal fluorescent probes amalgamate various detection methods, compensating for the limitations inherent in different imaging modalities and achieving synergistic effects. **d** Intelligent Probes: Intelligent fluorescent probes operate at the cellular and molecular levels to dynamically detect specific small molecules and changes within the cellular microenvironment. **e** AI Integration: The integration of artificial intelligence has accelerated the development of fluorescent probe design, application performance, and data analysis. **f** Personalized Medicine: Patient-specific probes address diverse requirements for personalized diagnosis and therapeutic monitoring. **g** Therapeutic Development: Fluorescent probes facilitate research and screening of new drugs and synergize with nanotechnology to advance the development of fluorescent nanoprobes that integrate diagnosis and treatment

greatly enhance the clinical utility of the probes. Currently, most fluorescent probes remain in the preclinical research phase; only after thorough verification through preclinical studies can human clinical trials commence. Aseptic Bevacizumab-800CW is the first NIR fluorescent molecular imaging agent approved for use in humans [289], and it is anticipated that more fluorescent probes will achieve clinical application in the future.

The quantum dot market, valued at $4 billion in 2021, is expected to reach $8.6 billion by 2026 [290]. This growth suggests significant potential for the clinical application of fluorescent probes; however, their clinical translation is fraught with challenges. First, an ideal fluorescent probe must exhibit biocompatibility and stable metabolism; nonetheless, many existing probes face issues related to long-term retention, which may result in chronic toxicity. Second, a critical challenge for future research involves the development of green, environmentally friendly synthesis methods for probes. These methods aim to minimize complexity, variability, and production costs in fluorescent probe development. As products that integrate diagnosis and therapy, fluorescent probes must adhere to dual regulations governing pharmaceuticals and medical devices to guarantee patient safety and promote the sustainable advancement of the fluorescent probe industry. For instance, compliance with the In Vitro Diagnostic Medical Devices Regulation (IVDR) is necessary to achieve regulatory approval and complete clinical trials prior to market entry [291].

Future perspectives

Integration and innovation of cutting-edge technologies

AD characterized by its intricate pathogenesis and dynamic progression, necessitates non-invasive in vivo monitoring tools that possess high sensitivity and spatiotemporal resolution. The Abbé diffraction limit imposes significant constraints on the resolution of conventional optical microscopes [292]. To overcome this limitation, researchers have developed super-resolution microscopy techniques (Fig. 5a), including Stimulated Emission

Depletion (STED) microscopy [293], Photoactivated Localization Microscopy (PALM) [294], and Stochastic Optical Reconstruction Microscopy (STORM) [295]. STED microscopy utilizes a toroidal depletion beam to induce stimulated emission, causing excited-state electrons at the periphery to return to the ground state while permitting only those in the central region to revert to the ground state in a spontaneously fluorescent manner, thereby achieving high-resolution imaging [296]. For example, the imaging resolution of the Lipi-BDTO probe can reach the nanoscale, enabling visualization of synaptic structures formed by neutrophils [297], T cells, and B cells, and illuminating the crucial role of neutrophils in autoimmune demyelinating diseases [298]. Nevertheless, STED microscopy continues to encounter challenges such as photobleaching [299] and background noise [300], which necessitate further optimization.

PALM overcomes the optical diffraction limit through fluorescence photoactivation and single-molecule localization [301]. Its fundamental principle involves the use of photoactivatable GFP to label proteins [294], followed by a repetitive cycle of activation, excitation, localization, and bleaching to achieve precise localization and counting of proteins, attaining nanoscale resolution [302]. In recent years, photoactivated BODIPY probes have been successfully utilized in PALM microscopy for sub-diffraction imaging of cellular substructures, providing a novel approach to studying dynamic processes within live cells [303].

Fluorescence-switching groups are a key feature of STORM, where different subsets of fluorophores are randomly activated during each imaging cycle [304]. This process allows for high-precision localization of each fluorophore and the construction of high-resolution images. Live-cell STORM imaging offers significant advantages for evaluating cellular structures and dynamic processes [305]. For instance, in studies examining the impact of autoantibodies on the distribution of cellular components, STORM technology can provide nanoscale quantitative assessments [306]. Furthermore, STORM technology enables high-precision three-dimensional imaging, visualizing interactions between presynaptic terminals and microglia, which enhances our understanding of intercellular interaction mechanisms [307].

In addition to high-resolution devices, near-infrared fluorescent probes (NIR-FPs) are emerging as a new generation of tools for elucidating autoimmune imbalances and guiding the precise treatment of AD, owing to their deep tissue penetration (NIR-I: 700–900 nm; NIR-II: 1000–2000 nm), minimal biological background interference, and multi-parametric responsiveness [308]. Zhang et al. developed an activatable NIR-II fluorescent probe that integrates a long-wavelength aggregation-induced emission unit with a manganese carbonyl cage motif, which can be activated within the inflammatory microenvironment of RA to release therapeutic carbon monoxide (CO) [309]. This probe can also be conjugated with anti-IL-6R antibodies, enabling active targeting of RA. Furthermore, NIR fluorescent probes have been widely applied in other inflammation-related diseases. The novel NIR two-photon probe HDM-Cl-HClO developed by Luo et al. can detect HClO in inflammatory and tumor mouse models, effectively tracking HClO levels in both cellular and animal contexts, thereby enhancing the understanding of the relationship between HClO, inflammation, and tumors [310]. In the future, NIR-FPs may focus on strategies that integrate treatment and immune regulation, effectively modulating the polarization state of immune cells and reducing inflammatory cell infiltration, thus providing new avenues for the treatment of AD. While challenges persist regarding biocompatibility, signal quantification standardization, and clinical translation, their integrated characteristics that link diagnosis and treatment hold significant promise for advancing precision medicine for various diseases.

Multifunctional fluorescent probes

The early diagnosis of diseases often necessitates the identification of multiple biomarkers. However, the concurrent use of several probes based on a single biomarker may result in issues related to fluorescence crosstalk [311]. Consequently, the synchronous detection of multiple biomarkers presents a significant challenge in the current advancement of fluorescent probes. To address this issue, researchers have proposed various strategies to optimize the design of multifunctional fluorescent probes (Fig. 5b). For instance, incorporating multiple specific binding sites within these probes permits the simultaneous detection of several target molecules [311]. Furthermore, combined triggering and serial activation strategies facilitate real-time detection of multiple biomarkers, effectively mitigating spectral overlap while significantly enhancing specificity and diagnostic accuracy [312]. Additionally, bimodal fluorescent probes that integrate both diagnostic and therapeutic functions further broaden the potential applications for disease management. These probes enable in vivo imaging of lesions while concurrently regulating drug release, providing a comprehensive solution for the diagnosis and treatment of autoimmune diseases [313].

Multimode fluorescent probes

The integration of various imaging modalities can address the limitations of individual techniques to achieve optimal synergistic effects. Multimodal fluorescent probes are capable of simultaneously detecting multiple signals,

offering high sensitivity, specificity, and the capacity to identify multiple target biomarkers, thereby presenting a promising strategy for precision medicine (Fig. 5c). Near-infrared fluorescent (NIRF) probes provide high sensitivity and non-invasive imaging; however, their practical application is often constrained by tissue penetration capabilities, rendering high-resolution visualization of deep tissues challenging. Photoacoustic (PA) imaging combines the benefits of fluorescence and ultrasound, further enhancing real-time imaging of deep tissues. By merging these two imaging approaches, Zhang et al. developed an activatable NIRF/PA dual-modal probe, hCy-Tf-CA, which successfully achieved real-time in situ imaging of the liver with enhanced sensitivity and improved signal feedback [227]. Gold nanoparticles possess excellent plasmonic properties that can amplify the Raman signals of nearby molecules, facilitating broad applications in photoacoustic imaging, surface-enhanced Raman scattering (SERS), and CT imaging. However, the paramagnetic characteristics of gold limit its applicability in MRI technology. By adsorbing gold nanoparticles onto pre-fabricated iron oxide cores, the resulting hybrid nanoprobes enable synchronized imaging using MRI, SERS, and CT modalities, providing high sensitivity and rapid deep tissue penetration imaging for in vitro cellular and ex vivo tissue studies, thereby revealing more detailed pathological information [255].

Multimodal fluorescent probes are progressing from simple diagnostic tools to integrated platforms for both diagnosis and therapy. The probe PiF is a multimodal imaging agent for pancreatic β-cells that combines fluorescence and positron emission tomography (PET), facilitating intraoperative imaging of islets and significantly shortening surgical duration [256]. Its imaging capabilities, compared to MRI and PET, demonstrate higher resolution, thereby greatly enhancing the application potential of fluorescent probes. Leveraging the complementary features of PA and fluorescence imaging, Sun et al. developed a photoacoustic-fluorescence (PA-FL) imaging system based on varying imaging contrasts, depths, and spatial resolutions [314]. This system enables real-time dual-modal imaging and opens new avenues for preclinical disease research, including monitoring systemic drug delivery dynamics, tracking cancer cells labeled with dual-modal molecular tracers, and investigating neurovascular coupling in both the central and peripheral nervous systems.

While multimodal fluorescent probes present significant application prospects, their future development is challenged by several critical issues. These include the need for systematic evaluation of probe biocompatibility, in vivo metabolic safety, and chronic toxicity. The synchronization of excitation and emission of multimodal signals, alongside the calibration of signal quantification, requires the standardization of various research protocols. Furthermore, the intricate interpretation of multimodal signals necessitates the development of innovative computational algorithms. It is anticipated that advancements and integration across toxicology, materials science, and big data algorithms will enable multimodal fluorescent probes to play a pivotal role in personalized medicine, real-time intraoperative navigation, and drug development.

Intelligent fluorescent probes

With advancements in fluorescent probe technology, small molecule probes have garnered significant attention from researchers due to their high sensitivity and selectivity (Fig. 5d). Enzymes, as fundamental regulators of biochemical reactions, play a crucial role in both physiological and pathological conditions, with their activity serving as a vital indicator of cellular metabolic status [315]. By monitoring the formation and breaking of chemical bonds during enzyme-catalyzed reactions, smart probes can effectively target hydrolases [316], oxidoreductases [317], and transferases [318], enabling both visualization and quantitative analysis of enzyme activity. This approach has demonstrated exceptional performance in monitoring enzyme expression both within and outside cells and has significant application value in drug delivery and high-throughput screening [319].

Abnormal fluctuations in pH are closely associated with cellular dysfunction and serve as indicators for the onset of various diseases [320]. For example, the pH in RA joints is lower than that of adjacent normal tissues. The Lyso-Cy probe selectively targets $ONOO^-$ within lysosomes and aids in the diagnosis of RA by visualizing pH levels [321]. The dynamic response mechanism of the probe's fluorescence intensity to changes in pH facilitates real-time monitoring of the tissue microenvironment, offering a novel concept for the design of intelligent probes.

Various biochemical reactions continuously occur within organisms. The future development of real-time imaging technologies for dynamic molecular tracking will be a central objective in the design of intelligent fluorescent probes. For instance, real-time monitoring of lysosomal pH can be accomplished through the dynamic reversible ICT mechanism of fluorescent dyes [322]. Additionally, interactions between organelles can be visualized using fluorescent lipid droplet probes [323]. Furthermore, integrating fluorescent probes into STED microscopy can significantly enhance

super-resolution dynamic imaging capabilities, offering new insights for cell biology research [324].

Artificial intelligence integration

The integration of fluorescent probes with artificial intelligence (AI) has emerged as a notable advancement in the biomedical field in recent years. AI technologies, particularly machine learning (ML) and deep learning algorithms, have revolutionized the design, optimization, and application of fluorescent probes (Fig. 5e). Zhao et al. developed predictive models by employing the ensemble learning algorithm LightGBM in conjunction with molecular fingerprints to analyze extensive datasets of experimental results and fluorescent dye databases [325]. Their model achieved an accuracy of 0.974 on the independent test set, significantly accelerating the development of novel fluorescent probes. Utilizing an AI-driven multi-level prediction system, they screened over 700 previously undiscovered excited-state intramolecular proton transfer (ESIPT) fluorescent molecules from a library of 570,000 compounds, thereby narrowing the gap between design and experiment [326]. This method streamlined the development process for ESIPT fluorescent molecules, while ensuring good biocompatibility and pharmacokinetic properties across various applications, ultimately reducing the development cycle of probes and enhancing overall efficiency.

AI technology not only enhances the design efficiency of fluorescent probes but also improves their performance in practical applications. ML in tandem with molecular evolution techniques, optimizes the functionality of GFP by guiding mutations to facilitate effective modifications in GFP's fluorescence color, thereby ensuring optimal probe performance in complex and dynamic environments [327]. The integration of algorithmic systems into fluorescence microscopy can reduce acquisition time and minimize the risks of photobleaching and cellular damage while sustaining high spatial, temporal, and spectral resolutions [328]. This approach not only accelerates the research and development process for novel probes but also significantly reduces development costs. Asadiatouei et al. developed software called DeepLASI, which can process multicolor fluorescence data and is characterized by strong adaptability, user-friendliness, and compatibility [329]. Each step in the software's workflow can be executed either manually or automatically using ML algorithms, thus addressing the growing analytical demands of the rapidly evolving field of probes.

Moreover, AI can be employed to enhance the subcellular targeting capabilities of fluorescent probes, enabling precise targeting of specific locations within cells and demonstrating significant potential for application in the biomedical field [330]. As AI technology continues to advance, the performance and range of applications for fluorescent probes are similarly expanding, resulting in a substantial reduction in data analysis time and research costs. This progress presents new opportunities and challenges for biomedical research and applications.

Personalized medicine

The foundation of personalized medicine lies in the precise identification of disease states through biomarkers, which are linked to the potential progression of diseases to formulate targeted treatment strategies (Fig. 5f). Fluorescent probes, due to their high selectivity and sensitivity toward specific biomarkers, have become essential tools in personalized medicine. Probes represented by quantum dots fulfill many of the requirements of personalized medicine by effectively delivering diagnostic probes and therapeutic drugs to lesions [331], releasing fluorescent signals and drugs at the lesion sites to achieve precise diagnosis and treatment [332]. In the study of autoimmune diseases, immune phenotype analysis provides critical evidence for personalized treatment [333]. By integrating the design of fluorescent probes with in vitro screening of immune-modulating drugs, nanoscale carriers can be developed to cater to the specific needs of individual patients. These carriers not only incorporate precise size and drug load designs but also establish a quantifiable relationship between fluorescent intensity and therapeutic potential [334], laying a solid foundation for the significant role of fluorescent probes in personalized medical services.

Development of novel therapeutic strategies

The incidence and prevalence of autoimmune diseases are on the rise, presenting an urgent challenge in developing efficient and precise treatment strategies. The role of fluorescent probes in drug development is particularly significant, as they can be utilized not only for high-throughput screening of drugs but also for evaluating the hepatotoxicity [335] and nephrotoxicity [336] of various medications, thereby aiding in the early diagnosis of drug-induced liver injury [337]. Natural products, as essential sources for new drug development, have recently been shown to function as both specific fluorescent probes and potential therapeutic candidates, significantly broadening the application scope of fluorescent natural products. For instance, natural alkaloid fluorescent probes can achieve both specific labeling and therapeutic efficacy in treatment [338].

Fluorescently labeled nanocarriers not only facilitate precise drug targeting and release but also enable real-time monitoring of drug distribution and efficacy. Their application in targeted drug delivery systems has emerged as a significant focus within biomedical

research. Chen et al. successfully developed a novel chitosan-based gated fluorescent mesoporous silica nanocarrier, CS-Na-MSN, characterized by its ICT properties, which utilizes fluorescence changes resulting from drug release to monitor the release process in real time [339]. This approach maximizes the avoidance of interference with drug activity and allows for the real-time monitoring of various drugs. The ratio-type fluorescent probe totalROX exhibits high sensitivity and excellent oxidative capacity in cells; however, it encounters practical limitations due to poor water solubility and insufficient targeting of diseased areas. Wang et al. combined the physical properties of pH-responsive nanoparticles, EHC NP, with the totalROX probe, which not only minimized probe release in the acidic gastrointestinal environment and accumulation in other organs but also significantly enhanced the ability to actively target inflamed areas in IBD [340]. Zhang et al. utilized polystyrene nanospheres as carriers to prepare nanoscale domain-enhanced fluorescent nanospheres, which possess both fluorescence and colorimetric dual signal recognition capabilities, with a fluorescence quantum yield reaching up to 98.21% [341]. This dual-mode multifunctional fluorescent nanosphere facilitates instrument-free, ultra-sensitive, and rapid detection, accommodating various applications in biomedical and environmental monitoring. Overall, the integration of fluorescent probes and nanocarriers provides robust technological support for targeted drug delivery systems (Fig. 5g). Future research will increasingly focus on integrating fluorescent probes with various targeting ligands, optimizing the performance of targeted nano-drug delivery systems under different physiological and pathological conditions, thereby facilitating the translation of fluorescent nanocarrier targeted drug delivery systems from laboratory research to clinical applications.

Conclusion

Autoimmune diseases pose a significant threat to human health and quality of life. Currently, the primary focus for most AD is achieving standard treatment, which underscores the importance of early disease detection and accurate diagnosis. This article reviews the fundamental principles and developmental history of fluorescent probes, systematically analyzing their applications in various autoimmune diseases, including RA, SLE, pemphigus, Sjögren's syndrome, and thyroid disorders. It highlights the significant potential of fluorescent probes in early diagnosis, disease progression monitoring, and the evaluation of immunotherapy. We are encouraged to observe that fluorescent probe technology, with its advantages of high sensitivity, real-time imaging, and non-invasive detection, has become an essential tool for diagnosing and monitoring autoimmune diseases.

Although fluorescent probes have demonstrated substantial value in clinical practice, they continue to face numerous challenges, including issues related to probe specificity, stability, imaging resolution, and clinical implementation. In particular, when diagnosing various disease subtypes and formulating individualized treatment plans, enhancing the precision and operability of fluorescent probes remains a pressing issue that requires resolution.

The development of fluorescent probes is highly interdisciplinary, requiring a comprehensive understanding of various fields, including organic chemistry, biochemistry, medicinal chemistry, and photophysics. As our understanding of the mechanisms underlying diseases deepens, along with ongoing advancements in biochemistry and medicinal chemistry, theoretical research on the binding sites between biomarkers and probes will become increasingly enriched, providing a robust theoretical foundation for the development of novel fluorescent probes. We believe that fluorescent probes represent not only an innovative technological breakthrough but also a pivotal force driving the transformation of diagnosis and treatment for autoimmune diseases. Their immense potential in medical research and clinical applications heralds a new era of personalized and precise treatment in future medical developments, warranting our continued attention and exploration.

Acknowledgements

We express our gratitude to ChatGPT for its exceptional support in English language editing. The language generation capabilities of ChatGPT have proven to be a valuable resource for our paper, facilitating a more precise communication of our research content. We sincerely appreciate the efforts and innovation of the OpenAI team, as their accomplishments have profoundly and positively influenced the advancement of our research.

Author contributions

JC collected the literature, created tables, drew images and wrote the manuscript. MC collected the literature and revised the manuscript. XY conceptualised the study and took overall responsibility for the work. Junli Chen: writing—original draft, investigation, data curation. Mingkai Chen: writing—review & editing, investigation. Xiaolong Yu: validation, supervision, resources, funding acquisition, conceptualization. All authors contributed to the article and approved the submitted version.

Funding

The study was supported by Changzhou High-Level Medical Talents Training Project (2022CZBJ109), and Open project of Jiangsu Key Laboratory of Laboratory Medicine (JSKLM-Y-2024-003).

Availability of data and materials

No data was used for the research described in the article.

Declarations

Competing interests
The authors declare that they have no known competing financial interests or personal relationships that could have appeared to influence the work reported in this paper.

Received: 21 January 2025 Accepted: 25 March 2025
Published online: 09 April 2025

References

1. Sanz I, Lund F. Complexity and heterogeneity - the defining features of autoimmune disease. Curr Opin Immunol. 2019;61:iii–vi.
2. Fugger L, Jensen LT, Rossjohn J. Challenges, progress, and prospects of developing therapies to treat autoimmune diseases. Cell. 2020;181:63–80.
3. Song Y, Li J, Wu Y. Evolving understanding of autoimmune mechanisms and new therapeutic strategies of autoimmune disorders. Signal Transduct Target Ther. 2024;9:263.
4. Miller FW. The increasing prevalence of autoimmunity and autoimmune diseases: an urgent call to action for improved understanding, diagnosis, treatment, and prevention. Curr Opin Immunol. 2023;80:102266.
5. Mohamed-Ahmed O, Shang L, Wang L, Chen Z, Kartsonaki C, Bragg F. Incidence and prevalence of autoimmune diseases in China: a systematic review and meta-analysis of epidemiological studies. Glob Epidemiol. 2024;8:100158.
6. Yu X, Chen M, Wu J, Song R. Research progress of SIRTs activator resveratrol and its derivatives in autoimmune diseases. Front Immunol. 2024;15:1390907.
7. Menichelli D, Cormaci VM, Marucci S, Franchino G, Del Sole F, Capozza A, Fallarino A, Valeriani E, Violi F, Pignatelli P, Pastori D. Risk of venous thromboembolism in autoimmune diseases: a comprehensive review. Autoimmun Rev. 2023;22:103447.
8. McGee EE, Castro FA, Engels EA, Freedman ND, Pfeiffer RM, Nogueira L, Stolzenberg-Solomon R, McGlynn KA, Hemminki K, Koshiol J. Associations between autoimmune conditions and hepatobiliary cancer risk among elderly US adults. Int J Cancer. 2019;144:707–17.
9. Song M, Engels EA, Clarke MA, Kreimer AR, Shiels MS. Autoimmune disease and the risk of anal cancer in the US population aged 66 years and over. J Natl Cancer Inst. 2024;116:309–15.
10. Zhou Z, Liu H, Yang Y, Zhou J, Zhao L, Chen H, Fei Y, Zhang W, Li M, Zhao Y, et al. The five major autoimmune diseases increase the risk of cancer: epidemiological data from a large-scale cohort study in China. Cancer Commun (Lond). 2022;42:435–46.
11. Igoe A, Merjanah S, Harley ITW, Clark DH, Sun C, Kaufman KM, Harley JB, Kaelber DC, Scofield RH, Program VAMV. Association between systemic lupus erythematosus and myasthenia gravis: a population-based National Study. Clin Immunol. 2024;260:109810.
12. Sumelahti ML, Verkko A, Kyto V, Sipila JOT. Stable excess mortality in a multiple sclerosis cohort diagnosed 1970–2010. Eur J Neurol. 2024;31:e16480.
13. Yang TH, Xirasagar S, Cheng YF, Chen CS, Lin HC. Increased prevalence of hearing loss, tinnitus and sudden deafness among patients with Sjogren's syndrome. RMD Open. 2024;10:e003308.
14. Zhang X, Cheng I, Liu S, Li C, Xue JH, Tam LS, Yu W. Automatic 3D joint erosion detection for the diagnosis and monitoring of rheumatoid arthritis using hand HR-pQCT images. Comput Med Imaging Graph. 2023;106:102200.
15. Di Matteo A, Smerilli G, Cipolletta E, Salaffi F, De Angelis R, Di Carlo M, Filippucci E, Grassi W. Imaging of joint and soft tissue involvement in systemic lupus erythematosus. Curr Rheumatol Rep. 2021;23:73.
16. Allen A, Carville S, McKenna F. Diagnosis and management of rheumatoid arthritis in adults: summary of updated NICE guidance. BMJ. 2018;362:k3015.
17. Tanaka N, Kim JS, Newell JD, Brown KK, Cool CD, Meehan R, Emoto T, Matsumoto T, Lynch DA. Rheumatoid arthritis–related lung diseases: CT findings. Radiology. 2004;232:81–91.
18. Suter LG, Fraenkel L, Braithwaite RS. Role of magnetic resonance imaging in the diagnosis and prognosis of rheumatoid arthritis. Arthritis Care Res (Hoboken). 2011;63:675–88.
19. Yu H, Nagafuchi Y, Fujio K. Clinical and immunological biomarkers for systemic lupus erythematosus. Biomolecules. 2021;11:928.
20. Derksen V, Huizinga TWJ, van der Woude D. The role of autoantibodies in the pathophysiology of rheumatoid arthritis. Semin Immunopathol. 2017;39:437–46.
21. Kwon OC, Park MC. Risk of systemic lupus erythematosus flares according to autoantibody positivity at the time of diagnosis. Sci Rep. 2023;13:3068.
22. Bugatti S, Manzo A, Montecucco C, Caporali R. The clinical value of autoantibodies in rheumatoid arthritis. Front Med (Lausanne). 2018;5:339.
23. Chandwar K, Aggarwal A. Systemic lupus erythematosus in children. Indian J Pediatr. 2024;91:1032–40.
24. Rodriguez-Gonzalez D, Garcia-Gonzalez M, Gomez-Bernal F, Quevedo-Abeledo JC, Gonzalez-Rivero AF, Fernandez-Cladera Y, Gonzalez-Lopez E, Ocejo-Vinyals JG, Jimenez-Sosa A, Gonzalez-Toledo B, et al. Complete description of the three pathways of the complement system in a series of 430 patients with rheumatoid arthritis. Int J Mol Sci. 2024;25:8360.
25. Tsokos GC. Systemic lupus erythematosus. N Engl J Med. 2011;365:2110–21.
26. Scott DL, Wolfe F, Huizinga TW. Rheumatoid arthritis. Lancet. 2010;376:1094–108.
27. Koyama K, Ohba T, Odate T, Wako M, Haro H. Pathological features of established osteoarthritis with hydrathrosis are similar to rheumatoid arthritis. Clin Rheumatol. 2021;40:2007–12.
28. Piga M, Tselios K, Viveiros L, Chessa E, Neves A, Urowitz MB, Isenberg D. Clinical patterns of disease: from early systemic lupus erythematosus to late-onset disease. Best Pract Res Clin Rheumatol. 2023;37:101938.
29. Li K, Li L-L, Zhou Q, Yu K-K, Kim JS, Yu X-Q. Reaction-based fluorescent probes for SO2 derivatives and their biological applications. Coord Chem Rev. 2019;388:310–33.
30. Sharma A, Verwilst P, Li M, Ma D, Singh N, Yoo J, Kim Y, Yang Y, Zhu JH, Huang H, et al. Theranostic fluorescent probes. Chem Rev. 2024;124:2699–804.
31. Yang Y, Tang M, Cui H, Zhang C, Liu X, Han J, Wang J, Yu X. Development of xanthine oxidase activated NIR fluorescence probe in vivo imaging. Sens Actuators B Chem. 2025;422:136563.
32. Dai J, Ma C, Zhang P, Fu Y, Shen B. Recent progress in the development of fluorescent probes for detection of biothiols. Dyes Pigm. 2020;177:108321.
33. Lu S, Dai Z, Cui Y, Kong DM. Recent development of advanced fluorescent molecular probes for organelle-targeted cell imaging. Biosensors (Basel). 2023;13:360.
34. Ceredig R: George Gabriel Stokes as a biologist. Philosophical Transactions of the Royal Society A: Mathematical, Physical and Engineering Sciences 2020, 378:20200105.
35. Lohani A, Durgapal S, Morganti P. Quantum dots: an emerging implication of nanotechnology in cancer diagnosis and therapy. In: Henini M, Rodrigues MO, editors. Quantum materials, devices, and applications. Amsterdam: Elsevier; 2023. p. 243–62.
36. Noelting E, Dziewoński K. Zur Kenntniss der Rhodamine. Ber Dtsch Chem Ges. 2006;38:3516–27.
37. Liu C. Studies of influenza infection in ferrets by means of fluorescein-labelled antibody. I. The pathogenesis and diagnosis of the disease. J Exp Med. 1955;101:665–76.
38. Hiramoto R, Engel K, Pressman D. Tetramethylrhodamine as immunohistochemical fluorescent label in the study of chronic thyroiditis. Proc Soc Exp Biol Med. 1958;97:611–4.
39. Litt M. Studies in experimental eosinophilia. VI. Uptake of immune complexes by eosinoPHILS. J Cell Biol. 1964;23:355–61.
40. Shimomura O, Johnson FH, Saiga Y. Extraction, purification and properties of aequorin, a bioluminescent protein from the luminous hydromedusan, Aequorea. J Cell Comp Physiol. 1962;59:223–39.

41. Chalfie M, Tu Y, Euskirchen G, Ward WW, Prasher DC. Green fluorescent protein as a marker for gene expression. Science. 1994;263:802–5.
42. Drummen GP. Quantum dots-from synthesis to applications in biomedicine and life sciences. Int J Mol Sci. 2010;11:154–63.
43. Bruchez M Jr, Moronne M, Gin P, Weiss S, Alivisatos AP. Semiconductor nanocrystals as fluorescent biological labels. Science. 1998;281:2013–6.
44. Matz MV, Fradkov AF, Labas YA, Savitsky AP, Zaraisky AG, Markelov ML, Lukyanov SA. Fluorescent proteins from nonbioluminescent Anthozoa species. Nat Biotechnol. 1999;17:969–73.
45. Campbell RE, Tour O, Palmer AE, Steinbach PA, Baird GS, Zacharias DA, Tsien RY. A monomeric red fluorescent protein. Proc Natl Acad Sci U S A. 2002;99:7877–82.
46. Shaner NC, Campbell RE, Steinbach PA, Giepmans BN, Palmer AE, Tsien RY. Improved monomeric red, orange and yellow fluorescent proteins derived from Discosoma sp. red fluorescent protein. Nat Biotechnol. 2004;22:1567–72.
47. Ullah Z, Roy S, Gu J, Ko Soe S, Jin J, Guo B. NIR-II fluorescent probes for fluorescence-imaging-guided tumor surgery. Biosensors (Basel). 2024;14:282.
48. Chen Y, Sun B, Jiang X, Yuan Z, Chen S, Sun P, Fan Q, Huang W. Double-acceptor conjugated polymers for NIR-II fluorescence imaging and NIR-II photothermal therapy applications. J Mater Chem B. 2021;9:1002–8.
49. Ding C, Ren T. Near infrared fluorescent probes for detecting and imaging active small molecules. Coord Chem Rev. 2023;482:215080.
50. Franco W, Gutierrez-Herrera E, Kollias N, Doukas A. Review of applications of fluorescence excitation spectroscopy to dermatology. Br J Dermatol. 2016;174:499–504.
51. Wenzel M, Mitric R. Internal conversion rates from the extended thawed Gaussian approximation: theory and validation. J Chem Phys. 2023;158:034105.
52. Vaishakh M, Nampoori VPN. Chapter 8 - Thermooptic techniques: a tool for interdisciplinary studies. In: Thakur SN, Rai VN, Singh JP, editors. Photoacoustic and photothermal spectroscopy. Amsterdam: Elsevier; 2023. p. 185–216.
53. Zhang X, Wei C, Li Y, Yu D. Shining luminescent graphene quantum dots: synthesis, physicochemical properties, and biomedical applications. TrAC, Trends Anal Chem. 2019;116:109–21.
54. Wu L, Huang C, Emery BP, Sedgwick AC, Bull SD, He XP, Tian H, Yoon J, Sessler JL, James TD. Forster resonance energy transfer (FRET)-based small-molecule sensors and imaging agents. Chem Soc Rev. 2020;49:5110–39.
55. Daly B, Ling J, de Silva AP. Current developments in fluorescent PET (photoinduced electron transfer) sensors and switches. Chem Soc Rev. 2015;44:4203–11.
56. Liu P, Xu J, Yan D, Zhang P, Zeng F, Li B, Wu S. A DT-diaphorase responsive theranostic prodrug for diagnosis, drug release monitoring and therapy. Chem Commun (Camb). 2015;51:9567–70.
57. Lee MH, Kim JS, Sessler JL. Small molecule-based ratiometric fluorescence probes for cations, anions, and biomolecules. Chem Soc Rev. 2015;44:4185–91.
58. Gu K, Xu Y, Li H, Guo Z, Zhu S, Zhu S, Shi P, James TD, Tian H, Zhu WH. Real-time tracking and in vivo visualization of beta-galactosidase activity in colorectal tumor with a ratiometric near-infrared fluorescent probe. J Am Chem Soc. 2016;138:5334–40.
59. Kokorina AA, Ponomaryova TS, Goryacheva IY. Photoluminescence-based immunochemical methods for determination of C-reactive protein and procalcitonin. Talanta. 2021;224:121837.
60. Chen Y. Advances in organic fluorescent probes for intracellular Zn(2+) detection and bioimaging. Molecules. 2024;29:2542.
61. Qi L, Liu S, Ping J, Yao X, Chen L, Yang D, Liu Y, Wang C, Xiao Y, Qi L, et al. Recent advances in fluorescent nanoparticles for stimulated emission depletion imaging. Biosensors (Basel). 2024;14:314.
62. Quan L, Sun T, Wei Y, Lin Y, Gong T, Pan C, Ding H, Liu W, Xie Z. Poly(ε-caprolactone) modified organic dyes nanoparticles for noninvasive long term fluorescence imaging. Colloids Surf, B. 2019;173:884–90.
63. Zheng Y, Nandakumar KS, Cheng K. Optimization of CAR-T cell-based therapies using small-molecule-based safety switches. J Med Chem. 2021;64:9577–91.
64. Terada N, Ohno N, Li Z, Fujii Y, Baba T, Ohno S. Detection of injected fluorescence-conjugated IgG in living mouse organs using "in vivo cryotechnique" with freeze-substitution. Microsc Res Tech. 2005;66:173–8.
65. Yeo SJ, Cuc BT, Kim SA, Kim DTH, Bao DT, Tien TTT, Anh NTV, Choi DY, Chong CK, Kim HS, Park H. Rapid detection of avian influenza A virus by immunochromatographic test using a novel fluorescent dye. Biosens Bioelectron. 2017;94:677–85.
66. Su M, Zhao C, Luo S. Therapeutic potential of chimeric antigen receptor based therapies in autoimmune diseases. Autoimmun Rev. 2022;21:102931.
67. He X, Hu L, Zou L, Zhong J, Luo H, Pu Z. Enhanced fluorescence properties of flexible waterborne polyurethane films by blocking fluorescein isothiocyanate (FITC). Mater Lett. 2021;293:129668.
68. Kim YJ, Jang M, Roh J, Lee YJ, Moon HJ, Byun J, Wi J, Ko SK, Tae J. Rhodamine-based cyclic hydroxamate as fluorescent ph probe for imaging of lysosomes. Int J Mol Sci. 2023;24:15073.
69. Sulistina DR, Ratnawati R, Wiyasa IWA. Rhodamine B increases hypothalamic cell apoptosis and disrupts hormonal balance in rats. Asian Pac J Reprod. 2014;3:180–3.
70. Chen XX, Wu Y, Ge X, Lei L, Niu LY, Yang QZ, Zheng L. In vivo imaging of heart failure with preserved ejection fraction by simultaneous monitoring of cardiac nitric oxide and glutathione using a three-channel fluorescent probe. Biosens Bioelectron. 2022;214:114510.
71. Jung S, Chen X. Quantum dot-dye conjugates for biosensing, imaging, and therapy. Adv Healthc Mater. 2018;7:e1800252.
72. Zhang L, Jean SR, Ahmed S, Aldridge PM, Li X, Fan F, Sargent EH, Kelley SO. Multifunctional quantum dot DNA hydrogels. Nat Commun. 2017;8:381.
73. Wang Y, Tang M. Dysfunction of various organelles provokes multiple cell death after quantum dot exposure. Int J Nanomed. 2018;13:2729–42.
74. Wang S, Li JJ, Lv Y, Wu R, Xing M, Shen H, Wang H, Li LS, Chen X. Synthesis of reabsorption-suppressed type-II/type-I ZnSe/CdS/ZnS core/shell quantum dots and their application for immunosorbent assay. Nanoscale Res Lett. 2017;12:380.
75. Ren D, Wang B, Hu C, You Z. Quantum dot probes for cellular analysis. Anal Methods. 2017;9:2621–32.
76. Fu C, Qin X, Shao W, Zhang J, Zhang T, Yang J, Ding C, Song Y, Ge X, Wu G, et al. Carbon quantum dots as immune modulatory therapy in a Sjogren's syndrome mouse model. Oral Dis. 2024;30:1183–97.
77. Shang A, Shao S, Zhao L, Liu B. Far-red fluorescent proteins: tools for advancing in vivo imaging. Biosensors (Basel). 2024;14:359.
78. Chen YL, Xie XX, Zhong N, Sun LC, Lin D, Zhang LJ, Weng L, Jin T, Cao MJ. Research progresses and applications of fluorescent protein antibodies: a review focusing on nanobodies. Int J Mol Sci. 2023;24:4307.
79. Harla I, Pawlus W, Zarebski M, Dobrucki JW. Induction of DNA single- and double-strand breaks by excited intra- or extracellular green fluorescent protein. J Photochem Photobiol B. 2024;259:113001.
80. Bousmah Y, Valenta H, Bertolin G, Singh U, Nicolas V, Pasquier H, Tramier M, Merola F, Erard M. tdLanYFP, a yellow, bright, photostable, and pH-insensitive fluorescent protein for live-cell imaging and förster resonance energy transfer-based sensing strategies. ACS Sens. 2021;6:3940–7.
81. Zheng X, Yu X, Wang C, Liu Y, Jia M, Lei F, Tian J, Li C. Targeted co-delivery biomimetic nanoparticles reverse macrophage polarization for enhanced rheumatoid arthritis therapy. Drug Delivery. 2022;29:1025–37.
82. Liu F, Yan JR, Chen S, Yan GP, Pan BQ, Zhang Q, Wang YF, Gu YT. Polypeptide-rhodamine B probes containing laminin/fibronectin receptor-targeting sequence (YIGSR/RGD) for fluorescent imaging in cancers. Talanta. 2020;212:120718.
83. Yan F, Fan K, Bai Z, Zhang R, Zu F, Xu J, Li X. Fluorescein applications as fluorescent probes for the detection of analytes. TrAC, Trends Anal Chem. 2017;97:15–35.
84. Zhang Y, Qiao L-L, Zhang Z-Q, Liu Y-F, Li L-S, Shen H, Zhao M-X. A mitochondrial-targetable fluorescent probe based on high-quality InP quantum dots for the imaging of living cells. Mater Des. 2022;219:110736.
85. Kong J, Wei Y, Zhou F, Shi L, Zhao S, Wan M, Zhang X. Carbon quantum dots: properties, preparation, and applications. Molecules. 2024;29:2002.

86. Kong J, Wang Y, Qi W, Huang M, Su R, He Z. Green fluorescent protein inspired fluorophores. Adv Colloid Interface Sci. 2020;285:102286.
87. Jang BS, Lim E, Hee Park S, Shin IS, Danthi SN, Hwang IS, Le N, Yu S, Xie J, Li KC, et al. Radiolabeled high affinity peptidomimetic antagonist selectively targets alpha(v)beta(3) receptor-positive tumor in mice. Nucl Med Biol. 2007;34:363–70.
88. Narode YM, Mokashi VM, Sharma GK. Rhodamine 6G capped gold nanoparticles: a fluorescent probe for monitoring the radiation induced oxidation of Glutathione. J Lumin. 2018;201:479–84.
89. Swanson WB, Durdan M, Eberle M, Woodbury S, Mauser A, Gregory J, Zhang B, Niemann D, Herremans J, Ma PX, et al. A library of Rhodamine6G-based pH-sensitive fluorescent probes with versatile in vivo and in vitro applications. RSC Chem Biol. 2022;3:748–64.
90. Torres MAM, Veglia AV, Pacioni NL. The fluorescence quenching of rhodamine 6G as an alternative sensing strategy for the quantification of silver and gold nanoparticles. Microchem J. 2021;160:105645.
91. Zhang T, He WH, Feng LL, Huang HG. Effect of doxorubicin-induced ovarian toxicity on mouse ovarian granulosa cells. Regul Toxicol Pharmacol. 2017;86:1–10.
92. Royall JA, Ischiropoulos H. Evaluation of 2',7'-dichlorofluorescin and dihydrorhodamine 123 as fluorescent probes for intracellular H2O2 in cultured endothelial cells. Arch Biochem Biophys. 1993;302:348–55.
93. Sun XY, Liu T, Sun J, Wang XJ. Synthesis and application of coumarin fluorescence probes. RSC Adv. 2020;10:10826–47.
94. Lv Y, Cheng Y, Lv K, Zhang G, Wu J. Felodipine determination by a CdTe quantum dot-based fluorescent probe. Micromachines (Basel). 2022;13:788.
95. Ning L, Geng Y, Lovett-Barron M, Niu X, Deng M, Wang L, Ataie N, Sens A, Ng HL, Chen S, et al. A bright, nontoxic, and non-aggregating red fluorescent protein for long-term labeling of fine structures in neurons. Front Cell Dev Biol. 2022;10:893468.
96. Fan Y, Chen Z, Ai HW. Monitoring redox dynamics in living cells with a redox-sensitive red fluorescent protein. Anal Chem. 2015;87:2802–10.
97. Aletaha D, Smolen JS. Diagnosis and management of rheumatoid arthritis: a review. JAMA. 2018;320:1360–72.
98. Aljohani RA, Aljanobi GA, Alderaan K, Omair MA. Exploring the quality of life and comorbidity impact among patients with systemic lupus erythematosus in Saudi Arabia. Saudi Med J. 2024;45:1071–9.
99. Yu X, Jin Z, Raza F, Zhang P, Wu J, Ren M, Wang J, Xi J. SIRT6 reduces rheumatoid arthritis injury by inhibiting MyD88-ERK signaling pathway. Front Biosci (Landmark Ed). 2024;29:5.
100. Tong X, Chen W, Ye L, Xiong Y, Xu Y, Luo Y, Xia X, Xu Z, Lin Y, Zhu X, et al. 5-Hydroxymethylcytosine in circulating cell-free DNA as a potential diagnostic biomarker for SLE. Lupus Sci Med. 2024;11:e001286.
101. Thiolat A, Semerano L, Pers YM, Biton J, Lemeiter D, Portales P, Quentin J, Jorgensen C, Decker P, Boissier MC, et al. Interleukin-6 receptor blockade enhances CD39+ regulatory T cell development in rheumatoid arthritis and in experimental arthritis. Arthritis Rheumatol. 2014;66:273–83.
102. Ragab D, Mobasher S, Shabaan E. Elevated levels of IL-37 correlate with T cell activation status in rheumatoid arthritis patients. Cytokine. 2019;113:305–10.
103. Moret FM, Hack CE, van der Wurff-Jacobs KM, de Jager W, Radstake TR, Lafeber FP, van Roon JA. Intra-articular CD1c-expressing myeloid dendritic cells from rheumatoid arthritis patients express a unique set of T cell-attracting chemokines and spontaneously induce Th1, Th17 and Th2 cell activity. Arthritis Res Ther. 2013;15:R155.
104. Koppejan H, Jansen D, Hameetman M, Thomas R, Toes REM, van Gaalen FA. Altered composition and phenotype of mucosal-associated invariant T cells in early untreated rheumatoid arthritis. Arthritis Res Ther. 2019;21:3.
105. Wen G, Lei H, Qi B, Duan S, Xiao Z, Han C, Xia Y, Jing C, Liu J, Li C. Non-invasive imaging OX40(+) activated T cells provides early warning of rheumatoid arthritis. Mol Imaging Biol. 2023;25:621–9.
106. Duan S, Han C, Xia Y, Jing C, Dong B, Zhang X, Wang W, Wang Y, Zhang M, Li P, et al. Fluorophore-conjugated 4–1BB antibody enables early detection of T-cell responses in inflammatory arthritis via NIRF imaging. Eur J Nucl Med Mol Imaging. 2022;50:38–47.
107. Lam AD, Styles IK, Senyschyn D, Cao E, Anshabo A, Abdallah M, Mikrani R, Nowell CJ, Porter CJH, Feeney OM, Trevaskis NL. Intra-articular injection of a B cell depletion antibody enhances local exposure to the joint-draining lymph node in mice with collagen-induced arthritis. Mol Pharm. 2023;20:2053–66.
108. Reijm S, Kwekkeboom JC, Blomberg NJ, Suurmond J, van der Woude D, Toes RE, Scherer HU. Autoreactive B cells in rheumatoid arthritis include mainly activated CXCR3+ memory B cells and plasmablasts. JCI Insight. 2023. https://doi.org/10.1172/jci.insight.172006.
109. You H, Cheng M, Ma C, Zheng W, Jiang Y, Chen D, Tang Y. Association among B lymphocyte subset and rheumatoid arthritis in a Chinese population. J Orthop Surg Res. 2021;16:732.
110. An Q, Yan W, Zhao Y, Yu K. Enhanced neutrophil autophagy and increased concentrations of IL-6, IL-8, IL-10 and MCP-1 in rheumatoid arthritis. Int Immunopharmacol. 2018;65:119–28.
111. Li W, Jiang W, Dai S, Wang L. Multiplexed detection of cytokines based on dual bar-code strategy and single-molecule counting. Anal Chem. 2016;88:1578–84.
112. Godmann L, Bollmann M, Korb-Pap A, König U, Sherwood J, Beckmann D, Mühlenberg K, Echtermeyer F, Whiteford J, De Rossi G, et al. Antibody-mediated inhibition of syndecan-4 dimerisation reduces interleukin (IL)-1 receptor trafficking and signalling. Ann Rheum Dis. 2020;79:481–9.
113. Symons RA, Colella F, Collins FL, Rafipay AJ, Kania K, McClure JJ, White N, Cunningham I, Ashraf S, Hay E, et al. Targeting the IL-6-Yap-Snail signalling axis in synovial fibroblasts ameliorates inflammatory arthritis. Ann Rheum Dis. 2022;81:214–24.
114. Ruscitti P, Liakouli V, Panzera N, Angelucci A, Berardicurti O, Di Nino E, Navarini L, Vomero M, Ursini F, Mauro D, et al. Tofacitinib may inhibit myofibroblast differentiation from rheumatoid-fibroblast-like synoviocytes induced by TGF-beta and IL-6. Pharmaceuticals (Basel). 2022;15:622.
115. de Paz B, Prado C, Alperi-Lopez M, Ballina-Garcia FJ, Rodriguez-Carrio J, Lopez P, Suarez A. Effects of glucocorticoid treatment on CD25(-) FOXP3(+) population and cytokine-producing cells in rheumatoid arthritis. Rheumatology (Oxford). 2012;51:1198–207.
116. Schlegel PM, Steiert I, Kotter I, Muller CA. B cells contribute to heterogeneity of IL-17 producing cells in rheumatoid arthritis and healthy controls. PLoS ONE. 2013;8:e82580.
117. Navratilova A, Becvar V, Hulejova H, Tomcik M, Stolova L, Mann H, Ruzickova O, Sleglova O, Zavada J, Pavelka K, et al. New pro-inflammatory cytokine IL-40 is produced by activated neutrophils and plays a role in the early stages of seropositive rheumatoid arthritis. RMD Open. 2023;9:e002894.
118. Senolt L, Prajzlerova K, Hulejova H, Sumova B, Filkova M, Veigl D, Pavelka K, Vencovsky J. Interleukin-20 is triggered by TLR ligands and associates with disease activity in patients with rheumatoid arthritis. Cytokine. 2017;97:187–92.
119. Fournelle M, Bost W, Tarner IH, Lehmberg T, Weiss E, Lemor R, Dinser R. Antitumor necrosis factor-alpha antibody-coupled gold nanorods as nanoprobes for molecular optoacoustic imaging in arthritis. Nanomedicine. 2012;8:346–54.
120. Chen Y, Dawes PT, Mattey DL. Polymorphism in the vascular endothelial growth factor A (VEGFA) gene is associated with serum VEGF-A level and disease activity in rheumatoid arthritis: differential effect of cigarette smoking. Cytokine. 2012;58:390–7.
121. Huang H, Li S, Han X, Zhang Y, Gao L, Wang X, Wang G, Chen Z. A rapid VEGF-gene-sequence photoluminescence detector for osteoarthritis. Front Bioeng Biotechnol. 2024;12:1338901.
122. Fuentelsaz-Romero S, Cuervo A, Estrada-Capetillo L, Celis R, Garcia-Campos R, Ramirez J, Sastre S, Samaniego R, Puig-Kroger A, Canete JD. GM-CSF expression and macrophage polarization in joints of undifferentiated arthritis patients evolving to rheumatoid arthritis or psoriatic arthritis. Front Immunol. 2020;11:613975.
123. Lu J, Li Z, Zheng X, Tan J, Ji Z, Sun Z, You J. A rapid response near-infrared ratiometric fluorescent probe for the real-time tracking of peroxynitrite for pathological diagnosis and therapeutic assessment in a rheumatoid arthritis model. J Mater Chem B. 2020;8:9343–50.
124. Zheng F, Luo S, Ouyang Z, Zhou J, Mo H, Schoonooghe S, Muyldermans S, De Baetselier P, Raes G, Wen Y. NIRF-molecular imaging with synovial macrophages-targeting Vsig4 nanobody for disease monitoring in a mouse model of arthritis. Int J Mol Sci. 2019;20:3347.
125. Toribio RE, Young N, Schlesinger LS, Cope FO, Ralph DA, Jarjour W, Rosol TJ. Cy3-tilmanocept labeling of macrophages in joints of mice

with antibody-induced arthritis and synovium of human patients with rheumatoid arthritis. J Orthop Res. 2021;39:821–30.
126. Tsen SD, Springer LE, Sharmah Gautam K, Tang R, Liang K, Sudlow G, Kucharski A, Pham CTN, Achilefu S. Non-invasive monitoring of arthritis treatment response via targeting of tyrosine-phosphorylated annexin A2 in chondrocytes. Arthritis Res Ther. 2021;23:265.
127. Wu H, Wu H, He Y, Gan Z, Xu Z, Zhou M, Liu S, Liu H. Synovitis in mice with inflammatory arthritis monitored with quantitative analysis of dynamic contrast-enhanced NIR fluorescence imaging using iRGD-targeted liposomes as fluorescence probes. Int J Nanomed. 2018;13:1841–50.
128. Lee JH, Jung SY, Park GK, Bao K, Hyun H, El Fakhri G, Choi HS. Fluorometric imaging for early diagnosis and prognosis of rheumatoid arthritis. Adv Sci (Weinh). 2020;7:1902267.
129. Brown PM, Anderson AE, Naamane N, Lendrem DW, Morgan AW, Isaacs JD, Pratt AG. Adenosine metabolic signature in circulating CD4+ T cells predicts remission in rheumatoid arthritis. RMD Open. 2024;10:e003858.
130. Feng H, Zhang Z, Meng Q, Jia H, Wang Y, Zhang R. Rapid response fluorescence probe enabled in vivo diagnosis and assessing treatment response of hypochlorous acid-mediated rheumatoid arthritis. Adv Sci (Weinh). 2018;5:1800397.
131. Kofoed Andersen C, Khatri S, Hansen J, Slott S, Pavan Parvathaneni R, Mendes AC, Chronakis IS, Hung SC, Rajasekaran N, Ma Z, et al. Carbon nanotubes-potent carriers for targeted drug delivery in rheumatoid arthritis. Pharmaceutics. 2021;13:453.
132. Wu H, He Y, Wu H, Zhou M, Xu Z, Xiong R, Yan F, Liu H. Near-infrared fluorescence imaging-guided focused ultrasound-mediated therapy against Rheumatoid Arthritis by MTX-ICG-loaded iRGD-modified echogenic liposomes. Theranostics. 2020;10:10092–105.
133. Lee SJ, Lee A, Hwang SR, Park JS, Jang J, Huh MS, Jo DG, Yoon SY, Byun Y, Kim SH, et al. TNF-alpha gene silencing using polymerized siRNA/thiolated glycol chitosan nanoparticles for rheumatoid arthritis. Mol Ther. 2014;22:397–408.
134. Tsokos GC, Lo MS, Reis PC, Sullivan KE. New insights into the immunopathogenesis of systemic lupus erythematosus. Nat Rev Rheumatol. 2016;12:716–30.
135. Bossuyt X, De Langhe E, Borghi MO, Meroni PL. Understanding and interpreting antinuclear antibody tests in systemic rheumatic diseases. Nat Rev Rheumatol. 2020;16:715–26.
136. Abozaid HSM, Hefny HM, Abualfadl EM, Ismail MA, Noreldin AK, Eldin ANN, Goda AM, Ali AH. Negative ANA-IIF in SLE patients: what is beyond? Clin Rheumatol. 2023;42:1819–26.
137. Chan EKL, von Mühlen CA, Fritzler MJ, Damoiseaux J, Infantino M, Klotz W, Satoh M, Musset L, García-De La Torre I, Carballo OG, et al. The international consensus on ANA patterns (ICAP) in 2021—The 6th workshop and current perspectives. J Appl Lab Med. 2022;7:322–30.
138. Damoiseaux J, Andrade LEC, Carballo OG, Conrad K, Francescantonio PLC, Fritzler MJ, Garcia de la Torre I, Herold M, Klotz W, Cruvinel WM, et al. Clinical relevance of HEp-2 indirect immunofluorescent patterns: the International Consensus on ANA patterns (ICAP) perspective. Ann Rheum Dis. 2019;78:879–89.
139. Zhang T, Du Y, Wu Q, Li H, Nguyen T, Gidley G, Duran V, Goldman D, Petri M, Mohan C. Salivary anti-nuclear antibody (ANA) mirrors serum ANA in systemic lupus erythematosus. Arthritis Res Ther. 2022;24:3.
140. Zhao Z, Xu B, Wang S, Zhou M, Huang Y, Guo C, Li M, Zhao J, Sung SJ, Gaskin F, et al. Tfh cells with NLRP3 inflammasome activation are essential for high-affinity antibody generation, germinal centre formation and autoimmunity. Ann Rheum Dis. 2022;81:1006–12.
141. Yang P, Zhang X, Chen S, Tao Y, Ning M, Zhu Y, Liang J, Kong W, Shi B, Li Z, et al. A novel serum tsRNA for diagnosis and prediction of nephritis in SLE. Front Immunol. 2021;12:735105.
142. Esfandiary L, Gupta N, Voigt A, Wanchoo A, Chan EK, Sukumaran S, Nguyen CQ. Single-cell antibody nanowells: a novel technology in detecting anti-SSA/Ro60- and anti-SSB/La autoantibody-producing cells in peripheral blood of rheumatic disease patients. Arthritis Res Ther. 2016;18:107.
143. Lood C, Blanco LP, Purmalek MM, Carmona-Rivera C, De Ravin SS, Smith CK, Malech HL, Ledbetter JA, Elkon KB, Kaplan MJ. Neutrophil extracellular traps enriched in oxidized mitochondrial DNA are interferogenic and contribute to lupus-like disease. Nat Med. 2016;22:146–53.
144. Han L, Shen L, Zhu Y, Qiu Y. A monoclonal antibody against CD86 and its protection in a murine lupus nephritis model of chronic graft-versus-host disease. Immunopharmacol Immunotoxicol. 2017;39:285–91.
145. Anders HJ, Saxena R, Zhao MH, Parodis I, Salmon JE, Mohan C. Lupus nephritis. Nat Rev Dis Primers. 2020;6:7.
146. Almaani S, Meara A, Rovin BH. Update on lupus nephritis. Clin J Am Soc Nephrol. 2017;12:825–35.
147. Hogan JJ, Mocanu M, Berns JS. The native kidney biopsy: update and evidence for best practice. Clin J Am Soc Nephrol. 2016;11:354–62.
148. Parikh SV, Alvarado A, Malvar A, Rovin BH. The kidney biopsy in lupus nephritis: past, present, and future. Semin Nephrol. 2015;35:465–77.
149. Iyama T, Takata T, Yamada K, Mae Y, Taniguchi S, Ida A, Ogawa M, Yamamoto M, Hamada S, Fukuda S, et al. A novel method for assessing the renal biopsy specimens using an activatable fluorescent probe. Sci Rep. 2020;10:12094.
150. Tang Y, Peng J, Guo R, Lu H, Lin W. A Cys-regulated two-photon lysosomal targetable fluorescent probe and its application for the diagnosis of kidney diseases. J Lumin. 2023;257:119745.
151. Garcia E, Lightley J, Kumar S, Kalita R, Gorlitz F, Alexandrov Y, Cook T, Dunsby C, Neil MA, Roufosse CA, French PM. Application of direct stochastic optical reconstruction microscopy (dSTORM) to the histological analysis of human glomerular disease. J Pathol Clin Res. 2021;7:438–45.
152. Okon LG, Werth VP. Cutaneous lupus erythematosus: diagnosis and treatment. Best Pract Res Clin Rheumatol. 2013;27:391–404.
153. Garelli CJ, Refat MA, Nanaware PP, Ramirez-Ortiz ZG, Rashighi M, Richmond JM. Current insights in cutaneous lupus erythematosus immunopathogenesis. Front Immunol. 2020;11:1353.
154. Udompanich S, Chanprapaph K, Suchonwanit P. Hair and scalp changes in cutaneous and systemic lupus erythematosus. Am J Clin Dermatol. 2018;19:679–94.
155. Niebel D, de Vos L, Fetter T, Bragelmann C, Wenzel J. Cutaneous lupus erythematosus: an update on pathogenesis and future therapeutic directions. Am J Clin Dermatol. 2023;24:521–40.
156. Vale E, Garcia LC. Cutaneous lupus erythematosus: a review of etiopathogenic, clinical, diagnostic and therapeutic aspects. An Bras Dermatol. 2023;98:355–72.
157. Reich A, Marcinow K, Bialynicki-Birula R. The lupus band test in systemic lupus erythematosus patients. Ther Clin Risk Manag. 2011;7:27–32.
158. Elbendary A, Zhou C, Valdebran M, Yu Y, Gad A, Kwon EJ, Elston DM. Specificity of granular IgM deposition in folliculosebaceous units and sweat gland apparatus in direct immunofluorescence (DIF) of lupus erythematosus. J Am Acad Dermatol. 2016;75:404–9.
159. Carlé C, Fortenfant F, Tauber M, Tournier E, Paul C, Bost C, Renaudineau Y. Lupus band test can be used in combination with anti-chromatin antibodies and complement analysis to predict transition from cutaneous to systemic lupus. Clin Immunol. 2022;234:108908.
160. Sinem Bağcı I, Aoki R, Vladimirova G, Ergün E, Ruzicka T, Sárdy M, French LE, Hartmann D. New-generation diagnostics in inflammatory skin diseases: Immunofluorescence and histopathological assessment using ex vivo confocal laser scanning microscopy in cutaneous lupus erythematosus. Exp Dermatol. 2021;30:684–90.
161. Kuhn A, Wenzel J, Weyd H. Photosensitivity, apoptosis, and cytokines in the pathogenesis of lupus erythematosus: a critical review. Clin Rev Allergy Immunol. 2014;47:148–62.
162. Kuhn A, Wozniacka A, Szepietowski JC, Glaser R, Lehmann P, Haust M, Sysa-Jedrzejowska A, Reich A, Oke V, Hugel R, et al. Photoprovocation in cutaneous lupus erythematosus: a multicenter study evaluating a standardized protocol. J Invest Dermatol. 2011;131:1622–30.
163. Lonnqvist S, Junker JPE, Sedell M, Nyman E, Kratz G. Tracking keratinocytes and melanocytes using carboxyfluorescein hydroxysuccinimidyl ester staining. PLoS ONE. 2019;14:e0221878.
164. Katsuyama Y, Sato Y, Okano Y, Masaki H. Intracellular oxidative stress induced by calcium influx initiates the activation of phagocytosis in keratinocytes accumulating at S-phase of the cell cycle after UVB irradiation. J Dermatol Sci. 2021;103:41–8.
165. May AL, Wood FM, Stoner ML. Assessment of adhesion assays for use with keratinocytes. Exp Dermatol. 2001;10:62–9.
166. Yap DYH, Chan TM. B cell abnormalities in systemic lupus erythematosus and lupus nephritis-role in pathogenesis and effect of immunosuppressive treatments. Int J Mol Sci. 2019;20:6231.

167. Vincent FB, Kandane-Rathnayake R, Koelmeyer R, Harris J, Hoi AY, Mackay F, Morand EF. Associations of serum soluble Fas and Fas ligand (FasL) with outcomes in systemic lupus erythematosus. Lupus Sci Med. 2020;7:e000375.
168. Yang F, He Y, Zhai Z, Sun E. Programmed cell death pathways in the pathogenesis of systemic lupus erythematosus. J Immunol Res. 2019;2019:3638562.
169. Liu X, Lu L, Zhang N, Jiang W. Regulator-carrying dual-responsive integrated AuNP composite fluorescence probe for in situ real time monitoring apoptosis progression. Talanta. 2024;269:125507.
170. Yang R, Zhu C, Yang X, Kuang Y, Jiang T, Wang S, Wei M. Simultaneous dual-color visualization of lysosome, mitochondria, nucleoli and monitoring apoptosis with a single fluorescent probe. Sens Actuators B Chem. 2025;424:136912.
171. Lyu X, Chi X, Li C, Niu J, Liu Y, Jin W, Hao Q, Liu Z, Wang K-N, Yu X. A hydrophilic lysosome-nucleolus immigration fluorescent probe for tracking normal cells from apoptosis to necrosis. Sens Actuators B Chem. 2024;406:135442.
172. Lin Z, Zhang L, Li D. Interpret the potential role of zinc against oxidative stress in inflammation with a practical fluorescent assay. Bioorg Chem. 2024;153:107886.
173. Meng Z, Liu J, Yu T, Shang Z, Wang Y, Shuang S. Novel ratiometric fluorescent probe with large Stokes shift for selective sensing and imaging of Zn(2+) in live cell. Spectrochim Acta A Mol Biomol Spectrosc. 2024;320:124645.
174. Ryo K, Yamada H, Nakagawa Y, Tai Y, Obara K, Inoue H, Mishima K, Saito I. Possible involvement of oxidative stress in salivary gland of patients with Sjogren's syndrome. Pathobiology. 2006;73:252–60.
175. Li M, Wang R, Lei P, Ma D, Shuang S, Dong C, Zhang L. Observation of polarity changes in Sjogren's syndrome mice using a targeting lysosomes and ratiometric fluorescent probe. Talanta. 2024;280:126787.
176. Abdul Sisak MA, Louis F, Aoki I, Lee SH, Chang YT, Matsusaki M. A near-infrared organic fluorescent probe for broad applications for blood vessels imaging by high-throughput screening via 3D-blood vessel models. Small Methods. 2021;5:e2100338.
177. Shoeibi A, Khodatars M, Jafari M, Moridian P, Rezaei M, Alizadehsani R, Khozeimeh F, Gorriz JM, Heras J, Panahiazar M, et al. Applications of deep learning techniques for automated multiple sclerosis detection using magnetic resonance imaging: a review. Comput Biol Med. 2021;136:104697.
178. Hodgson BM, Ossa AJ, Velasco FN, Urrejola NP, Arteaga LIA. Clinical picture at the onset of type 1 diabetes mellitus in children. Rev Med Chil. 2006;134:1535–40.
179. Correale J, Gaitan MI, Ysrraelit MC, Fiol MP. Progressive multiple sclerosis: from pathogenic mechanisms to treatment. Brain. 2017;140:527–46.
180. Kawakami N, Flugel A. Knocking at the brain's door: intravital two-photon imaging of autoreactive T cell interactions with CNS structures. Semin Immunopathol. 2010;32:275–87.
181. Othy S, Jairaman A, Dynes JL, Dong TX, Tune C, Yeromin AV, Zavala A, Akunwafo C, Chen F, Parker I, Cahalan MD. Regulatory T cells suppress Th17 cell Ca(2+) signaling in the spinal cord during murine autoimmune neuroinflammation. Proc Natl Acad Sci U S A. 2020;117:20088–99.
182. Lopez-Muguruza E, Matute C. Alterations of oligodendrocyte and myelin energy metabolism in multiple sclerosis. Int J Mol Sci. 2023;24:12912.
183. Zhao X, Jacob C. Mechanisms of demyelination and remyelination strategies for multiple sclerosis. Int J Mol Sci. 2023;24:6373.
184. Bourassa D, Elitt CM, McCallum AM, Sumalekshmy S, McRae RL, Morgan MT, Siegel N, Perry JW, Rosenberg PA, Fahrni CJ. Chromis-1, a ratiometric fluorescent probe optimized for two-photon microscopy reveals dynamic changes in labile Zn(II) in differentiating oligodendrocytes. ACS Sens. 2018;3:458–67.
185. Zia S, Hammond BP, Zirngibl M, Sizov A, Baaklini CS, Panda SP, Ho MFS, Lee KV, Mainali A, Burr MK, et al. Single-cell microglial transcriptomics during demyelination defines a microglial state required for lytic carcass clearance. Mol Neurodegener. 2022;17:82.
186. Kim B, Fukuda M, Lee JY, Su D, Sanu S, Silvin A, Khoo ATT, Kwon T, Liu X, Chi W, et al. Visualizing microglia with a fluorescence turn-on Ugt1a7c substrate. Angew Chem Int Ed Engl. 2019;58:7972–6.
187. Pinto MV, Santos FMF, Barros C, Ribeiro AR, Pischel U, Gois PMP, Fernandes A. BASHY dye platform enables the fluorescence bioimaging of myelin debris phagocytosis by microglia during demyelination. Cells. 2021;10:3163.
188. Morse SV, Boltersdorf T, Chan TG, Gavins FNE, Choi JJ, Long NJ. In vivo delivery of a fluorescent FPR2/ALX-targeted probe using focused ultrasound and microbubbles to image activated microglia. RSC Chem Biol. 2020;1:385–9.
189. Dai H, Navath RS, Balakrishnan B, Guru BR, Mishra MK, Romero R, Kannan RM, Kannan S. Intrinsic targeting of inflammatory cells in the brain by polyamidoamine dendrimers upon subarachnoid administration. Nanomedicine (Lond). 2010;5:1317–29.
190. Garg N, Smith TW. An update on immunopathogenesis, diagnosis, and treatment of multiple sclerosis. Brain Behav. 2015;5:e00362.
191. Monsma PC, Brown A. FluoroMyelin Red is a bright, photostable and non-toxic fluorescent stain for live imaging of myelin. J Neurosci Methods. 2012;209:344–50.
192. Condie AG, Gerson SL, Miller RH, Wang Y. Two-photon fluorescent imaging of myelination in the spinal cord. ChemMedChem. 2012;7:2194–203.
193. Wu MY, Wong AYH, Leung JK, Kam C, Wu KL, Chan YS, Liu K, Ip NY, Chen S. A near-infrared AIE fluorescent probe for myelin imaging: from sciatic nerve to the optically cleared brain tissue in 3D. Proc Natl Acad Sci U S A. 2021;118:e2106143118.
194. Benkowska-Biernacka D, Mucha SG, Firlej L, Formalik F, Bantignies JL, Anglaret E, Samoc M, Matczyszyn K. Strongly emitting folic acid-derived carbon nanodots for one- and two-photon imaging of lyotropic myelin figures. ACS Appl Mater Interfaces. 2023;15:32717–31.
195. Sun H, Du Y, Chen X, Jiang H, Li Y, Shen L. Design, synthesis, and evaluation of nile red analogs for myelin imaging as near-infrared fluorescence probe. Dyes Pigments. 2023;208:110804.
196. Lomakin Y, Kudriaeva A, Kostin N, Terekhov S, Kaminskaya A, Chernov A, Zakharova M, Ivanova M, Simaniv T, Telegin G, et al. Diagnostics of autoimmune neurodegeneration using fluorescent probing. Sci Rep. 2018;8:12679.
197. Wang C, Wu C, Popescu DC, Zhu J, Macklin WB, Miller RH, Wang Y. Longitudinal near-infrared imaging of myelination. J Neurosci. 2011;31:2382–90.
198. Liu Z, Li Y, Zhang J, Elias S, Chopp M. Evaluation of corticospinal axon loss by fluorescent dye tracing in mice with experimental autoimmune encephalomyelitis. J Neurosci Methods. 2008;167:191–7.
199. Hernandez-Torres G, Enriquez-Palacios E, Mecha M, Feliu A, Rueda-Zubiaurre A, Angelina A, Martin-Cruz L, Martin-Fontecha M, Palomares O, Guaza C, et al. Development of a fluorescent bodipy probe for visualization of the Serotonin 5-HT(1A) receptor in native cells of the immune system. Bioconjug Chem. 2018;29:2021–7.
200. Mi L, Niu C, Chen J, Han F, Ji X. Development of an activatable far-red fluorescent probe for rapid visualization of hypochlorous acid in live cells and mice with neuroinflammation. Front Chem. 2024;12:1355238.
201. Gonzalez LF, Acuna E, Arellano G, Morales P, Sotomayor P, Oyarzun-Ampuero F, Naves R. Intranasal delivery of interferon-beta-loaded nanoparticles induces control of neuroinflammation in a preclinical model of multiple sclerosis: a promising simple, effective, non-invasive, and low-cost therapy. J Control Release. 2021;331:443–59.
202. Moscarello MA, Mastronardi FG, Wood DD. The role of citrullinated proteins suggests a novel mechanism in the pathogenesis of multiple sclerosis. Neurochem Res. 2007;32:251–6.
203. Kunieda K, Kawaguchi M, Ieda N, Nakagawa H. Development of a highly sensitive fluorescence probe for peptidyl arginine deiminase (PAD) activity. Bioorg Med Chem Lett. 2019;29:923–8.
204. Atkinson MA, von Herrath M, Powers AC, Clare-Salzler M. Current concepts on the pathogenesis of type 1 diabetes–considerations for attempts to prevent and reverse the disease. Diabetes Care. 2015;38:979–88.
205. Babon JA, DeNicola ME, Blodgett DM, Crevecoeur I, Buttrick TS, Maehr R, Bottino R, Naji A, Kaddis J, Elyaman W, et al. Analysis of self-antigen specificity of islet-infiltrating T cells from human donors with type 1 diabetes. Nat Med. 2016;22:1482–7.
206. Musthaffa Y, Nel HJ, Ramnoruth N, Patel S, Hamilton-Williams EE, Harris M, Thomas R. Optimization of a method to detect autoantigen-specific T-cell responses in type 1 diabetes. Front Immunol. 2020;11:587469.
207. Bertrand R, Wolf A, Ivashchenko Y, Lohn M, Schafer M, Bronstrup M, Gotthardt M, Derdau V, Plettenburg O. Synthesis and characterization of a

promising novel FFAR1/GPR40 targeting fluorescent probe for beta-cell imaging. ACS Chem Biol. 2016;11:1745–54.
208. Reiner T, Thurber G, Gaglia J, Vinegoni C, Liew CW, Upadhyay R, Kohler RH, Li L, Kulkarni RN, Benoist C, et al. Accurate measurement of pancreatic islet beta-cell mass using a second-generation fluorescent exendin-4 analog. Proc Natl Acad Sci U S A. 2011;108:12815–20.
209. Komatsu H, Omori K, Parimi M, Rawson J, Kandeel F, Mullen Y. Determination of islet viability using a zinc-specific fluorescent dye and a semiautomated assessment method. Cell Transplant. 2016;25:1777–86.
210. Krinochkin A, Valieva M, Starnovskaya E, Slovesnova N, Minin A, Belousova A, Sadieva L, Taniya O, Khasanov A, Novikov A, et al. New fluorescent dye for the detection of Zn(2+) in living cells and fixed sections of the rat pancreas. J Fluoresc. 2024. https://doi.org/10.1007/s10895-024-03603-1.
211. Taghian T, Metelev VG, Zhang S, Bogdanov AA. Imaging NF-κB activity in a murine model of early stage diabetes. FASEB J. 2019;34:1198–210.
212. Yu X, Xing Y, Zhang Y, Zhang P, He Y, Ghamsari F, Ramasubramanian MK, Wang Y, Ai H, Oberholzer J. Smartphone-microfluidic fluorescence imaging system for studying islet physiology. Front Endocrinol (Lausanne). 2022;13:1039912.
213. Yang K, Tian Y, Zheng B, Wu F, Hu T, Yang Y, Pan J, Xiong H, Wang S. Fast-responsive HClO-activated near-infrared fluorescent probe for in vivo diagnosis of inflammatory bowel disease and ex vivo optical fecal analysis. Anal Chem. 2024;96:12065–73.
214. Liu S, Zhu Y, Wu P, Xiong H. Highly sensitive D-A-D-type near-infrared fluorescent probe for nitric oxide real-time imaging in inflammatory bowel disease. Anal Chem. 2021;93:4975–83.
215. Jin X, Wang Q, Xie T, Xu ST, Chen DA, Cao GY, Wang G, Wang J, Zhen L. Dual-locked chemiluminescent probe enables precise imaging and timely diagnosis of colitis via chymotrypsin/Vanin-1 cascade activation. Anal Chem. 2024;96:18635–44.
216. Xu W, He L, Xia Q, Jia C, Geng L, Yang M, Xu Z, Chen P, Cheng Y, Zhao J, et al. A far-red-emissive AIE active fluorescent probe with large stokes shift for detection of inflammatory bowel disease in vivo. J Mater Chem B. 2018;6:809–15.
217. Wang S, Zhang XF, Wang HS, Liu J, Shen SL, Cao XQ. A highly sensitive NIR fluorescence probe for hypoxia imaging in cells and ulcerative colitis. Talanta. 2023;252:123834.
218. Tian Y, Li Y, Jiang WL, Zhou DY, Fei J, Li CY. In-situ imaging of azoreductase activity in the acute and chronic ulcerative colitis mice by a near-infrared fluorescent probe. Anal Chem. 2019;91:10901–7.
219. Zeng M, Shao A, Li H, Tang Y, Li Q, Guo Z, Wu C, Cheng Y, Tian H, Zhu WH. Peptide receptor-targeted fluorescent probe: visualization and discrimination between chronic and acute ulcerative colitis. ACS Appl Mater Interfaces. 2017;9:13029–36.
220. Hong ST, Koh B, Choi SJ, Yoon E, Pyo MC, Choi JW, Kim MS, Lee EJ, Paik KC, Han MS, et al. Two-photon probe for TNF-alpha. Assessment of the transmembrane TNF-alpha level in human colon tissue by two-photon microscopy. Anal Chem. 2019;91:15769–76.
221. Fan X, Xia Q, Zhang Y, Li Y, Feng Z, Zhou J, Qi J, Tang BZ, Qian J, Lin H. Aggregation-induced emission (AIE) nanoparticles-assisted NIR-II fluorescence imaging-guided diagnosis and surgery for inflammatory bowel disease (IBD). Adv Healthc Mater. 2021;10:2101043.
222. Malik AM, Tupchong S, Huang S, Are A, Hsu S, Motaparthi K. An updated review of pemphigus diseases. Medicina (Kaunas). 2021;57:1080.
223. Schmidt E, Kasperkiewicz M, Joly P. Pemphigus. Lancet. 2019;394:882–94.
224. Horvath ON, Maurer M, Wietzke V, Fischer V, French LE, Sardy M. Intercellular, linear direct immunofluorescence staining pattern of sweat glands and hair follicles may be used as a diagnostic marker for pemphigus vulgaris in cases where epidermis is missing. Acta Derm Venereol. 2024;104:adv40620.
225. Kridin K, Patel PM, Jones VA, Cordova A, Amber KT. IgA pemphigus: a systematic review. J Am Acad Dermatol. 2020;82:1386–92.
226. Yang A, Xuan RR, Melbourne W, Hashimoto T, Uzun S, Daneshpazhooh M, Yamagami J, Di Zenzo G, Mascaro JM Jr, Mahmoudi H, et al. Inter-rater reliability of the BIOCHIP indirect immunofluorescence dermatology mosaic in bullous pemphigoid and pemphigus patients. J Eur Acad Dermatol Venereol. 2019;33:2327–33.
227. Zhang Y, Li W, Chen X, Xiong S, Bian Y, Yuan L, Gao X, Su D. Liver-targeted near-infrared fluorescence/photoacoustic dual-modal probe for real-time imaging of in situ hepatic inflammation. Anal Chem. 2023;95:2579–87.
228. Xu C, He S, Wei X, Huang J, Xu M, Pu K. Activatable sonoafterglow nanoprobes for T-cell imaging. Adv Mater. 2023;35:e2211651.
229. Wang K, Chen X-Y, Zhang R-W-Y, Yue Y, Wen X-L, Yang Y-S, Han C-Y, Ma Y, Liu H-J, Zhu H-L. Multifunctional fluorescence/photoacoustic bimodal imaging of γ-glutamyltranspeptidase in liver disorders under different triggering conditions. Biomaterials. 2024;310:122635.
230. Fahim A, Chong MC, Crooks MG, Hart SP. Idiopathic pulmonary fibrosis is associated with circulating antiepithelial antibodies. Lung. 2012;190:451–8.
231. He N, Wang Y, Huang Y, Wang X, Chen L, Lv C. A near-infrared fluorescent probe for evaluating glutamyl transpeptidase fluctuation in idiopathic pulmonary fibrosis cell and mice models. Sens Actuators B Chem. 2020;322:128565.
232. Xu F, Wang Q, Jiang L, Zhu F, Yang L, Zhang S, Song X. Evaluation of nitric oxide fluctuation via a fast, responsive fluorescent probe in idiopathic pulmonary fibrosis cells and mice models. Anal Chem. 2022;94:4072–7.
233. Liu L, Zhang L, Li M, Li Y, Wang Q, Wang X, Li S, Tian Y, Zhang Q. A Manganese(II) complex as high-order multiphoton fluorescent probe for detecting nitric oxide content change in idiopathic pulmonary fibrosis mice. Sens Actuators B Chem. 2023;394:134437.
234. Zhan Z, Liu R, Chai L, Dai Y, Lv Y. Visualization of lung inflammation to pulmonary fibrosis via peroxynitrite fluctuation. Anal Chem. 2019;91:11461–6.
235. Li S, Wang P, Liu Y, Yang K, Zhong R, Cheng D, He L. A mitochondrial-targeted near-infrared fluorescent probe for visualizing the fluctuation of hypochlorite acid in idiopathic pulmonary fibrosis mice. Anal Chim Acta. 2023;1239:340731.
236. Hou J, Huang Y, Fu L, Sun M, Wang L, Guo R, Chen L, Lv C. Evaluating the effect of hydrogen sulfide in the idiopathic pulmonary fibrosis model with a fluorescent probe. Anal Chem. 2023;95:5514–21.
237. He N, Bai S, Huang Y, Xing Y, Chen L, Yu F, Lv C. Evaluation of glutathione S-transferase inhibition effects on idiopathic pulmonary fibrosis therapy with a near-infrared fluorescent probe in cell and mice models. Anal Chem. 2019;91:5424–32.
238. Wei Y, Hou J, Lu P, Fu L, Wang X, Huang Y, Chen L, Lv C. A near-infrared fluorescent probe was used to evaluate the role of histone deacetylase in pulmonary fibrosis cells and mice. Sens Actuators B Chem. 2022;366:132012.
239. Schwenck J, Maurer A, Fehrenbacher B, Mehling R, Knopf P, Mucha N, Haupt D, Fuchs K, Griessinger CM, Bukala D, et al. Cysteine-type cathepsins promote the effector phase of acute cutaneous delayed-type hypersensitivity reactions. Theranostics. 2019;9:3903–17.
240. Ishimoto T, Arakawa Y, Vural S, Stohr J, Vollmer S, Galinski A, Siewert K, Ruhl G, Poluektov Y, Delcommenne M, et al. Multiple environmental antigens may trigger autoimmunity in psoriasis through T-cell receptor polyspecificity. Front Immunol. 2024;15:1374581.
241. Wei P, Guo Y, Liu L, Zhou X, Yi T. Hypochlorous acid triggered fluorescent probes for in situ imaging of a psoriasis model. J Mater Chem B. 2022;10:5211–7.
242. Zhao X, Hu X, Li L, Liu Y, Song B, Li Y, Cao Z, Zhou H, Peng C, Deng Y, Fang Y. Simultaneous visualization of lipid droplets and tracking of the endogenous hypochlorous acid in psoriatic mice models with a novel fluorescent probe in a wash-free fashion. Bioorg Chem. 2024;153:107967.
243. Lin Z, Xi L, Chen S, Tao J, Wang Y, Chen X, Li P, Wang Z, Zheng Y. Uptake and trafficking of different sized PLGA nanoparticles by dendritic cells in imiquimod-induced psoriasis-like mice model. Acta Pharm Sin B. 2021;11:1047–55.
244. Han J, Zhang J, Li M, Zhang Y, Lv J, Zhao X, Wang S, Wang L, Yang H, Han S, et al. A novel MuSK cell-based myasthenia gravis diagnostic assay. J Neuroimmunol. 2019;337:577076.
245. Pevzner A, Schoser B, Peters K, Cosma NC, Karakatsani A, Schalke B, Melms A, Kroger S. Anti-LRP4 autoantibodies in AChR- and MuSK-antibody-negative myasthenia gravis. J Neurol. 2012;259:427–35.
246. Alvarez-Velasco R, Dols-Icardo O, El Bounasri S, Lopez-Vilaro L, Trujillo JC, Reyes-Leiva D, Suarez-Calvet X, Cortes-Vicente E, Illa I, Gallardo E. Reduced number of thymoma CTLA4-positive cells is associated with a

higher probability of developing myasthenia gravis. Neurol Neuroimmunol Neuroinflamm. 2023;10:e200085.
247. Martinez MD, Trac DQ, Brown ME, Maher KO, Davis ME. Identification of targeting peptides for the diagnosis of myocarditis. Nanomedicine (Lond). 2018;13:787–801.
248. Konishi M, Erdem SS, Weissleder R, Lichtman AH, McCarthy JR, Libby P. Imaging granzyme B activity assesses immune-mediated myocarditis. Circ Res. 2015;117:502–12.
249. Sun Z, Hua X, Bao M, Xu W, Kang M, Mo H, Hu G, Yue G, Chen X, Mo S, et al. CXCL9+ Macrophage-targeted NIR-II aggregation-induced emission nanoprobes for the early diagnosis of myocarditis. Nano Today. 2024;54:102107.
250. Zhou Y, Dong H, Gu Z, Yang S, Ouyang M, Qing Z, Ma X, Hu S, Li J, Yang R. Self-immolative dye-doped polymeric probe for precisely imaging hydroxyl radicals by avoiding leakage. Anal Chem. 2021;93:12944–53.
251. Okuda K, Fu HY, Matsuzaki T, Araki R, Tsuchida S, Thanikachalam PV, Fukuta T, Asai T, Yamato M, Sanada S, et al. Targeted therapy for acute autoimmune myocarditis with nano-sized liposomal FK506 in rats. PLoS ONE. 2016;11:e0160944.
252. Xiong Y, Zhang Z, Liu S, Shen L, Zheng L, Ding L, Liu L, Wu L, Hu Z, Li L, et al. T lymphocyte-macrophage hybrid membrane-coated biomimetic nanoparticles alleviate myocarditis via suppressing pyroptosis by targeting gene silencing. Int J Nanomed. 2024;19:12817–33.
253. Zhang S, Ma M, Li J, Li J, Xu L, Gao D, Ma P, Han H, Song D. A pyroglutamate aminopeptidase 1 responsive fluorescence imaging probe for real-time rapid differentiation between thyroiditis and thyroid cancer. Anal Chem. 2024;96:5897–905.
254. Dong J, Miyake C, Yasuda T, Oyama H, Morita I, Tsukahara T, Takahashi M, Jeong HJ, Kitaguchi T, Kobayashi N, Ueda H. PM Q-probe: A fluorescent binding protein that converts many antibodies to a fluorescent biosensor. Biosens Bioelectron. 2020;165:112425.
255. de la Encarnación C, Lenzi E, Henriksen-Lacey M, Molina B, Jenkinson K, Herrero A, Colás L, Ramos-Cabrer P, Toro-Mendoza J, Orue I, et al. Hybrid magnetic-plasmonic nanoparticle probes for multimodal bioimaging. J Phys Chem C. 2022;126:19519–31.
256. Kang NY, Lee JY, Lee SH, Song IH, Hwang YH, Kim MJ, Phue WH, Agrawalla BK, Wan SYD, Lalic J, et al. Multimodal imaging probe development for pancreatic beta cells: from fluorescence to PET. J Am Chem Soc. 2020;142:3430–9.
257. Yao Y, Chen Z, Zhang T, Tang M. Adverse reproductive and developmental consequences of quantum dots. Environ Res. 2022;213:113666.
258. Liu J, Hu R, Liu J, Zhang B, Wang Y, Liu X, Law WC, Liu L, Ye L, Yong KT. Cytotoxicity assessment of functionalized CdSe, CdTe and InP quantum dots in two human cancer cell models. Mater Sci Eng C Mater Biol Appl. 2015;57:222–31.
259. Chen N, He Y, Su Y, Li X, Huang Q, Wang H, Zhang X, Tai R, Fan C. The cytotoxicity of cadmium-based quantum dots. Biomaterials. 2012;33:1238–44.
260. Lewinski N, Colvin V, Drezek R. Cytotoxicity of nanoparticles. Small. 2008;4:26–49.
261. Tarantola M, Pietuch A, Schneider D, Rother J, Sunnick E, Rosman C, Pierrat S, Sonnichsen C, Wegener J, Janshoff A. Toxicity of gold-nanoparticles: synergistic effects of shape and surface functionalization on micromotility of epithelial cells. Nanotoxicology. 2011;5:254–68.
262. Hu X, Gao X. Silica-polymer dual layer-encapsulated quantum dots with remarkable stability. ACS Nano. 2010;4:6080–6.
263. Aydemir D, Hashemkhani M, Acar HY, Ulusu NN. Evaluation of the biocompatibility of the GSH-coated Ag(2)S quantum dots in vitro: a perfect example for the non-toxic optical probes. Mol Biol Rep. 2020;47:4117–29.
264. Mao QX, Han L, Shu Y, Chen XW, Wang JH. Improving the biocompatibility of carbon nanodots for cell imaging. Talanta. 2016;161:54–61.
265. Fang X, Cui L, Yu H, Qi Y. Fe(III)-based fluorescent probe for high-performance recognition, test strip analysis, and cell imaging of carbon monoxide. Anal Chem. 2024;96:11588–94.
266. Ajith MP, Pardhiya S, Rajamani P. Carbon dots: an excellent fluorescent probe for contaminant sensing and remediation. Small. 2022;18:e2105579.
267. Geszke M, Murias M, Balan L, Medjahdi G, Korczynski J, Moritz M, Lulek J, Schneider R. Folic acid-conjugated core/shell ZnS:Mn/ZnS quantum dots as targeted probes for two photon fluorescence imaging of cancer cells. Acta Biomater. 2011;7:1327–38.
268. Rice LJ, Ecroyd H, van Oijen AM. Illuminating amyloid fibrils: fluorescence-based single-molecule approaches. Comput Struct Biotechnol J. 2021;19:4711–24.
269. Zhong S, Rivera-Molina F, Rivetta A, Toomre D, Santos-Sacchi J, Navaratnam D. Seeing the long tail: a novel green fluorescent protein, SiriusGFP, for ultra long timelapse imaging. J Neurosci Methods. 2019;313:68–76.
270. Wang H, Han G, Tang H, Zhang R, Liu Z, Sun Y, Liu B, Geng J, Zhang Z. Synchronous photoactivation-imaging fluorophores break limitations of photobleaching and phototoxicity in live-cell microscopy. Anal Chem. 2023;95:16243–50.
271. Sun Z, Liu S, Liu Z, Qin W, Chen D, Xu G, Wu C. FRET acceptor suppressed single-particle photobleaching in semiconductor polymer dots. Opt Lett. 2016;41:2370.
272. Platkov M, Tirosh R, Kaufman M, Zurgil N, Deutsch M. Photobleaching of fluorescein as a probe for oxidative stress in single cells. J Photochem Photobiol, B. 2014;140:306–14.
273. Kobayashi H, Ogawa M, Alford R, Choyke PL, Urano Y. New strategies for fluorescent probe design in medical diagnostic imaging. Chem Rev. 2010;110:2620–40.
274. Zanetti-Domingues LC, Tynan CJ, Rolfe DJ, Clarke DT, Martin-Fernandez M. Hydrophobic fluorescent probes introduce artifacts into single molecule tracking experiments due to non-specific binding. PLoS ONE. 2013;8:e74200.
275. Zhang B, Wang X, Liu F, Cheng Y, Shi D. Effective reduction of nonspecific binding by surface engineering of quantum dots with bovine serum albumin for cell-targeted imaging. Langmuir. 2012;28:16605–13.
276. Sato R, Kozuka J, Ueda M, Mishima R, Kumagai Y, Yoshimura A, Minoshima M, Mizukami S, Kikuchi K. Intracellular protein-labeling probes for multicolor single-molecule imaging of immune receptor-adaptor molecular dynamics. J Am Chem Soc. 2017;139:17397–404.
277. Zeng YS, Gao RC, Wu TW, Cho C, Tan KT. Fluorescent probe encapsulated in SNAP-tag protein cavity to eliminate nonspecific fluorescence and increase detection sensitivity. Bioconjug Chem. 2016;27:1872–9.
278. Wu TW, Lee FH, Gao RC, Chew CY, Tan KT. Fluorescent probe encapsulated in avidin protein to eliminate nonspecific fluorescence and increase detection sensitivity in blood serum. Anal Chem. 2016;88:7873–7.
279. Li H, Li J, Pan Z, Zheng T, Song Y, Zhang J, Xiao Z. Highly selective and sensitive detection of Hg(2+) by a novel fluorescent probe with dual recognition sites. Spectrochim Acta A Mol Biomol Spectrosc. 2023;291:122379.
280. Zhou R, Liu G, Fu S, Zheng H, Li D, Dai J, Wei J, Li B, Wang C, Lu G. Labeling selectivity of lipid droplets fluorescent probes: Twisted intramolecular charge transfer (TICT) vs intramolecular charge transfer (ICT). Biosens Bioelectron. 2024;264:116624.
281. Hanaoka K, Iwaki S, Yagi K, Myochin T, Ikeno T, Ohno H, Sasaki E, Komatsu T, Ueno T, Uchigashima M, et al. General design strategy to precisely control the emission of fluorophores via a twisted intramolecular charge transfer (TICT) process. J Am Chem Soc. 2022;144:19778–90.
282. Tu B, Feng Z, Wang H, Zhang W, Ye W, Wang H, Xiao X, Zhao W, Wu T. Development of a background signal suppression probe for 8-oxoguanine DNA glycosylase detection. Anal Chim Acta. 2021;1175:338741.
283. Long L, Wu Y, Wang L, Gong A, Hu R, Zhang C. Complete suppression of the fluorophore fluorescence by combined effect of multiple fluorescence quenching groups: a fluorescent sensor for Cu(2)(+) with zero background signals. Anal Chim Acta. 2016;908:1–7.
284. Mela C, Papay F, Liu Y. Enhance fluorescence imaging and remove motion artifacts by combining pixel tracking, interleaved acquisition, and temporal gating. IEEE Photonics J. 2021;13:1–13.
285. Wu S, Zhong Y, Zhou Y, Song B, Chu B, Ji X, Wu Y, Su Y, He Y. Biomimetic preparation and dual-color bioimaging of fluorescent silicon nanoparticles. J Am Chem Soc. 2015;137:14726–32.
286. Wang HX, Yang Z, Liu ZG, Wan JY, Xiao J, Zhang HL. Facile preparation of bright-fluorescent soft materials from small organic molecules. Chemistry. 2016;22:8096–104.
287. Jing Y, Chen Z, Ding E, Yuan R, Liu B, Xu B, Zhang P. High-yield production of g-C3N4 quantum dots as photocatalysts for the degradation of organic pollutants and fluorescent probes for detection of Fe3+ ions with live cell application. Appl Surf Sci. 2022;586:152812.

288. Wang L, Wu B, Li W, Li Z, Zhan J, Geng B, Wang S, Pan D, Wu M. Industrial production of ultra-stable sulfonated graphene quantum dots for Golgi apparatus imaging. J Mater Chem B. 2017;5:5355–61.
289. ter Weele EJ, van Terwisscha Scheltinga AGT, Linssen MD, Nagengast WB, Lindner I, Jorritsma-Smit A, de Vries EGE, Kosterink JGW, de Lub Hooge MN. Development, preclinical safety, formulation, and stability of clinical grade bevacizumab-800CW, a new near infrared fluorescent imaging agent for first in human use. Eur J Pharm Biopharm. 2016;104:226–34.
290. Abdellatif AAH, Younis MA, Alsharidah M, Al Rugaie O, Tawfeek HM. Biomedical applications of quantum dots: overview, challenges, and clinical potential. Int J Nanomed. 2022;17:1951–70.
291. Hoffmüller P, Brüggemann M, Eggermann T, Ghoreschi K, Haase D, Hofmann J, Hunfeld KP, Koch K, Meisel C, Michl P, et al. Advisory opinion of the AWMF Ad hoc Commission In-vitro Diagnostic Medical Devices regarding in-vitro diagnostic medical devices manufactured and used only within health institutions established in the Union according to Regulation (EU) 2017/746 (IVDR). Ger Med Sci. 2021;19:Doc08.
292. Hell SW. Far-field optical nanoscopy. Science. 2007;316:1153–8.
293. Hell SW, Wichmann J. Breaking the diffraction resolution limit by stimulated emission: stimulated-emission-depletion fluorescence microscopy. Opt Lett. 1994;19:780–2.
294. Betzig E, Patterson GH, Sougrat R, Lindwasser OW, Olenych S, Bonifacino JS, Davidson MW, Lippincott-Schwartz J, Hess HF. Imaging intracellular fluorescent proteins at nanometer resolution. Science. 2006;313:1642–5.
295. Rust MJ, Bates M, Zhuang X. Sub-diffraction-limit imaging by stochastic optical reconstruction microscopy (STORM). Nat Methods. 2006;3:793–5.
296. Vicidomini G, Bianchini P, Diaspro A. STED super-resolved microscopy. Nat Methods. 2018;15:173–82.
297. Liu G, Peng G, Dai J, Zhou R, Wang C, Yan X, Jia X, Liu X, Gao Y, Wang L, Lu G. STED nanoscopy imaging of cellular lipid droplets employing a superior organic fluorescent probe. Anal Chem. 2021;93:14784–91.
298. Whittaker Hawkins RF, Patenaude A, Dumas A, Jain R, Tesfagiorgis Y, Kerfoot S, Matsui T, Gunzer M, Poubelle PE, Larochelle C, et al. ICAM1+ neutrophils promote chronic inflammation via ASPRV1 in B cell-dependent autoimmune encephalomyelitis. JCI Insight. 2017;2:e96882.
299. Heine J, Reuss M, Harke B, D'Este E, Sahl SJ, Hell SW. Adaptive-illumination STED nanoscopy. Proc Natl Acad Sci. 2017;114:9797–802.
300. Lee J-C, Ma Y, Han KY, Ha T. Accurate background subtraction in STED nanoscopy by polarization switching. ACS Photonics. 2019;6:1789–97.
301. Saladin L, Le Berruyer V, Bonnevial M, Didier P, Collot M. Targeted photoactivatable green-emitting BODIPY based on directed photooxidation-induced activation and its application to live dynamic super-resolution microscopy. Chemistry. 2024;30:e202403409.
302. Lee SH, Shin JY, Lee A, Bustamante C. Counting single photoactivatable fluorescent molecules by photoactivated localization microscopy (PALM). Proc Natl Acad Sci U S A. 2012;109:17436–41.
303. Zhang Y, Zheng Y, Tomassini A, Singh AK, Raymo FM. Photoactivatable BODIPYs for live-cell PALM. Molecules. 2023;28:2447.
304. Samanta S, Gong W, Li W, Sharma A, Shim I, Zhang W, Das P, Pan W, Liu L, Yang Z, et al. Organic fluorescent probes for stochastic optical reconstruction microscopy (STORM): recent highlights and future possibilities. Coord Chem Rev. 2019;380:17–34.
305. Erstling JA, Hinckley JA, Bag N, Hersh J, Feuer GB, Lee R, Malarkey HF, Yu F, Ma K, Baird BA, Wiesner UB. Ultrasmall, bright, and photostable fluorescent core-shell aluminosilicate nanoparticles for live-cell optical super-resolution microscopy. Adv Mater. 2021;33:e2006829.
306. Ladepeche L, Planaguma J, Thakur S, Suarez I, Hara M, Borbely JS, Sandoval A, Laparra-Cuervo L, Dalmau J, Lakadamyali M. NMDA receptor autoantibodies in autoimmune encephalitis cause a subunit-specific nanoscale redistribution of NMDA receptors. Cell Rep. 2018;23:3759–68.
307. Grabner CP, Jansen I, Neef J, Weihs T, Schmidt R, Riedel D, Wurm CA, Moser T. Resolving the molecular architecture of the photoreceptor active zone with 3D-MINFLUX. Sci Adv. 2022;8:eabl7560.
308. Li C, Guan X, Zhang X, Zhou D, Son S, Xu Y, Deng M, Guo Z, Sun Y, Kim JS. NIR-II bioimaging of small molecule fluorophores: from basic research to clinical applications. Biosens Bioelectron. 2022;216:114620.
309. Zhang Y, Liu D, Chen W, Tao Y, Li W, Qi J. Microenvironment-activatable probe for precise nir-ii monitoring and synergistic immunotherapy in rheumatoid arthritis. Adv Mater. 2024;36:2409661.
310. Luo X, Yu F, Wang R, Su T, Luo P, Wen P, Yu F. A near-infrared two-photon fluorescent probe for the detection of HClO in inflammatory and tumor-bearing mice. Chin Chem Lett. 2024. https://doi.org/10.1016/j.cclet.2024.110531.
311. Tang H, Qiang X, Gao Y, Teng H, Chen X, Zhang Y, Tian J, Qin B, Guo Y. Real-time tracking and dual-mode imaging of hypochlorous acid in vivo by a small-sized fluorescence probe. Dyes Pigments. 2021;188:109219.
312. Zhou L, Zhang X, Dong Y, Pan Y, Li J, Zang Y, Li X. A tandemly activated fluorescence probe for detecting senescent cells with improved selectivity by targeting a biomarker combination. ACS Sens. 2022;7:1958–66.
313. Zhou X, Su X, Hu D, Li Y, Guo L, Yuan W, Yuan H, Chen L, Xu M, Luo S, et al. Ratiometric fluorescence and afterglow lifetime dual-channel nanoprobe for simultaneous imaging of HOCl and temperature in arthritis. ACS Appl Mater Interfaces. 2023;15:50916–25.
314. Sun Y, Wang Y, Li W, Li C. Real-time dual-modal photoacoustic and fluorescence small animal imaging. Photoacoustics. 2024;36:100593.
315. Li YX, Xie DT, Yang YX, Chen Z, Guo WY, Yang WC. Development of small-molecule fluorescent probes targeting enzymes. Molecules. 2022;27:4501.
316. Guo WY, Fu YX, Mei LC, Chen Z, Zhang ZY, Wang F, Yang WC, Liu G, Yang GF. Rational design of esterase-insensitive fluorogenic probes for in vivo imaging. ACS Sens. 2023;8:2041–9.
317. Sidhu JS, Kaur N, Singh N. Trends in small organic fluorescent scaffolds for detection of oxidoreductase. Biosens Bioelectron. 2021;191:113441.
318. Iwatate RJ, Kamiya M, Umezawa K, Kashima H, Nakadate M, Kojima R, Urano Y. Silicon rhodamine-based near-infrared fluorescent probe for gamma-glutamyltransferase. Bioconjug Chem. 2018;29:241–4.
319. Liu J, Schleyer KA, Bryan TL, Xie C, Seabra G, Xu Y, Kafle A, Cui C, Wang Y, Yin K, et al. Ultrasensitive small molecule fluorogenic probe for human heparanase. Chem Sci. 2020;12:239–46.
320. Xue XL, Wang Y, Chen S, Wang KP, Niu SY, Zong QS, Jiang Y, Hu ZQ. Monitoring intracellular pH using a hemicyanine-based ratiometric fluorescent probe. Spectrochim Acta A Mol Biomol Spectrosc. 2023;284:121778.
321. Chen W, Liu H, Song F, Xin L, Zhang Q, Zhang P, Ding C. pH-switched near-infrared fluorescent strategy for ratiometric detection of ONOO(-) in lysosomes and precise imaging of oxidative stress in rheumatoid arthritis. Anal Chem. 2023;95:1301–8.
322. Zhang H, Wang Y, Xuan X, Wang G, Guo H, Fan J. A dynamic invertible intramolecular charge-transfer fluorescence probe: real-time monitoring of mitochondrial ATPase activity. Chem Commun (Camb). 2017;53:5535–8.
323. Cao M, Liu Y, Xiang C, Zheng G, Xiong Q, Niu G. Versatile organic fluorescent probes for visualizing the dynamics of lipid droplets. Coord Chem Rev. 2025;522:216181.
324. Gao X, Cai S, Wang L, Guo Y, Liu L, Weng X, Huang K, Yan W, Qu J. Rhodamine-based fluorescent probe for dynamic STED imaging of mitochondria. Biomed Opt Express. 2024;15:1595–604.
325. Zhao Y, Chen K, Yu B, Wan Q, Wang Y, Tang F, Li X. Development of organic aggregation-induced emission fluorescent materials based on machine learning models and experimental validation. J Mol Struct. 2024;1317:139126.
326. Huang W, Huang S, Fang Y, Zhu T, Chu F, Liu Q, Yu K, Chen F, Dong J, Zeng W. AI-powered mining of highly customized and superior ESIPT-based fluorescent probes. Adv Sci. 2024. https://doi.org/10.1002/advs.202405596.
327. Saito Y, Oikawa M, Nakazawa H, Niide T, Kameda T, Tsuda K, Umetsu M. Machine-learning-guided mutagenesis for directed evolution of fluorescent proteins. ACS Synth Biol. 2018;7:2014–22.
328. Ghezzi A, Lenz AJM, Soldevila F, Tajahuerce E, Vurro V, Bassi A, Valentini G, Farina A, D'Andrea C. Computational based time-resolved multispectral fluorescence microscopy. APL Photonics. 2023;8:046110.
329. Asadiatouei P, Salem CB, Wanninger S, Ploetz E, Lamb DC. Deep-LASI, single-molecule data analysis software. Biophys J. 2024;123:2682–95.
330. Zhu Y, Fang Y, Huang W, Zhang W, Chen F, Dong J, Zeng W. AI-driven precision subcellular navigation with fluorescent probes. J Mater Chem B. 2024;12:11054–62.

331. Zrazhevskiy P, Gao X. Multifunctional quantum dots for personalized medicine. Nano Today. 2009;4:414–28.
332. Sun L, Ouyang J, Zeng Z, Zeng C, Ma Y, Zeng F, Wu S. Targeted and activatable nanosystem for fluorescent and optoacoustic imaging of immune-mediated inflammatory diseases and therapy via inhibiting NF-kappaB/NLRP3 pathways. Bioact Mater. 2022;10:79–92.
333. Preglej T, Brinkmann M, Steiner G, Aletaha D, Goschl L, Bonelli M. Advanced immunophenotyping: a powerful tool for immune profiling, drug screening, and a personalized treatment approach. Front Immunol. 2023;14:1096096.
334. Manshian BB, Jimenez J, Himmelreich U, Soenen SJ. Personalized medicine and follow-up of therapeutic delivery through exploitation of quantum dot toxicity. Biomaterials. 2017;127:1–12.
335. Wang N, Wang H, Zhang J, Ji X, Su H, Liu J, Wang J, Zhao W. Endogenous peroxynitrite activated fluorescent probe for revealing anti-tuberculosis drug induced hepatotoxicity. Chin Chem Lett. 2022;33:1584–8.
336. Lv Y, Dan C, Dongdong S, Chen M, Yin BC, Yuan L, Zhang XB. Visualization of oxidative injury in the mouse kidney using selective superoxide anion fluorescent probes. Chem Sci. 2018;9:7606–13.
337. Dong J, Yang Y, Fan X, Zhu H-L, Li Z. Accurate imaging in the processes of formation and inhibition of drug-induced liver injury by an activable fluorescent probe for ONOO−. Mater Today Bio. 2023;21:100689.
338. Zheng D, Zuo Y, Li L, McDowell A, Cao Y, Ye X, Zhou H, Peng C, Deng Y, Lu J, Fang Y. Natural harmaline acts as novel fluorescent probe for hypochlorous acid and promising therapeutic candidate for rheumatoid arthritis. J Photochem Photobiol B. 2024;258:112995.
339. Chen Y, Lu W, Guo Y, Zhu Y, Song Y. Chitosan-gated fluorescent mesoporous silica nanocarriers for the real-time monitoring of drug release. Langmuir. 2020;36:6749–56.
340. Wang Y, Wang X, Lv Y, Guo Y, He M, Lan M, Zhao Y, Gao F. A ROS-responsive fluorescent probe detecting experimental colitis by functional polymeric nanoparticles. Int J Pharm. 2021;609:121125.
341. Zhang Y, Feng N, Hu X, Wang X, Tao J, Ji Z, Yang Y, Ma J, Chen Y. Nanodomain-enhanced stable and multifunctional probes with near 100% quantum yield for versatile biosensing. Nano Lett. 2024;24:14427–36.

Publisher's Note